Confluentes Mathematici, Vol. 4, No. 3 (2012) 1230001 (80 pages)

DOI: 10.1142/S1793744212300012

SINGULARITIES OF DIVERGENCE-FREE VECTOR FIELDS WITH VALUES INTO S^1 OR S^2. APPLICATIONS TO MICROMAGNETICS

RADU IGNAT

Laboratoire de Mathématiques, Université Paris-Sud 11,
bât. 425, 91405 Orsay, France
Radu.Ignat@math.u-psud.fr

Received 24 August 2012
Revised 18 September 2012
Accepted 18 September 2012
Published 22 November 2012

In this survey, we present several results on the regularizing effect, rigidity and approximation of 2D unit-length divergence-free vector fields. We develop the concept of entropy (coming from scalar conservation laws) in order to analyze singularities of such vector fields. In particular, based on entropies, we characterize lower semicontinuous line-energies in 2D and we study by Γ-convergence method the associated regularizing models (like the 2D Aviles–Giga and the 3D Bloch wall models). We also present some applications to the analysis of pattern formation in micromagnetics. In particular, we describe domain walls in the thin ferromagnetic films (e.g. symmetric Néel walls, asymmetric Néel walls, asymmetric Bloch walls) together with interior and boundary vortices.

Keywords: Eikonal equation; regularity; Sobolev spaces; approximation; vortices; kinetic formulation; entropy; singular perturbation; Γ-convergence; compactness; micromagnetics; domain walls; Ginzburg–Landau theory.

AMS Subject Classification: 35A15, 35B25, 49L25, 49J45, 49Q20, 49S05, 58E20, 58E50, 78A25, 74G65, 82D40

Contents

1. Introduction

This survey concerns recent results on the structure of 2D and 3D unit-length vector fields of vanishing divergence and applications to micromagnetics. It contains two parts:

(I) We start by analyzing the regularizing effect, rigidity and approximation results of 2D unit-length divergence-free vector fields. This amounts to the study of the 2D eikonal equation which can be viewed as a scalar conservation law. A key tool in the analysis is the notion of entropy, classical in the theory of scalar conservation laws, which is adapted here to the framework of S^1-valued maps. Our first aim is to characterize the structure of singularities such as point-singularities (vortices) under the hypothesis of Sobolev regularity $W^{\frac{1}{p},p}$ of these vector fields. A second issue concerns the study of line-energies concentrated on singularities of codimension 1 of S^1-valued BV vector fields of vanishing divergence. More precisely, for vector fields $m \in BV(\Omega, S^1)$ with $\nabla \cdot m = 0$ in $\Omega \subset \mathbf{R}^2$, we consider energy functionals

$$\mathcal{I}_f(m) := \int_{J(m)} f(|m^+ - m^-|) d\mathcal{H}^1$$

concentrated on the jump "lines" $J(m)$ of m that depend only on the jump size $|m^+ - m^-|$ via the *cost function* $f : [0, 2] \to \mathbf{R}_+$. Using the concept of entropies, we characterize the cost functions f that generate lower semicontinuous line-energies $\mathcal{I}_f$ for a relevant topology. We also deduce existence of minimizers under certain boundary conditions. In particular, we characterize the situations where the viscosity solution is a minimizing configuration. Finally, we discuss the case of 3D unit-length vector fields satisfying a divergence constraint; typically, for vector fields

$m : \omega = \Omega \times (0, h) \to S^2$ with $m = m(x_1, x_2)$ (i.e. invariant in x_3-direction) and $\nabla \cdot m = 0$ in $\omega \subset \mathbf{R}^3$, we analyze the Γ-convergence of the singularly perturbed functionals G_ε (as $\varepsilon \to 0$):

$$G_\varepsilon(m_\varepsilon) = \varepsilon \int_\omega |\nabla m|^2 + \frac{1}{\varepsilon} \int_\omega g(m),$$

for certain potential $g : S^2 \to \mathbf{R}_+$. For that, we focus on the concept of generalized entropy defined on $\mathbf{R}^2$ or S^2. On the one hand, these generalized entropies are used for proving compactness of uniformly bounded energy configurations $G_\varepsilon(m_\varepsilon) \leq C$ as $\varepsilon \to 0$. On the other hand, they are the main tool in showing (optimal) lower bounds for G_ε as $\varepsilon \to 0$. We highlight the fact that this strategy works for potentials g generating one-dimensional transition layers (e.g. the Aviles–Giga and Bloch wall models) but also in the case where 2D microstructure appears instead of one-dimensional transition layers (e.g. the cross-tie wall and the zigzag pattern models).

(II) The second part focuses on micromagnetics, more precisely, on the analysis of pattern formation of the magnetization. In certain asymptotic regimes, the magnetization is described (at the mesoscopic level) by a 3D vector field m of vanishing divergence and taking values into S^2. Thus, there is a close link with the first part of this survey, our aim consisting in characterizing the singularities of the magnetization. These singular phenomena correspond (at the microscopic level) to domain walls (i.e. either one-dimensional transition layers, or 2D–3D microstructures) and topological defects of vortex type. We will discuss the general context of micromagnetics, in particular, a classification of the domain walls in the thin-film regime: *symmetric Néel walls*, *asymmetric Néel walls*, *asymmetric Bloch walls* together with interior vortices (*Bloch lines*) and boundary vortices.

We start our analysis by dealing with the predominant domain wall in thin ferromagnetic films, the (symmetric) Néel wall: it is a one-dimensional transition layer corresponding to an in-plane rotation between two directions of angle $-\theta$ and θ of the magnetization. We prove the asymptotic behavior of Néel walls through the method of Γ-convergence. The entropy method is not adapted in this case since the energetic cost of Néel wall is quartic in θ; we use instead a duality argument and failing Gagliardo–Nirenberg interpolation embedding with logarithmic rate. Second, we investigate the behavior of a vortex defect induced by a 360° Néel wall. The particularity of this vortex structure consists in carrying a zero topological degree at the microscopic level which is completely different from the well-known Ginzburg–Landau vortices. The analysis is closely related to the structure of 2D unit-length divergence-free vector fields, in particular, this model provides the optimal topology of the approximation result of $W^{\frac{1}{p},p}$ vector fields in Theorem 3.

Next, we deal with a common pattern in thin-films, the Landau state, corresponding to the global minimizer of the micromagnetic energy. It involves formation of Néel walls and Ginzburg–Landau type vortices, called Bloch lines in the micromagnetic jargon. Our main result concerns the compactness of magnetization of energy close to the Landau state in the regime where a vortex is energetically more expensive than a Néel wall. The method uses techniques developed for the Ginzburg–Landau type problems for the concentration of energy on vortex balls, together with an approximation argument of S^2-vector fields by S^1-vector fields away from the vortex balls.

We then analyze in details the topological defects of the magnetization. In particular, we study the asymptotic behavior of boundary vortices and their interaction energy; the fundamental object is based on the notion of "boundary" Jacobian that detects boundary vortices. The concentration of the micromagnetic energy around boundary vortices is proved by a Γ-convergence type argument. We also determine the renormalized energy corresponding to the interaction between boundary vortices and governing the localization of these defects.

Finally, we investigate a critical thin-film regime where a bifurcation phenomenon occurs between symmetric and asymmetric domain walls. We prove that for small transition angles θ, the optimal transition layer corresponds to the (symmetric) Néel wall. Then there exists a critical angle θ^* where a symmetry breaking occurs and an asymmetric domain wall (the asymmetric Néel wall) nucleates in the core of the transition. We study the asymptotic behavior of this transition layer and we prove the energy separation between the symmetric part (tails) and the asymmetric part (core) of the transition layer. In order to determine the critical angle θ^*, we compute the asymptotic expansion of the energy of the asymmetric wall at order θ^4. It amounts to study the minimization of Dirichlet energy over divergence-free vector fields with values into S^2 where a transition angle from $-\theta$ to θ is imposed.

We highlight the close relation between the two parts of the survey: The connecting thread is given by the structure of unit-length vector fields of vanishing divergence. On the one hand, the topic treated in the first part is often inspired by questions related to micromagnetics. On the other hand, the pattern formation of the magnetization (at the mesoscopic level) studied in the second part strongly relies on the analysis of 3D divergence-free vector fields m taking values into S^2. Depending on the asymptotic regime or the ansatz, the vector field m is invariant in one direction so that the divergence constraint only acts on two variables. Moreover, certain restrictions imposed by the asymptotic regime enforce m to take in-plane values, i.e. $m \in S^1$. This justifies the study on 2D unit-legth divergence-free vector fields developed at the beginning of the survey.

This survey is based on the "mémoire d'habilitation" of the author.[a] New parts have been added, in particular a simplified proof of Proposition 2 in Sec. 6.1, Lemma 1 and Remark 10 in Sec. 5.3, Theorem 9 in Sec. 5, Remark 6 in Sec. 4.2 and Remark 13 in Sec. 6.2.

[a]The habilitation was defended at Université Paris-Sud 11 in December 2011 in front of the Jury composed by F. Alouges, Y. Brenier, P. Gérard, F. Otto, B. Perthame and S. Serfaty and after referee reports of F. Alouges, L. Ambrosio and B. Perthame.

2. 2D Divergence-Free Unit-Length Vector Fields

Let $\Omega \subset \mathbf{R}^2$ be an open bounded set. We will focus on measurable vector fields $m : \Omega \to \mathbf{R}^2$ that satisfy

$$|m| = 1 \text{ a.e.} \quad \text{in } \Omega \quad \text{and} \quad \nabla \cdot m = 0 \quad \text{in } \mathcal{D}'(\Omega). \tag{2.1}$$

One can equivalently consider measurable vector fields $v : \Omega \to \mathbf{R}^2$ such that

$$|v| = 1 \text{ a.e.} \quad \text{in } \Omega \quad \text{and} \quad \nabla \times v = 0 \quad \text{in } \mathcal{D}'(\Omega). \tag{2.2}$$

[The passage from (2.1) to (2.2) is done via $v = m^\perp = (-m_2, m_1)$. The notation m comes from micromagnetics and stands for the magnetization.] Locally, m (respectively, v) can be written in terms of a stream function ψ, i.e. $m = \nabla^\perp \psi$ (respectively, $v = -\nabla\psi$) so that we get to the eikonal equation through ψ:

$$|\nabla \psi| = 1. \tag{2.3}$$

Typically, one can construct such vector fields by considering stream functions of the form $\psi = \operatorname{dist}(\cdot, K)$ for some closed set $K \subset \mathbf{R}^2$; these vector fields are called Landau states in micromagnetic jargon (see Fig. 1). However, not every stream function can be written as a distance function (up to a sign ± 1 and an additive constant); for example, if $\psi(x) = \max\{\operatorname{dist}(x, P_1), \operatorname{dist}(x, P_2)\}$ for two different points $P_1, P_2 \in \mathbf{R}^2$, then (2.3) holds even if ψ is not a distance function.

We denote

$$C^\infty_{\operatorname{div}}(\Omega, S^1) = \{m \in C^\infty(\Omega, \mathbf{R}^2) : m \text{ satisfies (2.1)}\}.$$

Idem, $W^{s,p}_{\operatorname{div}}(\Omega, S^1)$ stands for Sobolev spaces of order $s > 0$ and $p \geq 1$ of divergence-free unit-length vector fields, as well as $BV_{\operatorname{div}}(\Omega, S^1)$ for vector fields of bounded total variation. For a vector field $m \in BV_{\operatorname{div}}(\Omega, S^1)$, we denote the jump set of m by $J(m)$ which is a $\mathcal{H}^1$-rectifiable set oriented by a unit vector field $\nu : J(m) \to S^1$ and $m^\pm : J(m) \to S^1$ stand for the traces of m on $J(m)$ with respect to ν. Notice that the divergence-free hypothesis on m ensures that the normal component $m \cdot \nu$ is continuous across the jump set $J(m)$. So, for $\mathcal{H}^1$-almost every $x \in J(m)$, we can characterize the jump of m by a so-called "wall angle" $\theta(x)$ such that $m^\pm(x) = \cos\theta(x)\nu(x) \pm \sin\theta(x)\nu^\perp(x)$ (see Fig. 2).

3. Entropies

In the study of vector fields (2.1), the main tool we use in the following is the concept of entropies coming from scalar conservation laws. The starting point consists in

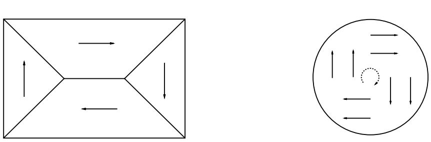

Fig. 1. Landau states in a rectangle and a disc.

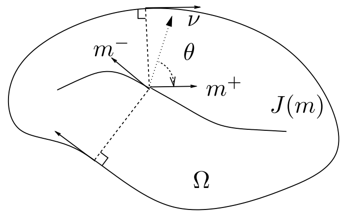

Fig. 2. Configuration m in $BV_{\text{div}}(\Omega, S^1)$.

regarding the structure (2.1) of our vector fields as a scalar conservation law. Indeed, writing $m = (u, h(u))$ for the flux $h(u) = \pm\sqrt{1-u^2}$, the vanishing divergence condition in m turns into the nonlinear transport equation

$$\partial_t u + \partial_s[h(u)] = 0, \tag{3.1}$$

where $(t, s) := (x_1, x_2)$ correspond to (time, space) variables. Let us recall some definitions from the theory of scalar conservation laws. Since the flux h is nonlinear, there is in general no smooth solution of the Cauchy problem associated to (3.1). Therefore, the solutions of (3.1) are to be understood in the sense of distributions and in general, there are infinitely many weak solutions for the Cauchy problem. The concept of entropy solution has been formulated in order to have uniqueness (see Kružkov [52]). To introduce this notion, the pair (entropy, entropy-flux) is defined as a couple of scalar functions (η, q) such that $\frac{dq}{du} = \frac{dh}{du}\frac{d\eta}{du}$ which entails that every smooth solution u of (3.1) has vanishing entropy production, i.e.

$$\partial_t[\eta(u)] + \partial_s[q(u)] = 0.$$

A solution u of (3.1) (in the sense of distributions) is called entropy solution if for every convex entropy η, the entropy production $\partial_t[\eta(u)] + \partial_s[q(u)] \leq 0$ is a non-positive measure. Moreover, such solutions u have the property that for every pair (η, q), the entropy production is a (signed) measure that concentrates on lines (corresponding to "shocks" of u). It suggests the interest of using "global" quantities (η, q) to detect "local" line-singularities of u. This idea has been used when dealing with reduced models in micromagnetics, e.g. Jin–Kohn [50], Aviles–Giga [6], DeSimone–Kohn–Müller–Otto [26], Ambrosio–DeLellis–Mantegazza [2], Alouges–Riviere–Serfaty [1], Ignat–Merlet [42, 43], Ignat–Moser [44].

In the sequel we will always use the following notion of entropy introduced in [26] (see also [50, 20, 43]). It corresponds to the pair (entropy, entropy-flux) from the scalar conservation laws, but here the pair is defined in terms of the couple $(u, h(u))$ and not only on u.

Definition 1. (DKMO [26]) We will say that $\Phi \in C^\infty(S^1, \mathbf{R}^2)$ is an entropy if

$$\frac{d}{d\theta}\Phi(z) \cdot z = 0, \quad \text{for every } z = e^{i\theta} = (\cos\theta, \sin\theta) \in S^1. \tag{3.2}$$

Here, $\frac{d}{d\theta}\Phi(z) := \frac{d}{d\theta}[\Phi(e^{i\theta})]$ stands for the angular derivative of Φ. The set of all entropies is denoted by ENT.

We will often use a second characterization of entropies that provides a way to construct entropies:

Proposition 1. (DKMO [26]) *Let $\Phi \in C^\infty(S^1, \mathbf{R}^2)$. Then $\Phi \in ENT$ if and only if there exists a (unique) 2π-periodic $\varphi \in C^\infty(\mathbf{R})$ such that for every $z = e^{i\theta} \in S^1$,*

$$\Phi(z) = \varphi(\theta)z + \frac{d\varphi}{d\theta}(\theta)z^\perp. \tag{3.3}$$

In this case,

$$\frac{d}{d\theta}\Phi(z) = \lambda(\theta)z^\perp, \tag{3.4}$$

where $\lambda \in C^\infty(\mathbf{R})$ is the 2π-periodic function defined by $\lambda = -\Lambda\varphi := \varphi + \frac{d^2}{d\theta^2}\varphi$ in $\mathbf{R}$.

Remark 1. There exists a unique extension of $\Lambda : C^\infty(S^1 \approx \frac{\mathbf{R}}{2\pi\mathbb{Z}}) \to C^\infty(S^1)$ as a linear unbounded operator $\Lambda : L^2(S^1) \to L^2(S^1)$ with the domain $D(\Lambda) = H^2(S^1)$. Moreover, the kernel of Λ is given by $\ker\Lambda = \mathbf{R}\sin \oplus \mathbf{R}\cos$, the spectrum of Λ is $\sigma(\Lambda) = \{k^2 - 1 : k \in \mathbb{N}^*\}$ and the range of Λ is $R(\Lambda) = (\ker\Lambda)^\perp$. Consequently, for every $\lambda \in (\ker\Lambda)^\perp$, there exists a unique $\varphi \in \frac{L^2(S^1)}{\ker\Lambda}$ such that $-\Lambda\varphi = \lambda$ and the corresponding entropy Φ given by (3.3) is uniquely defined by λ up to a constant.

This notion is coherent with the property that a smooth vector field m satisfying (2.1) induces vanishing entropy production $\nabla \cdot [\Phi(m)] = 0$. In fact, it is equivalent[b] to Definition 1 as stated in the following property:

Proposition 2. (Ignat [39]) *Let $\Phi \in C^\infty(S^1, \mathbf{R}^2)$. Then Φ is an entropy if and only if for every $m \in W^{\frac{1}{p},p}_{\mathrm{div}}(\Omega, S^1)$, $p \in [1, 2]$ (in particular, for every $m \in C^\infty_{\mathrm{div}}(\Omega, S^1)$), the following identity holds*:

$$\nabla \cdot [\Phi(m)] = 0 \quad \textit{in } \mathcal{D}'(\Omega). \tag{3.5}$$

As we explain later, the assumption $m \in W^{\frac{1}{p},p}$ is a critical regularity to avoid jump line-singularities. We conjecture that Proposition 2 should hold also for $p > 2$. However, for $m \in BV_{\mathrm{div}}(\Omega, S^1)$, the *entropy production*

$$\mu_\Phi(m) := \nabla \cdot [\Phi(m)]$$

is a measure supported on the jump set of m.

Proposition 3. (Ignat–Merlet [43]) *Let $\Phi \in ENT$ be an entropy and $m \in BV_{\mathrm{div}}(\Omega, S^1)$. Then we have*

$$\mu_\Phi(m) = \{\Phi(m^+) - \Phi(m^-)\} \cdot \nu\mathcal{H}^1 \llcorner J(m), \tag{3.6}$$

[b] In fact, (3.2) can be deduced from (3.5) by choosing m to be an appropriate vortex configuration (see [43]).

where $J(m)$ is the $\mathcal{H}^1$-rectifiable jump set of m oriented by ν and $m^\pm$ are the traces of m on $J(m)$.

Observe that for the orientation $\nu = e^{i\beta}$ ($\beta \in \mathbf{R}$) and traces $m^\pm = e^{i(\beta\pm\theta)}$ where $\theta \in [-\pi, \pi)$ is the "wall angle" of the jump of m at some point $x \in J(m)$, the entropy production density can be written as a convolution formula via (3.4):

$$[\Phi(m^+) - \Phi(m^-)] \cdot \nu = (\lambda \star \sin_\theta)(\beta), \quad \beta \in \mathbf{R}, \tag{3.7}$$

where

$$\sin_\theta(\beta) = \begin{cases} \operatorname{sgn}(\theta)\sin\beta & \text{for } |\beta| \le |\theta|, \\ 0 & \text{for } |\beta| > |\theta|. \end{cases}$$

Remark 2. The proofs of Propositions 2 and 3 in [39] and [43] strongly rely on the structure of lifting of vector fields $m \in BV(\Omega, S^1)$ (respectively, $m \in W^{\frac{1}{p},p}(\Omega, S^1)$) and an appropriate chain rule. More precisely, if $m \in BV(\Omega, S^1)$, then there exists a lifting $\Theta \in BV(\Omega, \mathbf{R})$ such that $m = e^{i\Theta}$ a.e. in Ω (see e.g. [30, 12, 18, 35]). While if $m \in W^{\frac{1}{p},p}(\Omega, S^1)$ with $p \ge 1$, then one can find a lifting $\Theta = \Theta_1 + \Theta_2$ of m with $\Theta_1 \in W^{\frac{1}{p},p}$, $\Theta_2 \in SBV$ and $e^{i\Theta_2} \in W^{\frac{1}{p},p} \cap W^{1,1}$ (see [11, 59, 58]). Recall that $SBV(\Omega, \mathbf{R}^d)$ is the subspace of vector fields $m \in BV(\Omega, \mathbf{R}^d)$ whose differential Dm has vanishing Cantor part $D^c m$ (i.e. $D^c m \equiv 0$ as a measure in Ω). In Sec. 6.1, we will present a *new and easier* proof of Proposition 2 that avoids the properties of lifting of $W^{\frac{1}{p},p}(\Omega, S^1)$ vector fields, but uses the concept of generalized entropy.

As shown in [43], these properties can be extended for nonsmooth entropies. Moreover, there is a special class of BV entropies that play an important role in the following: for each $\xi \in S^1$, we call "elementary entropies" the maps $\Phi^\xi : S^1 \to \mathbf{R}^2$ given by

$$\Phi^\xi(z) := \begin{cases} \xi & \text{for } z \cdot \xi > 0, \\ 0 & \text{for } z \cdot \xi \le 0. \end{cases} \tag{3.8}$$

Although Φ^ξ is not a smooth entropy (in fact, Φ^ξ has a jump at the points $\pm\xi^\perp \in S^1$), the equality (3.2) trivially holds in $\mathcal{D}'(S^1)$. Moreover, as shown in [26], there exists a sequence of smooth entropies $\{\Phi_k\} \subset ENT$ such that $\{\Phi_k\}$ is uniformly bounded and $\lim_k \Phi_k(z) = \Phi^\xi(z)$ for every $z \in S^1$ (this approximation result follows via (3.3)).

4. The Space $W^{\frac{1}{p},p}_{\mathrm{div}}(\Omega, S^1)$. Vortices

The aim of this section consists in the study of vector fields (2.1) of critical regularity $m \in W^{\frac{1}{p},p}$ that insures avoidance of jump line-singularities. In this case, we expect that such vector fields m present vortex singular points.

Remark 3. Note that a vector field $m \in W^{\frac{1}{p},p}(\Omega \subset \mathbb{R}^2, S^1)$ (not satisfying the divergence-free constraint) may have line-singularities (that are not jump line-singularities). For example, if $p = 2$, then the function $\varphi : (-\frac{1}{2}, \frac{1}{2}) \to \mathbb{R}$ defined as $\varphi(x_1) = \log|\log|x_1||$ for $x_1 \neq 0$ belongs to $H^{\frac{1}{2}}((-\frac{1}{2}, \frac{1}{2}))$. So, setting $\Omega = (-\frac{1}{2}, \frac{1}{2})^2 \subset \mathbb{R}^2$, then the function $m(x_1, x_2) := e^{i\varphi(x_1)}$ belongs to $H^{\frac{1}{2}}(\Omega, S^1)$ and obviously, $L = \{(0, x_2) : x_2 \in (-\frac{1}{2}, \frac{1}{2})\} \subset \Omega$ is a line-singularity of m.

The main feature of vector fields in $W^{\frac{1}{p},p}_{\mathrm{div}}(\Omega, S^1)$ relies on a kinetic formulation. It comes via Propositions 2 and 3 when writing the entropy production for the "elementary entropies" $\Phi^\xi = \xi\tilde{\chi}$ (see (3.8)). We succeed to prove in [38, 39] the following kinetic formulation for $W^{\frac{1}{p},p}_{\mathrm{div}}(\Omega, S^1)$ with $p \in [1, 2]$ and we conjecture that it still holds for $p > 2$.

Proposition 4. (Kinetic formulation) *Let $m \in W^{\frac{1}{p},p}_{\mathrm{div}}(\Omega, S^1)$ with $p \in [1, 2]$. For every direction $\xi \in S^1$, we define $\chi(\cdot, \xi) : \Omega \to \{0, 1\}$ (respectively, $\tilde{\chi}(\cdot, \xi) : S^1 \to \{0, 1\}$) by*

$$\chi(x, \xi) = \tilde{\chi}(m(x), \xi) = \begin{cases} 1 & \text{for } m(x) \cdot \xi > 0, \\ 0 & \text{for } m(x) \cdot \xi \leq 0. \end{cases}$$

Then the following kinetic equation holds for every $\xi \in S^1$:

$$\xi \cdot \nabla\chi(\cdot, \xi) = 0 \quad \text{in } \mathcal{D}'(\Omega). \tag{4.1}$$

Here, χ corresponds to the concept of characteristic of a weak solution m satisfying (2.1). Indeed, if m is smooth around a point $x \in \Omega$, then the characteristic of m at x (by means of the eikonal equation (2.3) with $m = \nabla^\perp\psi$ around x) is given by $\dot{X}(t, x) = m^\perp(X(t, x))$ with the initial condition $X(0, x) = x$; then the orbit $\{X(t, x)\}_t$ is a straight line (i.e. $X(t, x) = x + tm^\perp(x)$ for t in some interval around 0) along which m is perpendicular and constant. Therefore, in the direction $\xi := m^\perp(x)$, either $\nabla\chi(\cdot, \xi)$ locally vanishes (if m is constant in a neighborhood of x), or it concentrates on $\{X(t, x)\}_t$ and is oriented by $\xi^\perp$ (see Fig. 3). The knowledge of $\chi(\cdot, \xi)$ in every direction $\xi \in S^1$ determines completely the vector field m due to the straightforward formula

$$m(x) = \frac{1}{2}\int_{S^1} \xi\chi(x, \xi)d\xi \quad \text{for a.e. } x \in \Omega. \tag{4.2}$$

Remark 4. Classical kinetic averaging lemma (see e.g. Golse–Lions–Perthame–Sentis [32]) shows that a measurable vector-field $m : \Omega \to S^1$ satisfying (4.1) belongs to $H^{\frac{1}{2}}_{\mathrm{loc}}$ (due to (4.2)). This property can be read as the converse of Proposition 4 for the case $m \in H^{\frac{1}{2}}(\Omega, S^1)$.

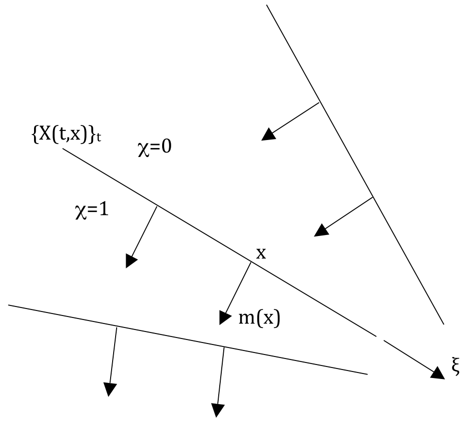

Fig. 3. Characteristics of m.

4.1. *Regularity results*

The first goal is to prove the following regularity result:

Theorem 1. (Ignat [39]) *If $m \in W^{\frac{1}{p},p}_{\mathrm{div}}(\Omega, S^1)$ with $p \in [1,2]$, then m is locally Lipschitz continuous inside Ω except at a locally finite number of singular points. Moreover, every singular point P of m corresponds to a vortex singularity of degree 1 of m, i.e. there exists a sign $\alpha = \pm 1$ such that*

$$m(x) = \alpha \frac{(x-P)^\perp}{|x-P|} \quad \text{for every } x \neq P \text{ in any convex neighborhood of } P \text{ in } \Omega.$$

In particular, if $m \in H^1_{\mathrm{div}}(\Omega, S^1)$ then m is locally Lipschitz.

Remark 5. The above result was proved by Jabin–Otto–Perthame [47] in the particular case of zero-energy states of a line-energy Ginzburg–Landau model. More precisely, for $\varepsilon > 0$, one defines the functional $E_\varepsilon : H^1(\Omega, \mathbf{R}^2) \to \mathbf{R}_+$ by

$$E_\varepsilon(m_\varepsilon) = \varepsilon \int_\Omega |\nabla m_\varepsilon|^2 dx + \frac{1}{\varepsilon} \int_\Omega (1 - |m_\varepsilon|^2)^2 dx$$
$$+ \frac{1}{\varepsilon} \|\nabla \cdot m_\varepsilon\|^2_{H^{-1}(\Omega)}, \quad m_\varepsilon \in H^1(\Omega, \mathbf{R}^2)$$

(we refer to [2, 6, 50, 26, 48, 68, 47] for the analysis of this model). A vector field $m : \Omega \subset \mathbf{R}^2 \to \mathbf{R}^2$ is called zero-energy state if there exists a family $\{m_\varepsilon \in H^1(\Omega, \mathbf{R}^2)\}_{\varepsilon \to 0}$ satisfying

$$m_\varepsilon \to m \quad \text{in } L^1(\Omega) \quad \text{and} \quad E_\varepsilon(m_\varepsilon) \to 0 \quad \text{as } \varepsilon \to 0.$$

Then m satisfies (2.1). Moreover, it is proved in [47] that a zero-energy state satisfies the kinetic formulation (4.1) and furthermore, m shares the structure in Theorem 1. Therefore, the proof of Theorem 1 strongly relies on [47] and Proposition 4 (via Proposition 2).

As a consequence of Theorem 1, one has for $p \in [1, 2]$:

$$\{m \in W^{\frac{1}{p},p}_{\text{loc}}(\Omega, \mathbf{R}^2) : m \text{ satisfies } (2.1)\} = \{m \in H^{\frac{1}{2}}_{\text{loc}}(\Omega, \mathbf{R}^2) : m \text{ satisfies } (2.1)\}.$$

Let us now discuss the optimality of the result in Theorem 1: Firstly, observe that Lipschitz regularity cannot be improved.

Proposition 5. (Ignat [39]) *There exist Lipschitz vector fields $m : \Omega \to \mathbf{R}^2$ that satisfy* (2.1) *and are not C^1 in Ω.*

In general, a vector field $m \in W^{\frac{1}{p},p}_{\text{div}}(\Omega, S^1)$ with $p \in [1, 2]$ (without interior vortex singularities) is only locally Lipschitz, and not necessary globally Lipschitz in Ω. This is the case of a "boundary vortex" vector field, e.g. $m(x) = \frac{(x-P)^\perp}{|x-P|}$ for every $x \in \Omega$ where P is some point on $\partial\Omega$. If the domain Ω has a cusp in $P \in \partial\Omega$, the "boundary vortex" vector field could belong even to $H^1(\Omega, \mathbf{R}^2)$; moreover, there even exist convex domains Ω and $m \in H^1_{\text{div}}(\Omega, S^1)$ such that m is not globally Lipschitz in Ω.

The geometry of Ω influences the number of vortex singularities of $W^{\frac{1}{p},p}$-vector fields satisfying (2.1). For example, if Ω is convex, then every vector field $m \in W^{\frac{1}{p},p}_{\text{div}}(\Omega, S^1)$ with $p \in [1, 2]$ is either a "vortex" vector field (i.e. $m(x) = \pm\frac{(x-P)^\perp}{|x-P|}$ for every $x \in \Omega$ where P is some point in Ω), or locally Lipschitz (i.e. no interior vortex); therefore, convex domains do not allow for more than one interior vortex. However, we prove that there are nonconvex domains where configurations with arbitrary number of vortices do exist.

Proposition 6. (Ignat [39]) *There exist an open simply-connected nonconvex piecewise Lipschitz domain Ω and a vector field $m \in W^{1,q}_{\text{div}}(\Omega, S^1)$ for every $q \in [1, 2)$ that has infinitely many vortices $\{P_1, P_2, \ldots\}$.*

Observe that $W^{1,q}_{\text{loc}}(\Omega, S^1) \subset W^{\frac{1}{p},p}_{\text{loc}}(\Omega, S^1)$ for $q > 1$ and $p \geq 1$, and the embedding fails for $q = 1$. Also notice that configurations with infinitely many (interior) vortices can occur only in a non-Lipschitz domain Ω; indeed, if $\partial\Omega$ is Lipschitz, then a configuration $m \in W^{\frac{1}{p},p}_{\text{div}}(\Omega, S^1)$ with $p \in [1, 2]$ has only a finite number of interior vortex singularities.

We address the following open problem:

Open Problem 1. *Does Theorem* 1 *hold in the case $m \in W^{\frac{1}{p},p}_{\text{div}}(\Omega, S^1)$ with $p > 2$?*

A positive answer is equivalent to proving Proposition 2 for $m \in W^{\frac{1}{p},p}_{\text{div}}(\Omega, S^1)$ with $p > 2$ which would yield the kinetic formulation (4.1) for such m. However, a duality issue prevents us from establishing (4.1) when $p > 2$ (see the proof of Proposition 2 in Sec. 6.1). A natural question concerns higher dimensions $d \geq 3$ in the same context of the eikonal equation. We mention that the above techniques seem to be typical for the two-dimensional case and do not adapt to the case $d \geq 3$. Indeed, if $d = 3$, the system of scalar conservation laws associated to (2.3) admits only the trivial entropies (see Remark 10). Moreover, the regularity result in Theorem 1 is based on a certain order relation between the characteristics of m. Obviously, such an order relation does not exist in higher dimensions. We conjecture the following for dimension $d = 3$:

Open Problem 2. *Let $\Omega \subset \mathbf{R}^3$ be a bounded open set and $v \in H^1(\Omega, S^2)$ be a gradient field, i.e. $v = \nabla\psi$ with* (2.3). *Is it true that v is locally Lipschitz continuous inside Ω except at a locally finite number of vortex singularities of v and $v(x) = \alpha\frac{(x-P)}{|x-P|}$ in any convex neighborhood of a vortex point P in Ω with a sign $\alpha = \pm 1$?*

A partial answer was recently given by Caffarelli–Crandall [14]: Under the stronger hypothesis that the function ψ given in (2.3) is *differentiable in a pointwise sense* except on a set of zero Hausdorff measure $\mathcal{H}^1$, then the conclusion of Open Problem 2 holds true.

4.2. *Density results*

The second goal of the section is to present approximation results for the class of vector fields $W^{\frac{1}{p},p}_{\mathrm{div}}(\Omega, S^1)$ with $p \in [1, 2]$: Our subsets are formed either by divergence-free vector fields that are smooth except at a finite number of points and the approximation result holds in the $W^{\frac{1}{p},p}$-topology, or by everywhere smooth S^1-valued vector fields (not necessarily divergence-free) and the approximation result holds in a weaker topology. We start by extending Bethuel–Zheng's density result (see [8]) for $W^{1,1}(\Omega, S^1)$ vector fields, respectively Riviere's density result (see [67]) for $H^{\frac{1}{2}}(\Omega, S^1)$ vector fields to the case of divergence-free vector fields:

Theorem 2. (Ignat [39]) *Let Ω be a Lipschitz bounded simply-connected domain and $m \in W^{\frac{1}{p},p}_{\mathrm{div}}(\Omega, S^1)$ with $p \in [1, 2]$. Then m has a finite number $N \geq 0$ of vortices $\{P_1, \ldots, P_N\}$ and m can be approximated in $W^{1,q}_{\mathrm{loc}}(\Omega)$ (for any $q \in [1, 2)$) by divergence-free vector fields $m_k \in C^\infty(\Omega\backslash\{P_{1,k}, \ldots, P_{N,k}\}, S^1)$ that are smooth except at the N vortex points of m_k. In particular, if $m \in H^1_{\mathrm{div}}(\Omega, S^1)$, the sequence $\{m_k\}$ can be chosen to be smooth everywhere in Ω and the approximation result holds in $H^1_{\mathrm{loc}}(\Omega)$.*

Remark 6. We highlight the fact that in general the vortices of the approximating vector fields m_k in Theorem 2 cannot coincide with the set of vortex points of m. Let us consider the vector field m given in Fig. 4. More precisely, set $f, g : \mathbf{R} \to \mathbf{R}$ with $f(t) = |t|$ and

$$g(t) = \begin{cases} 2(t+1) & \text{for } t \leq -1, \\ -\dfrac{1}{2}(t+1) & \text{for } t \geq -1 \end{cases}$$

and define the curves

$$\gamma^+ = \{(x_1, f(x_1)) : x_1 \in [-2, 1]\} \quad \text{and} \quad \gamma^- = \{(x_1, g(x_1)) : x_1 \in [-2, 1]\}.$$

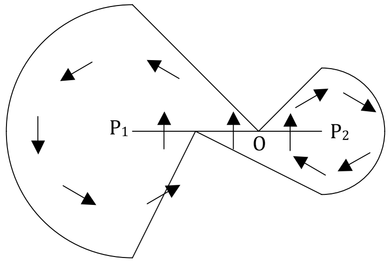

Fig. 4. Two vortex-point singularities of different orientation.

Fixing the vortex points $P_1 := (-2, 0)$ and $P_2 = (1, 0)$, we define the domain

$$\Omega := (B(P_1, 2) \cap \{x_1 \leq -2\}) \cup \{(x_1, x_2) : x_1 \in [-2, 1], g(x_1) < x_2 < f(x_1)\}$$
$$\cup (B(P_2, 1) \cap \{x_1 \geq 1\})$$

(see Fig. 4). We define $m : \Omega \to S^1$ as follows:

$$m(x) = \begin{cases} \dfrac{(x - P_1)^\perp}{|x - P_1|} & \text{in } \Omega_1 := \{x \in \Omega : x_1 \leq -1 \text{ or } (x_1 \in (-1, 0) \text{ and } x_2 > 0)\}, \\ -\dfrac{(x - P_2)^\perp}{|x - P_2|} & \text{in } \Omega_2 := \{x \in \Omega : x_1 \geq 0 \text{ or } (x_1 \in (-1, 0) \text{ and } x_2 < 0)\}. \end{cases}$$

Then $m \in W^{\frac{1}{p},p}_{\text{div}}(\Omega, S^1)$ for any $p \geq 1$ and is locally Lipschitz in $\Omega \backslash \{P_1, P_2\}$ with two vortex-point singularities P_1 and P_2 of degree 1. Now observe that any other configuration $\tilde{m} \in W^{\frac{1}{p},p}_{\text{div}}(\Omega, S^1)$ (for some $p \in [1, 2]$) with the same vortex points P_1 and P_2 satisfies the rigidity structure proved in Theorem 1, implying that $\tilde{m}$ is uniquely determined in Ω_1 and Ω_2. More precisely, the flow of characteristics coming from the vortex points P_1 and P_2 constraints $\tilde{m}$ to coincide with m or $-m$. Therefore, the characteristic $[P_1 P_2]$ represents a jump line-singularity of $\nabla \tilde{m}$, i.e. $\tilde{m}$ does not belong to $C^\infty(\Omega \backslash \{P_1, P_2\}, S^1)$. We conclude that the approximating vector fields $m_k \in C^\infty(\Omega \backslash \{P_{1,k}, P_{2,k}\}, S^1)$ of m (given in Theorem 2) must satisfy $\{P_{1,k}, P_{2,k}\} \neq \{P_1, P_2\}$.

In various applications (see e.g. Remark 7 below), we need to approximate vector fields m (with the structure given in Theorem 1) by $H^1(\Omega, S^1)$ vector fields. But $H^1(\Omega, S^1)$-vector fields cannot allow for vortices. Therefore, an approximation result by everywhere smooth S^1-valued vector fields is needed in some weaker topology than in Theorem 2. What is the optimal weak topology where such a density result holds? The following result shows that L^1-topology is too strong for having density of smooth vector fields of vanishing divergence and values in S^1.

Proposition 7. (Ignat [39]) *Let $m : B^2 \to S^1$ be the vortex configuration $m(x) = \frac{x^\perp}{|x|}$ in the unit disc B^2. Then there exists no sequence of vector fields $m_k \in C^\infty_{\text{div}}(\Omega, S^1)$ such that $m_k \to m$ a.e. in B^2 as $k \to \infty$.*

We now generalize this property: The density result still fails if we relax the divergence-free constraint on the approximated smooth vector fields, but we impose this restriction on the limit in L^1-topology (or H^{-s} weak topology for some $s \in [0, \frac{1}{2})$).

Proposition 8. (Ignat [39]) *Let $m : B^2 \to S^1$ be the vortex configuration $m(x) = \frac{x^\perp}{|x|}$ in B^2. Then there exists no sequence of vector fields $m_k \in C^\infty(\Omega, S^1)$ such that $m_k \to m$ a.e. in B^2 as $k \to \infty$ and one of the following two conditions holds*:

(a) $\nabla \cdot m_k \to 0$ *in* $L^1(B^2)$;
(b) $\nabla \cdot m_k \rightharpoonup 0$ *weakly in* $H^{-s}(B^2)$ *for some* $s \in [0, \frac{1}{2})$.

Finally, we prove an approximation result in L^1-topology by smooth vector fields with values in S^1 (not necessary divergence-free), but the divergence-free constraint holds in the limit in the $H^{-\frac{1}{2}}$-topology. This topology is optimal (due Proposition 8(b)).

Theorem 3. (Ignat [39]) *Let Ω be a Lipschitz bounded simply-connected domain and $m \in W^{\frac{1}{p},p}_{\mathrm{div}}(\Omega, S^1)$ with $p \in [1, 2]$. Then there exists a sequence of vector fields $m_k \in C^\infty(\Omega, S^1)$ such that $m_k \to m$ a.e. in Ω and $(\nabla \cdot m_k)\mathbf{1}_\Omega \to 0$ in $\dot{H}^{-\frac{1}{2}}(\mathbf{R}^2)$ as $k \to \infty$.*

Remark 7. The motivation of Theorem 3 comes from thin-film micromagnetics. The following 2D energy (see [23]) is considered as an approximation of the 3D micromagnetic model in a thin-film regime: For $\varepsilon > 0$, one defines the functional $\tilde{E}_\varepsilon : H^1(\Omega, S^1) \to \mathbf{R}_+$ by

$$\tilde{E}_\varepsilon(m_\varepsilon) = \varepsilon \int_\Omega |\nabla m_\varepsilon|^2 dx + \|(\nabla \cdot m_\varepsilon)\mathbf{1}_\Omega\|^2_{\dot{H}^{-\frac{1}{2}}(\mathbf{R}^2)}, \quad m_\varepsilon \in H^1(\Omega, S^1).$$

This model was analyzed in [21, 45, 40]. In particular, it is proved in [40] that a vortex configuration $m(x) = \frac{x^\perp}{|x|}$ in B^2 is a zero-energy state, i.e. there exists a family $\{m_\varepsilon\} \subset H^1(B^2, S^1)$ such that $m_\varepsilon \to m$ a.e. in B^2 and $\tilde{E}_\varepsilon(m_\varepsilon) \to 0$ as $\varepsilon \to 0$. The role of Theorem 3 is to generalize this approximation result for every vector field $m \in W^{\frac{1}{p},p}$ (with $p \in [1, 2]$) satisfying (2.1).

5. The BV Case. Line-Energies

The topic of this section concerns vector fields m satisfying (2.1) that present jump line-singularities. The context is the following: Let $\Omega \subset \mathbf{R}^2$ be a bounded domain with piecewise Lipschitz boundary that is oriented by the outer unit normal vector n. We start by addressing the following conjecture concerning the regularity of vector fields $m \in BV_{\mathrm{div}}(\Omega, S^1)$: The measure Dm does not concentrate on sets of Hausdorff dimension $d \in (1, 2)$.

Open Problem 3. *Is it true that every $m \in BV_{\mathrm{div}}(\Omega, S^1)$ satisfies $m \in SBV$?*

This question is related with a recent work of Bianchini–DeLellis–Robyr [9]: They show that the viscosity solution ψ of a Hamilton–Jacobi equation $H(\nabla\psi) = 0$ in Ω (with a uniformly convex hamiltonian H) satisfies $\nabla\psi \in SBV$. Open Problem 3 asks whether for the particular case of the eikonal equation (2.3), the result in [9] still holds when replacing the assumption of viscosity solution with the hypothesis of a general solution ψ of (2.3) with $\nabla\psi \in BV$.

In the following, we focus on line-energies, i.e. energy functionals that concentrate on the jump set of $m \in BV_{\mathrm{div}}(\Omega, S^1)$:

$$\mathcal{I}_f(m) := \int_{J(m)} f(|m^+ - m^-|)d\mathcal{H}^1.$$

We only consider energy densities that depend on the jump size $|m^+ - m^-|$ via a *cost function* $f : [0, 2] \to \mathbf{R}_+$ which satisfies $f(0) = 0$ and is assumed to be *lower semicontinuous*. Notice that if $\theta(x)$ is the "wall angle" of the jump of m at $x \in J(m)$, then $|m^+(x) - m^-(x)| = 2|\sin\theta(x)|$. Since m is of vanishing divergence, the trace of the normal component $m \cdot n$ is well-defined on $\partial\Omega$ and we will consider the minimization problem in the subset

$$\mathcal{S}_0(\Omega) = \{m \in BV_{\mathrm{div}}(\Omega, S^1) : m \cdot n = 0 \text{ on } \partial\Omega\}$$

(see Fig. 2).

Our problem can be equivalently interpreted in terms of the stream function $\psi : \Omega \to \mathbf{R}$ associated to $m = \nabla^\perp\psi \in \mathcal{S}_0(\Omega)$. Then the above variational principle turns in analyzing the following energy functional

$$\int_{J(\nabla\psi)} f(|(\nabla\psi)^+ - (\nabla\psi)^-|)d\mathcal{H}^1 \tag{5.1}$$

over the set of solutions of the Dirichlet problem associated to the eikonal equation

$$|\nabla\psi| = 1 \quad \text{in } \Omega \quad \text{and} \quad \psi = 0 \quad \text{on } \partial\Omega.$$

The method of characteristics shows that for a simply-connected bounded domain there is no smooth solution of the eikonal equation $|\nabla\psi| = 1$ in Ω satisfying the constaint $\psi = 0$ on $\partial\Omega$. Typical singularities are jump discontinuities of $\nabla\psi$ (equivalently of m) through line-singularities or vortices.

5.1. *Motivation*

Line-energy functionals $\mathcal{I}_f$ appear as natural candidates for the asymptotic energy of family of singularly perturbed functionals $\{G_\varepsilon\}_{\varepsilon\downarrow 0}$,

$$G_\varepsilon(m_\varepsilon) = \varepsilon\int_\Omega |\nabla m_\varepsilon|^2 + \frac{1}{\varepsilon}\int_\Omega g(|1 - |m_\varepsilon|^2|), \tag{5.2}$$

defined for $m_\varepsilon \in H^1(\Omega, \mathbf{R}^2)$ satisfying the constraints $\nabla \cdot m_\varepsilon = 0$ in Ω. One can eventually impose a boundary condition $m_\varepsilon \cdot n = 0$ on $\partial\Omega$. Here, $\varepsilon > 0$ is a small parameter and $g : \mathbf{R}_+ \to \mathbf{R}_+$ is some lower semicontinuous function such that

$g(0) = 0$ and $g(t) > 0$ for $t > 0$. Variational models (5.2) arise in several physical applications such as smectic liquid crystals, film blisters or convective pattern formation (see e.g. [4, 64, 50, 42]).

Observe that the vector fields m_ε in (5.2) are not S^1-valued but their distance to S^1 is penalized by the second term of G_ε. As ε tends to 0, we expect that families $\{m_\varepsilon\}$ of uniformly bounded energies (5.2) will converge (up to extraction and in a certain topology, see below) to some limit m_0 satisfying (2.1).

A natural question arises: If $\mathcal{I}_f$ is indeed the asymptotic energy of $\{G_\varepsilon\}$ as $\varepsilon \to 0$, what is the relation between the energy density f and the function g? The ansatz consists in reducing the 2D variational problem to a 1D asymptotic analysis: Assume that m_0 is of bounded variation and satisfies (2.1), i.e. $m_0 \in BV_{\mathrm{div}}(\Omega, S^1)$. We also assume that at level $\varepsilon > 0$ the energy $G_\varepsilon(m_\varepsilon)$ concentrates on 1D transition layers of length scale ε through the jump line-singularities of m_0. With the above notation, let x_0 be a jump point of m_0, θ_0 be the "wall angle" defining the jump $m_0^\pm(x_0)$ and ν_0 be the orientation of the jump set at x_0 (see Fig. 5). At level $\varepsilon > 0$, a 1D transition layer in the direction ν_0 has the form

$$m_\varepsilon(x_0 + t\nu_0) = \cos\theta_0 \nu_0 + u\left(\frac{t}{\varepsilon}\right)\nu_0^\perp,$$

where $u : \mathbf{R} \to \mathbf{R}$ is the rescaled profile of the tangential component of the layer satisfying $u(s) \xrightarrow{\pm s\uparrow\infty} \pm\sin\theta_0$. (Observe that a divergence-free 1D transition layer has a constant normal component.) Using this ansatz, we obtain that the limit energy is given by $\mathcal{I}_f$ with the cost function computed as follows:

$$\begin{aligned} f(|2\sin\theta_0|) &= \min\left\{\int_{\mathbf{R}}\left(\left|\frac{du}{ds}(s)\right|^2 + g(|\sin^2\theta_0 - u^2(s)|)\right)ds : u : \mathbf{R}\to\mathbf{R},\right.\\ &\qquad\qquad \left. u \xrightarrow{\pm s\uparrow\infty} \pm\sin\theta_0\right\}\\ &= 4\int_0^{\sin\theta_0}\sqrt{g(\sin^2\theta_0 - u^2)}\,du, \quad \theta_0 \in \left[0, \frac{\pi}{2}\right], \end{aligned} \tag{5.3}$$

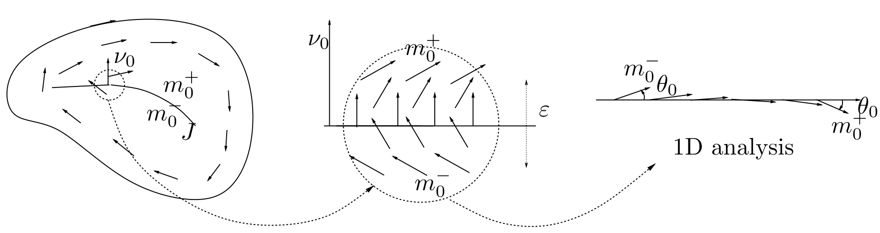

Fig. 5. 1D ansatz: A line-singularity of a limit configuration m_0 (left picture) is regularized by a smooth 1D transition layer at the level $\varepsilon > 0$ connecting two limit states $m_0^\pm$ (middle picture). The full transition occurs in the normal direction ν_0 as represented in the right picture.

which yields the connection between f and g. In particular, every power function $f(t) = t^p$ corresponds to $g(t) = ct^{p-1}$ in (5.3) where the constant $c = c(p)$ depends only on p.

For $g(t) = t^2$, the above ansatz is known to be relevant. The corresponding functional (5.2) has been introduced by Aviles and Giga [4] and we will explain in Sec. 6.2 why $\mathcal{I}_f$ with $f(t) = \frac{t^3}{3}$ (given by (5.3)) is indeed the asymptotic energy of $\{G_\varepsilon\}$ (in the sense of Γ-convergence in the strong L^1-topology). However, let us stress that for a general function g, the above 1D ansatz may be wrong. Indeed, in some cases, it is possible to decrease strictly the energy by substituting 2D mesoscopic structures with 1D transition layers. In these cases, the 1D asymptotic energy $\mathcal{I}_f$ (with f given by (5.3)) does not match the 2D Γ-limit energy of (5.2). Such counterexamples are obtained with functionals $\mathcal{I}_f$ that are not lower-semicontinuous (see Definition 2 below). Indeed, a Γ-limit functional over a metric space (which is the space L^1 in our case) must be lower semicontinuous with respect to the induced topology. A first counterexample is given in [2]: It is shown that power functions $f(t) = t^p$ lead to non-lower semicontinuous functional $\mathcal{I}_f$ for $p > 3$. A second counterexample is described in [1]: The cost function $f_{ARS}(2\sin\theta) = \sin\theta - \theta\cos\theta$ for $0 \le \theta \le \frac{\pi}{2}$ (stemmed from the energy of 1D transition layers associated to a particular asymptotics of the micromagnetic energy). It turns out that $\mathcal{I}_{f_{ARS}}$ is not lower semicontinuous. In both cases it is possible to build a 2D mesoscopic structure with length scale $\eta \ll 1$ between two limit states m^- and m^+ with an energetic cost strictly smaller than the cost of a direct 1D jump. An example of such 2D structure is described in [1] (see Fig. 6) and stands for the cross-tie wall pattern in micromagnetics.

5.2. *Lower semicontinuity*

As explained above, lower semicontinuity implies the optimality of the 1D structure, i.e. it is not possible to decrease the energy of a (direct) jump by constructing 2D

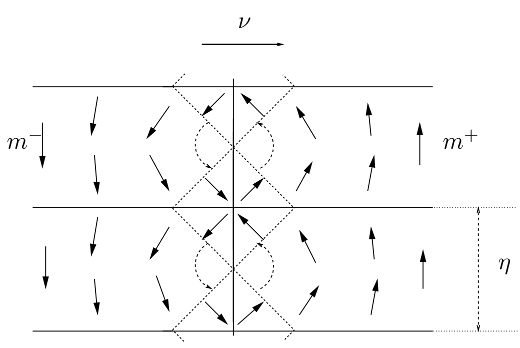

Fig. 6. A cross-tie wall. As $\eta \downarrow 0$, the 2D microstructure tends to a jump configuration (m^-, m^+) in direction ν and has less energy than the initial cost $f_{ARS}(2)$ corresponding to the 1D jump $m^\pm$ of angle $\theta = 90°$.

mesoscopic structures. So it is important to characterize cost functions f such that the line-energy $\mathcal{I}_f$ is lower semicontinuous in a relevant functional space. In general, the weak BV-topology is too strong for this aim; due to applications (see Sec. 6), it is natural to weaken the regularity by using the topology of L^1. Of course, in order for the constraint $|m_0| = 1$ to be stable under convergence, we need to use the strong L^1-topology. Then, let us extend the functional $\mathcal{I}_f$ in $L^1(\Omega, \mathbf{R}^2)$ by $+\infty$, i.e.

$$\mathcal{I}_f(m) = +\infty \quad \text{if } m \in L^1(\Omega, \mathbf{R}^2)\backslash BV_{\text{div}}(\Omega, S^1)$$

and let us introduce the relaxed functional $\overline{\mathcal{I}_f}$, i.e. the lower semicontinuous envelope of $\mathcal{I}_f$ with respect to the strong L^1-topology: $\overline{\mathcal{I}_f} : L^1(\Omega, \mathbf{R}^2) \to \mathbf{R} \cup \{+\infty\}$ is defined as

$$\overline{\mathcal{I}_f}(m) = \inf \left\{ \liminf_{k\to\infty} \mathcal{I}_f(m_k) : m_k \to m \text{ strongly in } L^1 \right\}, \quad \forall\, m \in L^1(\Omega, \mathbf{R}^2).$$

Obviously, $\overline{\mathcal{I}_f} \leq \mathcal{I}_f$ and all configurations of finite relaxed energy $\overline{\mathcal{I}_f}(m) < +\infty$ belong to

$$\mathcal{L}(\Omega) = \{m \in L^1(\Omega, \mathbf{R}^2) : |m| = 1 \text{ and } \nabla \cdot m = 0 \text{ in } \Omega\}$$

which is a closed set in L^1. Recall that the normal component of $m \in \mathcal{L}(\Omega)$ at the boundary $\partial\Omega$ is well-defined. In particular,

$$\mathcal{L}_0(\Omega) = \{m \in \mathcal{L}(\Omega) : m \cdot n = 0 \text{ on } \partial\Omega\} \tag{5.4}$$

is a closed subset of $\mathcal{L}(\Omega)$.

Definition 2. We say that the line-energy $\mathcal{I}_f : L^1(\Omega, \mathbf{R}^2) \to \mathbf{R} \cup \{+\infty\}$ is *lower semicontinuous* (*l.s.c.*) if $\mathcal{I}_f(m) = \overline{\mathcal{I}_f}(m)$ for every $m \in BV_{\text{div}}(\Omega, S^1)$.

Remark 8. The above definition is weaker than asking for $\mathcal{I}_f$ to be lower semicontinuous in L^1 (i.e. $\mathcal{I}_f = \overline{\mathcal{I}_f}$ in $L^1(\Omega, \mathbf{R}^2)$). Indeed, for the Aviles–Giga model with cubic jump costs, it is proved in [2] that $\mathcal{I}_{t\mapsto t^3}(m) = \overline{\mathcal{I}}_{t\mapsto t^3}(m)$ for every $m \in BV_{\text{div}}(\Omega, S^1)$ (so, $\mathcal{I}_{t\mapsto t^3}$ is lower semicontinuous after Definition 2), but one can construct a limit configuration $m_0 \in L^1\backslash BV$ with finite relaxed energy $\overline{\mathcal{I}}_{t\mapsto t^3}(m_0) < +\infty = \mathcal{I}_{t\mapsto t^3}(m_0)$. The crucial point in the construction of m_0 relies on the cubic cost of small jumps of m_0 in $\mathcal{I}_{t\mapsto t^3}$ that cannot control the linear cost of the jump part of Dm_0. Therefore, finite limit energy configurations m_0 do not belong in general to BV; however, m_0 always shares the structure of BV functions, in particular, an equivalent notion of jump set can be defined for m_0 (see [20]).

A first result states the following necessary condition: In order for the line-energy functional $\mathcal{I}_f$ to be lower semicontinuous, the cost function f should also be lower semicontinuous.

Proposition 9. (Ignat–Merlet [43]) *Let* $f : [0, 2] \to \mathbf{R}_+$ *be a measurable function. If* $\mathcal{I}_f$ *is lower semicontinuous, then* f *is lower semicontinuous on* $[0, 2]$.

Recall that Aviles and Giga [6] proved that $\mathcal{I}_{t\mapsto t^3}$ is lower semicontinuous and afterwards, Ambrosio, De Lellis and Mantegazza [2] established that $\mathcal{I}_f$ is not lower semicontinuous for power cost functions $f(t) = t^p$ with $p > 3$. We address the following question raised in [2].

Conjecture 1. *$\mathcal{I}_f$ is lower semicontinuous for power cost functions $f(t) = t^p$ if $1 \leq p < 3$.*

First of all, we give a partial positive answer to this question: The behavior as a power function t^p for $1 \leq p \leq 3$ at the origin $t = 0$ is natural for appropriate cost function.

Theorem 4. (Ignat–Merlet [43]) *For every $p \in [1, 3]$, there exists an appropriate cost function $f : [0, 2] \to \mathbf{R}_+$ such that $f(t) = t^p$ for $t \in [0, \sqrt{2}]$ and $\mathcal{I}_f$ is lower semicontinuous.*

We mention that our method does not work for $p < 1$, therefore we do not know if the condition $p \geq 1$ is a necessary condition in Conjecture 1.

Next, we will establish a positive answer to Conjecture 1 for $p = 2$. Our interest for this case has a physical motivation, associated with the study of the energetic behavior of Bloch walls in micromagnetics as we will explain in Sec. 6.2.

Theorem 5. (Ignat–Merlet [43]) *If $f(t) = t^2$, then $\mathcal{I}_f$ is lower semicontinuous.*

In fact the quadratic cost function stated in Theorem 5 is a particular case of a large family of cost functions that we will introduce via entropies in Sec. 5.3 and which induce lower semicontinuous line-energies.

5.3. *Cost functions*

The concept of entropies introduced in Sec. 3 reveals to be fundamental for cost functions f leading to l.s.c. functionals $\mathcal{I}_f$. More precisely, we will associate an appropriate cost function to every subset of entropies $S \subset ENT$:

Definition 3. For a subset $S \subset ENT$, we define the cost function $c_S : [0, 2] \to \mathbf{R}_+$ by

$$c_S(t) := \sup\{[\Phi(z^+) - \Phi(z^-)] \cdot \nu : \Phi \in S, (z^-, z^+, \nu) \in \mathcal{T}, |z^+ - z^-| = t\},$$

where $\mathcal{T}$ defines the set of admissible jump discontinuities:

$$\mathcal{T} := \{(z^-, z^+, \nu) \in (S^1)^3 : (z^+ - z^-) \cdot \nu = 0\}.$$

Remark 9. The set $\mathcal{T}$ is motivated by the structure of jump discontinuities of divergence-free vector fields $m \in BV_{\mathrm{div}}(\Omega, S^1)$. Indeed, one has $(m^+ - m^-) \cdot \nu = 0$ $\mathcal{H}^1$-a.e. on the jump set $J(m)$ oriented by the normal ν with the traces $m^\pm \in L^\infty(J(m), S^1)$. The cost function c_S is non-negative since one can switch from ν to $-\nu$ so that $[\Phi(z^+) - \Phi(z^-)] \cdot \nu \geq 0$.

Observe that these cost functions depend only on the jump size. To be consistent with this isotropic property, we will impose the following geometric constraints on our sets of entropies.

Definition 4. A subset $S \subset ENT$ is *symmetric* if $S = -S$ and it is said to be equivariant if $R^{-1}SR = S$ for every rotation $R \in \mathrm{SO}(2)$. For any subset of entropies $S \subset ENT$, we will denote by

$$\langle S\rangle := \{\pm R^{-1}\Phi R : \Phi \in S, R \in \mathrm{SO}(2)\},$$

the smallest symmetric and equivariant subset of entropies which contains S.

In terms of the bijective correspondence $\varphi \mapsto \Phi$ given by (3.3), the notion of equivariance of S is equivalent to having the set $\{\varphi \in C^\infty_{\mathrm{per}}(\mathbf{R}) : \Phi \in S\}$ invariant by translations. For proving that $\mathcal{I}_{c_S}$ is lower semicontinuous for nonempty symmetric equivariant subsets $S \subset ENT$, we introduce the following functionals (inspired by (3.6)) which generalize Theorem 2.1 in [6].

Definition 5. Let $S \subset ENT$. We define $\mathcal{E}_S : L^1(\Omega, \mathbf{R}^2) \to \bar{\mathbf{R}}$ by

$$\mathcal{E}_S(m) := \sup\left\{\sum_{i=1}^n \langle \mu_{\Phi_i}(m), \alpha_i\rangle : n \geq 0, (\Phi_i, \alpha_i) \subset S \times C_c^\infty(\Omega, \mathbf{R}_+),\right.$$
$$\left.\sum_{i=1}^n \alpha_i \leq 1\right\} \quad \text{if } m \in \mathcal{L}(\Omega);$$

otherwise, we set $\mathcal{E}_S(m) = +\infty$ for $m \in L^1(\Omega, \mathbf{R}^2)\backslash\mathcal{L}(\Omega)$.

As a supremum of continuous functionals over L^1, this new energy $\mathcal{E}_S$ is lower semicontinuous with respect to the strong L^1 topology. In the above definition we use a partition of unity to localize the entropy production. In particular, in the neighborhood of a jump discontinuity $x \in J(m)$ of $m \in BV_{\mathrm{div}}(\Omega, S^1)$, we can choose a sequence of entropies maximizing the local entropy production as in the definition of $c_S(|m^+(x) - m^-(x)|)$. Using this property, we prove that $\mathcal{E}_S$ coincides with $\mathcal{I}_{c_S}$ on $BV_{\mathrm{div}}(\Omega, S^1)$:

Theorem 6. (Ignat–Merlet [43]) *Let $S \subset ENT$ be nonempty, symmetric and equivariant. For every $m \in BV_{\mathrm{div}}(\Omega, S^1)$, we have*

$$\mathcal{E}_S(m) = \mathcal{I}_{c_S}(m) = \overline{\mathcal{I}_{c_S}}(m).$$

In particular, $\mathcal{I}_{c_S}$ is lower semicontinuous and $\mathcal{E}_S \leq \overline{\mathcal{I}_{c_S}}$ in $L^1(\Omega, \mathbf{R}^2)$.

We deduce that the class of cost functions in Definition 3 leads to lower semicontinuous line-energy functionals. Finally, for proving Theorems 4 and 5 we will construct a subset $S \subset ENT$ so that $f = c_S$. Let us give some examples. The simplest case is given by sets $S = \langle\Phi\rangle$ generated by a single entropy $\Phi \in ENT$. If

$\lambda(\theta) = \frac{d}{d\theta}\Phi(z) \cdot z^\perp$ (as in (3.4)), then the combination of (3.7) and Definition 3 leads to

$$c_{\langle\Phi\rangle}(2\sin\beta) = \sup_{x\in[0,2\pi]} |\lambda \star \sin_\beta|(x), \quad \beta \in \left[0, \frac{\pi}{2}\right]. \tag{5.5}$$

We obtained a criteria depending on λ that computes the supremum in (5.5): If λ is an odd π-periodic function and its restriction to $(0, \frac{\pi}{2})$ is convex and even with respect to $\frac{\pi}{4}$, then the supremum in (5.5) is achieved at $x = 0$ so that

$$c_{\langle\Phi\rangle}(2\sin\beta) = -2\int_0^\beta \lambda(\theta)\sin(\theta)d\theta.$$

In particular, this criteria leads to the cost functions mentioned in Examples 1 and 2 below, corresponding to the Aviles–Giga and "cross-tie wall" models.

Example 1. (Aviles–Giga cost function) There exists a subset $S_1 = \langle\{\Phi_1\}\rangle \subset$ *ENT* generated by one entropy $\Phi_1(z) = \frac{4}{3}(z_2^3, z_1^3)$ for $z \in S^1$ (i.e. $\lambda_1(\theta) = -6\sin(2\theta)$ in (3.4)) such that $c_{S_1}(t) = \frac{t^3}{3}$ for $t \in [0, 2]$.

Example 2. ("Cross-tie wall" cost function) There exists a subset $S_2 = \langle\{\Phi_2\}\rangle \subset$ *ENT* generated by one entropy $\Phi_2 \in C^{1,1}(S^1, \mathbf{R}^2)$ (i.e. λ_2 in (3.4) is a π-periodic odd function given by $\lambda_2(\theta) = |\theta - \frac{\pi}{4}| - \frac{\pi}{4}$ on $(0, \frac{\pi}{2})$) such that

$$c_{S_2}(2\sin\theta) = \begin{cases} \sin\theta - \theta\cos\theta & \text{if } 0 \le \theta \le \dfrac{\pi}{4}, \\ \sqrt{2} - \left(\dfrac{\pi}{2} - \theta\right)\cos\theta - \sin\theta & \text{if } \dfrac{\pi}{4} < \theta \le \dfrac{\pi}{2}. \end{cases}$$

For these examples, the corresponding entropies have been introduced in [50] and [1] respectively. Obviously, not all appropriate cost functions can be associated to subsets of entropies generated by only one entropy. For example, if $c_S(t) = t^2$ for every $t \in [0, 2]$, we are compelled to construct a subset S generated by an infinite family of entropies.

Conjecture 2. *Is it true that every lower semicontinuous line-energy $\mathcal{I}_f$ has the form $\mathcal{I}_{c_S}$ for some subset of entropies $S \subset ENT$?*

Remark 10. One can address problem (5.1) for higher dimensions $N \ge 3$. In this case, DeLellis proved in [19] that the power function $f(t) = t^3$ (in the Aviles–Giga model) does not lead anymore to a lower semicontinuous hypersurface-energy as in the two-dimensional case. The microscopic structure breaking the one-dimensional ansatz considered in [19] can be adapted to other power functions $f(t) = t^p$. Also we highlight the fact that our approach for treating lower semicontinuous line-energies via entropy method cannot be extended to hypersurface-energy functionals if $N \ge 3$. In fact, for $N = 3$, the only entropies associated to the system of conservation laws generated by

$$v : \Omega \subset \mathbf{R}^3 \to \mathbf{R}^3, \quad |v| = 1 \quad \text{and} \quad \nabla \times v = 0 \quad \text{in } \Omega \tag{5.6}$$

are the trivial entropies. Let us explain this fact. If $v = (v_1, v_2, v_3)$ is a smooth solution of (5.6), then one has

$$\begin{cases} \partial_{x_1} v_2 - \partial_{x_2} v_1 = 0, \\ \partial_{x_1} v_3 - \partial_{x_3} v_1 = 0. \end{cases}$$

Write $U := (v_2, v_3)$. Since $|v| = 1$, we have that $v_1 = \pm(1 - |U|^2)^{\frac{1}{2}} =: F(U)$. Denoting the diagonal matrix $A(U) = (A_1(U), A_2(U)) = -F(U)\mathrm{Id}$, we deduce the following 2D system of conservation laws:

$$\partial_t U + \nabla_s \cdot [A(U)] = 0, \tag{5.7}$$

where $t := x_1$ and $(s_1, s_2) := (x_2, x_3)$ stand for the (time, space) variables and $\nabla_s \cdot [A(U)] = \partial_{s_1}[A_1(U)] + \partial_{s_2}[A_2(U)]$. The pair (entropy, entropy-flux) is defined as a couple (η, Q) with $\eta : \mathbf{B}^2 \to \mathbf{R}$ and $Q = (Q_1, Q_2) : \mathbf{B}^2 \to \mathbf{R}^2$ that satisfies the compatibility identities:

$$\partial_{U_i} Q_j = \partial_{U_i} A_j \cdot \nabla_U \eta \quad \text{in } \mathbf{B}^2 \text{ and for } i, j = 1, 2, \tag{5.8}$$

where $\mathbf{B}^2 = \overline{B^2}$ is the closed unit disk in $\mathbf{R}^2$. It entails that for every smooth solution U of (5.7), we have a vanishing entropy production:

$$\partial_t[\eta(U)] + \nabla_s \cdot [Q(U)] = 0.$$

(This follows by multiplying (5.7) with $\nabla \eta(U)$.) Then we have the following result:

Lemma 1. *If (η, Q) is a smooth couple (entropy, entropy-flux) in the open disk B^2 satisfying (5.8), then the entropy η is an affine function, i.e. $D^2\eta \equiv 0$ in B^2.*

Proof. Since A is a diagonal matrix valued map, by (5.8), we deduce that for every point $U \in B^2$ (i.e. $|U| < 1$), $\partial_{U_i} Q_j(U) = -\partial_{U_j}\eta(U)\partial_{U_i}F(U)$, $i, j = 1, 2$. Then, by the Schwarz theorem, i.e. $\partial_{U_j}\partial_{U_i} Q_k(U) = \partial_{U_i}\partial_{U_j} Q_k(U)$, $i, j, k = 1, 2$, it follows that

$$U_1 \partial_{U_1 U_2} \eta(U) = U_2 \partial_{U_1 U_1} \eta(U), \tag{5.9}$$

$$U_2 \partial_{U_1 U_2} \eta(U) = U_1 \partial_{U_2 U_2} \eta(U). \tag{5.10}$$

Differentiating (5.9) in U_2 and (5.10) in U_1 respectively, by summation, we obtain that $\Delta\eta(U) = 0$. Assume now that $U_1, U_2 \neq 0$. Then dividing (5.9) by U_2 and (5.10) by U_1 respectively, by summation, we deduce that

$$\left(\frac{U_1}{U_2} + \frac{U_2}{U_1}\right) \partial_{U_1 U_2} \eta(U) = \Delta\eta(U) = 0$$

which entails that $\partial_{U_1 U_2}\eta(U) = 0$ and then, by (5.9) and (5.10), it implies that $D^2\eta(U) = 0$ for every $U \in B^2$ with $U_1, U_2 \neq 0$. By hypothesis, η is smooth so that we conclude $D^2\eta \equiv 0$ in B^2, i.e. η is an affine function. $\square$

5.4. *Existence of minimizers for relaxed line-energies*

Now we deal with a second issue: The existence of minimizers of the relaxed energy functional $\overline{\mathcal{I}_f}$ under certain boundary conditions. (Without imposed boundary conditions, the problem is trivial, $\overline{\mathcal{I}_f}$ has vanishing minimal value and every constant unit vector field is a minimizer.) We impose the following boundary condition $m \cdot n = 0$ on $\partial\Omega$ to our configurations m, so we are looking for minimizers in $\mathcal{L}_0(\Omega)$ (see (5.4)). Suppose that the cost function f is equal to c_S for some subset $S \subset ENT$. Then the relative compactness in L^1 of the sublevel sets of $\overline{\mathcal{I}_f}$ would imply the existence of minimizers of the relaxed functional $\overline{\mathcal{I}_f}$ in $\mathcal{L}_0(\Omega)$. For that, one should be able to rule out oscillations for configurations of uniformly bounded energy. It turns out that this statement holds true if the symmetric and equivariant set,

$$S_f := \{\Phi \in ENT : [\Phi(z^+) - \Phi(z^-)] \cdot \nu \leq f(|z^+ - z^-|), \forall\, (z^-, z^+, \nu) \in \mathcal{T}\},$$

composed of the admissible entropies associated with f, is large enough. More precisely, we will obtain compactness if

$$t^3 \lesssim f(t) \quad \text{in } [0, 2] \tag{5.11}$$

(see Theorem 7 below) which means in fact that up to multiplicative constants, S_f coincides with ENT, i.e. $\mathbf{R}S_f = ENT$.

Remark 11. Note that $c_{S_f} \leq f$ in $[0, 2]$ and S_f is the maximal subset of ENT such that this inequality holds.

Theorem 7. (Ignat–Merlet [43]) *Let f be a cost function such that* $\inf_{t\in(0,2]} \frac{f(t)}{t^3} > 0$ *and $c_{S_f} = f$. Then $\overline{\mathcal{I}_f}$ (respectively, $\mathcal{E}_{S_f}$) admits at least one minimizer over $\mathcal{L}_0(\Omega)$.*

It means that a minimizer $m \in \mathcal{L}_0(\Omega)$ of $\overline{\mathcal{I}_f}$ can be written as a limit of a sequence $\{m_k\}$ in $\mathcal{S}_0(\Omega)$ such that $\overline{\mathcal{I}_f}(m) = \lim_k \mathcal{I}_f(m_k)$. However, we do not know whether these minimizers m belong to $\mathcal{S}_0(\Omega)$, in other words, we do not know if $\mathcal{I}_f$ admits a minimizer over $\mathcal{S}_0(\Omega)$.

Remark 12. The existence result in Theorem 7 is still valid if we replace $\mathcal{L}_0(\Omega)$ by any closed subset of $\mathcal{L}(\Omega)$. But this does not cover the case of general Dirichlet boundary conditions. However, the following strategy can be adopted for Dirichlet boundary condition $m = u_{\mathrm{bd}}$ on $\partial\Omega$. If we can extend $u_{\mathrm{bd}} : \partial\Omega \to S^1$ as a divergence-free vector field $u \in BV(O, S^1)$ for some smooth open set $O \supset \bar{\Omega}$, then the argument in Theorem 7 shows the existence of minimizers of the functional $F(m) := \mathcal{I}_f(m; O) - \mathcal{I}_f(u; O\backslash\bar{\Omega})$ in the closed set

$$\{m \in \mathcal{L}(O) : m \equiv u \text{ a.e. in } O\backslash\bar{\Omega}\}.$$

Observe that finite energy configurations $F(m) < \infty$ satisfy $m \in BV(O, S^1)$, $m \cdot n = u_{\mathrm{bd}} \cdot n$ $\mathcal{H}^1$-a.e. on $\partial\Omega$ (since m is of vanishing divergence) and the jump of the tangential component $[m \cdot n^\perp]$ on $\partial\Omega$ is penalized through $F(m)$ by the boundary term:

$$\int_{\partial\Omega} f(|m^+ - m^-|)d\mathcal{H}^1,$$

where $m^\pm$ denote the inner and outer traces of m on $\partial\Omega$ with respect to n (here, $m^+ = u_{\mathrm{bd}}$ on $\partial\Omega$). The minimizing problem does not depend on the extended domain O or on the extension vector field u.

5.5. *Viscosity solution*

We are also interested in the minimization problem under the more restrictive boundary condition $m = n^\perp$ on $\partial\Omega$. This condition makes sense for $m \in BV$ and defines a new subset of $\mathcal{S}_0(\Omega)$:

$$\mathcal{S}_\perp(\Omega) := \{m \in \mathcal{S}_0(\Omega) : m = n^\perp \text{ on } \partial\Omega\}.$$

For configurations in this set, no change of orientation is allowed along the boundary. The motivation comes from micromagnetics where the boundary vortices are strongly penalized in certain asymptotic regimes (see Sec. 7.2).

The natural question in this context is whether the minimizer of $\mathcal{I}_f$ over $\mathcal{S}_\perp(\Omega)$ exists and is associated to the viscosity solution of the Dirichlet problem for the eikonal equation, i.e. letting ψ_* be the distance function to the boundary

$$\psi_* = \mathrm{dist}(x, \partial\Omega),$$

we will always denote the corresponding map in $\mathcal{S}_\perp(\Omega)$ by

$$m_* = \nabla^\perp \mathrm{dist}(x, \partial\Omega). \tag{5.12}$$

We will still call m_* the *viscosity solution* on Ω (or Landau state in micromagnetic jargon). In relation with (5.1), this amounts to considering stream functions ψ satisfying $m = \nabla^\perp\psi \in BV(\Omega, S^1)$ and the boundary conditions $\psi = 0$ and $\frac{\partial\psi}{\partial n} = -1$ $\mathcal{H}^1$-a.e. on $\partial\Omega$.

In [50], Jin and Kohn suggested that when the domain Ω is convex, the viscosity solution minimizes $\mathcal{I}_f$ in $\mathcal{S}_\perp(\Omega)$ for $f(t) = t^p$, $1 \le p \le 3$. The result is proved for $p = 3$ when Ω is an ellipse in [50]. For $p = 1$ and if Ω a convex polygon, it is proved in [5] that m_* minimizes $\mathcal{I}_f$ over the set $\{m \in \mathcal{S}_\perp(\Omega) : \nabla m \text{ is piecewise constant}\}$. We first give a positive answer in the case of a stadium domain Ω and general appropriate cost functions:

Theorem 8. (Ignat–Merlet [43]) *Let $S \subset ENT$ be nonempty, symmetric and equivariant. We consider the stadium-shaped domain Ω (see Fig. 7)*

$$\Omega = (-L, L) \times (-1, 1) \cup B((-L, 0), 1) \cup B((L, 0), 1),$$

for some $L \ge 0$. Then the viscosity solution m_* minimizes $\mathcal{I}_{c_S}$ over $\mathcal{S}_\perp(\Omega)$.

We also prove positive results for some other special domains not necessarily convex (in particular, ellipse and union of two discs) and some special appropriate

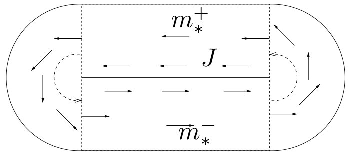

Fig. 7. Stadium shaped domain and the corresponding viscosity solution.

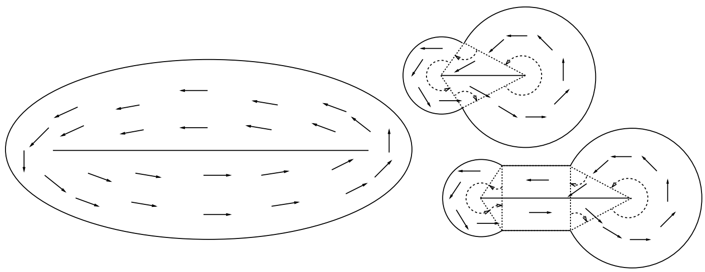

Fig. 8. Viscosity solutions $m_\star$ for an ellipse, the union of two disks, and a bone-shaped domain (with the jump set oriented by $\nu_\star := \mathbf{e}_2$).

cost functions. These results can be extended to the Aviles–Giga model presented in Sec. 5.1. In particular, one has the following result (similar to Proposition 5.1 in [50]):

Theorem 9. *Let $\Omega \subset \mathbf{R}^2$ be an open bounded domain with piecewise Lipschitz boundary $\partial\Omega$ such that the viscosity solution $m_\star = \nabla^\perp \mathrm{dist}(x, \partial\Omega)$ has the jump set J oriented by one fixed direction $\nu_\star$ (see Fig.* 8). *We consider the Aviles–Giga energy*

$$G_\varepsilon(m) = \int_\Omega \left(\varepsilon|\nabla m|^2 + \frac{1}{\varepsilon}(1-|m|^2)^2\right) dx, \quad m \in H^1_{\mathrm{div}}(\Omega, \mathbf{R}^2). \tag{5.13}$$

Then there exists a constant $C = C(\partial\Omega)$ such that for every $\varepsilon > 0$ and $m \in H^1_{\mathrm{div}}(\Omega, \mathbf{R}^2)$ with $m = n^\perp$ on $\partial\Omega$, we have:

$$\frac{1}{3}\int_J |m_\star^+ - m_\star^-|^3 d\mathcal{H}^1 \le G_\varepsilon(m) + \varepsilon C. \tag{5.14}$$

We will present the proof of Theorem 9 in Sec. 6.2.

For nonconvex domains, it is proved in [5] that for power cost functions $f(t) = t^p$ with $p \le \frac{4}{3}$, there exists a nonconvex polygonal domain Ω such that m_* does not minimize $\mathcal{I}_f$ over $\mathcal{S}_\perp(\Omega)$. Moreover, the same counterexamples indicate that for every power cost function with $p > 0$, m_* does not minimize $\mathcal{I}_f$ in $\mathcal{S}_0(\Omega)$. In [50], the authors exhibit a nonconvex Lipschitz domain (a union of two intersecting discs) such that m_* is not a minimizer of $\mathcal{I}_f$ in $\mathcal{S}_\perp(\Omega)$ for every $f(t) = t^p$ with $p \ne 3$; in the case $f(t) = t^3$, m_* is a minimizer of $\mathcal{I}_f$, but it is not unique. It was conjectured in [50] that for some other nonconvex domains, m_* is not a minimizer of $\mathcal{I}_{t\mapsto t^3}$. In

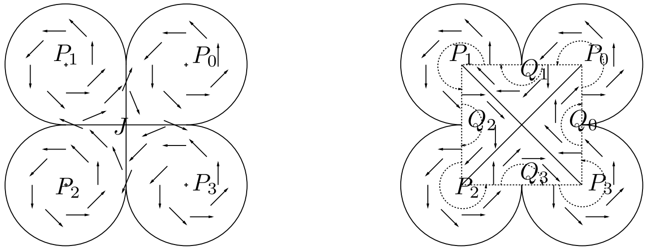

Fig. 9. The configuration $\tilde{m}$ (on the left) is given by "vortex" type vector fields centered at P_k, $k = 1, \dots, 4$. It has less energy $\mathcal{I}_f$ than the viscosity solution m_* (on the right).

the following, we prove this conjecture. In fact, we show a more general fact: There exists a nonconvex domain such that *for any* fixed positive cost function f, the viscosity solution is not optimal in $\mathcal{S}_\perp(\Omega)$.

Theorem 10. (Ignat–Merlet [43]) *There exists a nonconvex piecewise Lipschitz domain Ω such that the viscosity solution is not a minimizer of $\mathcal{I}_f$ over $\mathcal{S}_\perp(\Omega)$ for every lower semicontinuous function $f : [0,2] \to \mathbf{R}_+$ such that $\int_{\sqrt{2}}^{2} f(t)dt > 0$.*

The above domain Ω (a union of four discs and a square, see Fig. 9) is nonsmooth, but universal for every positive cost function f. Moreover, by slightly modifying the boundary of Ω, we can show that the result is not restricted to nonsmooth domains. However, the modified smooth domain is no longer universal with respect to the cost function.

Theorem 11. (Ignat–Merlet [43]) *For every bounded lower semicontinuous function $f : [0,2] \to \mathbf{R}_+$ such that $\int_{\sqrt{2}}^{2} f(t)dt > 0$, there exists a nonconvex $C^{1,1}$ domain Ω such that the viscosity solution is not a minimizer of $\mathcal{I}_f$ over $\mathcal{S}_\perp(\Omega)$.*

6. Generalized Entropies

In the previous section we characterized lower semicontinuous line-energies $\mathcal{I}_f$. For such a line-energy, one may wonder whether $\mathcal{I}_f$ is indeed the Γ-limit of functionals (5.2) (or of some perturbation functional of (5.2)). If this is the case, how entropies can be used in proving the Γ-convergence program (in order to have compactness and lower bounds)?

6.1. *Compactness*

We focus here on the first step in the method of Γ-convergence, i.e. the compactness issue for functionals G_ε in (5.2):

Claim 1. *Any family $\{m_\varepsilon\}_{\varepsilon\downarrow 0} \subset H^1_{\mathrm{div}}(\Omega, \mathbf{R}^2)$ of uniformly bounded energy $G_\varepsilon(m_\varepsilon) \le C$ is relatively compact in $L^1(\Omega)$ and any limit configuration m_0 satisfies* (2.1).

We will assume here the following hypothesis:

$$g(t) \geq Ct^2, \quad \text{for every } t \geq 0, \tag{6.1}$$

where $C > 0$ denotes a generic constant. This assumption is motivated by the following. We want that the energy G_ε asymptotically concentrates on line-energies $\mathcal{I}_f$ as $\varepsilon \to 0$; as discussed in the previous section (see (5.11)), the lower semicontinuity of $\mathcal{I}_f$ is related to the condition $f(t) \geq Ct^3$ (so that $\mathbf{R}S_f = ENT$) and in this case, the 1D ansatz (5.3) suggests (6.1).

Under the assumption (6.1), the compactness issue reduces to the case $g(t) = t^2$ in (5.2), known as the Aviles–Giga model. It is in fact a Ginzburg–Landau model for gradient fields and appears either in solid mechanics, liquid crystals or in micromagnetics (see [13, 33]). It gives rise to a series of articles [50, 6, 2, 26, 17, 66] that justify that $\mathcal{I}_f$ with $f(t) = \frac{t^3}{3}$ (given by (5.3)) is indeed the asymptotic energy of $\{G_\varepsilon\}$ in the sense of Γ-convergence under the strong L^1-topology.

In particular, Claim 1 was proved by Ambrosio, De Lellis and Mantegazza [2] and DeSimone, Kohn, Müller and Otto [26]. The entropy method comes out to be fruitful in this matter, too. We explain here the ideas in [26]. Since the vector fields m_ε are no longer of values in S^1, the strategy used in [26] consists in firstly extending the notion of entropies to maps defined in the whole space $\mathbf{R}^2$:

Definition 6. (DKMO [26]) We will say that $\Phi \in C_c^\infty(\mathbf{R}^2, \mathbf{R}^2)$ is a *DKMO*-entropy if

$$\Phi(0) = 0, \quad D\Phi(0) = 0 \quad \text{and (3.2) holds for all } z \in \mathbf{R}^2.$$

Let us discuss some properties of this extension: First of all, any entropy $\Phi \in ENT$ can be extended at a *DKMO*-entropy by considering

$$\tilde{\Phi}(z) := \rho(|z|)\Phi\left(\frac{z}{|z|}\right) \quad \text{for every } z \in \mathbf{R}^2 \backslash \{0\}, \tag{6.2}$$

where $\rho \in C_c^\infty(\mathbf{R}_+)$ with $\rho(1) = 1$. Indeed, by (3.2), we have that

$$(D\tilde{\Phi}(z)z^\perp) \cdot z = |z|\frac{\partial \tilde{\Phi}}{\partial \theta}(z) \cdot z = |z|\rho(|z|)\frac{d\Phi}{d\theta}\left(\frac{z}{|z|}\right) \cdot z = 0, \quad z \in \mathbf{R}^2.$$

A second property concerns the entropy production: For every *DKMO*-entropy Φ, there exist $\Psi \in C_c^\infty(\mathbf{R}^2, \mathbf{R}^2)$ and $\gamma \in C_c^\infty(\mathbf{R}^2, \mathbf{R})$ such that[c]

$$D\Phi(z) = -2\Psi(z) \otimes z + \gamma(z)\mathrm{Id} \quad \text{for every } z \in \mathbf{R}^2, \tag{6.3}$$

consequently, for every $m \in H^1(\Omega, \mathbf{R}^2)$, the entropy production is given by:

$$\nabla \cdot \{\Phi(m)\} - \gamma(m)\nabla \cdot m = \Psi(m) \cdot \nabla(1 - |m|^2) \quad \text{a.e. in } \Omega \tag{6.4}$$

(see [26]).

[c]The function γ is an extension of the function given in (3.4) to the whole plane $\mathbf{R}^2$.

The main feature of *DKMO*-entropies with respect to Claim 1 is the following: For every *DKMO*-entropies Φ, the family of entropy productions $\{\nabla \cdot [\Phi(m_\varepsilon)]\}_{\varepsilon\downarrow 0}$ is asymptotically bounded as measure for every family $\{m_\varepsilon\}_{\varepsilon\downarrow 0} \subset H^1_{\mathrm{div}}(\Omega, \mathbf{R}^2)$ of uniformly bounded energy. In fact, integration of (6.4) yields (due to (6.1)):

$$\begin{aligned}\limsup_{\varepsilon\to 0} &\left| \int_\Omega \nabla \cdot \{\Phi(m_\varepsilon)\}\zeta \right| \\ &\leq C_\Phi \|\zeta\|_\infty \limsup_{\varepsilon\to 0} G_\varepsilon(m_\varepsilon), \quad \text{for every } \zeta \in C_c^\infty(\Omega), \end{aligned} \tag{6.5}$$

where $C_\Phi = 2\|\nabla\Psi\|_\infty$.

On the one hand, this property yields Claim 1 by a nice combination of the theory of Young measures and the div–curl lemma of Murat and Tartar (see e.g. [72, 62]) applied to families $\{\Phi(m_\varepsilon) \wedge \tilde{\Phi}(m_\varepsilon)\}_{\varepsilon\downarrow 0}$ where $\Phi, \tilde{\Phi} \in C^\infty(\mathbf{R}^2, \mathbf{R}^2)$ are two arbitrary *DKMO*-entropies (see in [26]).

On the other hand, the entropy method also yields the structure of the limiting configurations m_0 (that obviously satisfy (2.1)). First, observe that (6.5) implies that the entropy production $\nabla \cdot [\Phi(m_0)]$ is a measure for every *DKMO*-entropy Φ. Moreover, this property holds true for every entropy $\Phi \in ENT$ (by (6.2)). De Lellis and Otto [20] characterized this class of vector fields m_0 where the entropy production is a measure for every entropy. Essentially, every limiting configuration m_0 shares some structure properties of maps of bounded variation $BV(\Omega)$; in particular it is possible to give a rigorous definition of the jump set $J(m_0)$ as a $\mathcal{H}^1$-rectifiable set so that $\mathcal{I}_f$ makes sense. (A similar result was independently obtained by Ambrosio, Kirchheim, Lecumberry and Rivière [3] using the characterization of m_0 in terms of its phase θ_0.) The main obstacle is that limiting finite-energy configurations m_0 are not in BV as we already mentioned in Remark 8. However, the situation is better if we focus on either zero-energy configurations (see Remark 5) or dilation invariant configurations (see [31]).

Let us now present a *new and easier* proof of Proposition 2 that avoids the properties of lifting of $W^{\frac{1}{p},p}(\Omega, S^1)$ vector fields, but uses the generalized entropies in (6.2).

Proof of Proposition 2. Let $\Phi \in C^\infty(S^1, \mathbf{R}^2)$ be an entropy, i.e. (3.2) holds. We want to prove that if $m \in W^{\frac{1}{p},p}_{\mathrm{div}}(\Omega, S^1)$ (with $p \in [1, 2]$) then (3.5) holds. (For the converse implication we refer to [39] and [43] where an appropriate vortex configuration m is used.) Let $B \subset \Omega$ be a ball inside Ω and $\{\eta_\varepsilon\}_{\varepsilon>0}$ be a family of positive mollifiers. For $\varepsilon > 0$ small enough, we consider the approximation

$$m_\varepsilon = m \star \eta_\varepsilon \text{ in } B.$$

Then $m_\varepsilon \in C^\infty(B, \mathbf{R}^2)$, $\nabla \cdot m_\varepsilon = 0$ and $|m_\varepsilon| \leq 1$ in B. Now let us extend the entropy Φ to a generalized entropy $\tilde{\Phi}$ on $\mathbf{R}^2$ as in (6.2); for that, we consider a smooth function $\rho : [0, \infty) \to \mathbf{R}$ such that $\rho = 0$ on $[0, \frac{1}{2}] \cup [2, \infty)$ and $\rho(1) = 1$ and let $\tilde{\Phi} \in C_c^\infty(\mathbf{R}^2, \mathbf{R}^2)$ be given by (6.2). Therefore, there exist $\Psi \in C_c^\infty(\mathbf{R}^2, \mathbf{R}^2)$ and

$\gamma \in C_c^\infty(\mathbf{R}^2, \mathbf{R})$ such that (6.3) holds, leading by (6.4) to

$$\nabla \cdot [\tilde{\Phi}(m_\varepsilon)] = \Psi(m_\varepsilon) \cdot \nabla(1 - |m_\varepsilon|^2) \quad \text{in } B \tag{6.6}$$

because m_ε is of vanishing divergence in B. The final issue consists in passing to the limit as $\varepsilon \to 0$.

Case 1. $p = 1$. On one hand, the chain rule implies that $\tilde{\Phi}(m_\varepsilon) \to \tilde{\Phi}(m) = \Phi(m)$ in $W^{1,1}(B)$, in particular,

$$\nabla \cdot [\tilde{\Phi}(m_\varepsilon)] \to \nabla \cdot [\Phi(m)] \quad \text{in } L^1(B). \tag{6.7}$$

On the other hand, the chain rule leads to $1 - |m_\varepsilon|^2 \to 1 - |m|^2 = 0$ in $W^{1,1}(B)$, in particular,

$$\nabla(1 - |m_\varepsilon|^2) \to 0 \quad \text{in } L^1(B).$$

Since $\{\Psi(m_\varepsilon)\}$ is uniformly bounded, the duality $\langle \cdot\,, \cdot \rangle_{L^\infty(B), L^1(B)}$ leads to

$$\Psi(m_\varepsilon) \cdot \nabla(1 - |m_\varepsilon|^2) \to 0 \quad \text{in } L^1(B),$$

which by (6.6) and (6.7) yield $\nabla \cdot [\Phi(m)] = 0$ (in $L^1(B)$).

Case 2. $p = 2$. We repeat the above argument using the duality

$$\langle \cdot\,, \cdot \rangle_{\mathbf{H}^{-\frac{1}{2}}(B), H_{00}^{\frac{1}{2}}(B)},$$

where $\mathbf{H}^{-\frac{1}{2}}(B)$ is the dual space of $H_{00}^{\frac{1}{2}}(B)$:

$$H_{00}^{\frac{1}{2}}(B) = \left\{ \zeta \in H^{\frac{1}{2}}(B) : \int_B \int_B \frac{|\zeta(x) - \zeta(y)|^2}{|x - y|^3} dx dy + \int_B \frac{|\zeta(x)|^2}{d(x)} dx < \infty \right\},$$

where $d(x) = \operatorname{dist}(x, \partial B)$. In fact, $H_{00}^{\frac{1}{2}}(B)$ can be seen as the closure of $C_c^\infty(B)$ in $H^{\frac{1}{2}}(\mathbf{R}^2)$ (see e.g. [39] for more details). More precisely, on one hand, the chain rule implies that $\tilde{\Phi}(m_\varepsilon) \to \tilde{\Phi}(m) = \Phi(m)$ in $H^{\frac{1}{2}}(B)$, in particular,

$$\nabla \cdot [\tilde{\Phi}(m_\varepsilon)] \to \nabla \cdot [\Phi(m)] \quad \text{in } \mathbf{H}^{-\frac{1}{2}}(B). \tag{6.8}$$

On the other hand, the chain rule leads to $1 - |m_\varepsilon|^2 \to 1 - |m|^2 = 0$ in $H^{\frac{1}{2}}(B)$, in particular,

$$\nabla(1 - |m_\varepsilon|^2) \to 0 \quad \text{in } \mathbf{H}^{-\frac{1}{2}}(B).$$

Since $\Psi(m_\varepsilon) \to \Psi(m)$ in $H^{\frac{1}{2}}(B)$, we conclude that for every $\zeta \in C_c^\infty(B)$,

$$\langle \nabla(1 - |m_\varepsilon|^2), \zeta \Psi(m_\varepsilon) \rangle_{\mathbf{H}^{-\frac{1}{2}}(B), H_{00}^{\frac{1}{2}}(B)} \to 0,$$

which by (6.6) and (6.8) yield

$$\langle \nabla \cdot [\Phi(m)], \zeta \rangle_{\mathbf{H}^{-\frac{1}{2}}(B), H_{00}^{\frac{1}{2}}(B)} = 0.$$

Hence, $\nabla \cdot [\Phi(m)] = 0$ in $\mathcal{D}'(B)$.

Case 3. $p \in (1,2)$. By Gagliardo–Nirenberg embedding: $L^\infty \cap W^{\frac{1}{p},p} \subset H^{\frac{1}{2}}$ (see [10], Lemma D.1) and thus, one concludes by Case 2.

Since $B \subset \Omega$ was an arbitrarily chosen ball, (3.5) follows in Ω. $\square$

6.2. *Entropies for S^2-valued vector fields. The Aviles–Giga and Bloch wall models*

In this section we will introduce a different extension of entropies *ENT* (than the *DKMO*-entropy) that is adapted for solving the second issue in the Γ-convergence program, i.e. to show that $\mathcal{I}_f$ is a lower bound of (5.2). We treat this issue for slightly more general functionals $E_{\varepsilon,\beta}$ defined for S^2-vector fields $m = (m', m_3) \in H^1(\Omega, S^2)$ (with $m' = (m_1, m_2)$) that are not necessarily divergence-free, but the divergence $\nabla \cdot m = \nabla \cdot m'$ is penalized by the energy $E_{\varepsilon,\beta}$:

$$E_{\varepsilon,\beta}(m) = \int_\Omega \left(\varepsilon|\nabla m|^2 + \frac{1}{\varepsilon} g(m_3^2) + \frac{1}{\beta} ||\nabla|^{-1} \nabla \cdot m|^2 \right) dx,$$

where $\varepsilon > 0$ and $\beta > 0$ are small parameters. We will always assume the following regime

$$\beta = \beta(\varepsilon) \ll \varepsilon \ll 1$$

and that (6.1) holds. (The opposite regime, i.e. $\varepsilon \ll \beta \ll 1$, entails different asymptotic behavior: The energy $E_{\varepsilon,\beta}$ enforces m to take values into S^1 much stronger than satisfying the flux closure condition. This situation is adapted for "cross-tie" walls, see [1, 68, 69].) Notice that $E_{\varepsilon,\beta}$ controls the functional G_ε in (5.2) (for divergence-free configurations): Indeed, the second term coincides for both functionals (since $m_{3,\varepsilon}^2 = 1 - |m'_\varepsilon|^2$), while the first-term in $E_{\varepsilon,\beta}$ controls the one in G_ε since $|\nabla m_\varepsilon| \geq |\nabla m'_\varepsilon|$. Moreover, the compactness issue discussed in the previous section is still valid for uniformly bounded energy configurations $E_{\varepsilon,\beta}(m_\varepsilon) \leq C$ (due to (6.1)).

In order to obtain sharp lower bounds for $E_{\varepsilon,\beta}$ we introduce a class of *generalized entropies* Φ for which the entropy production is controlled by the energy (with constant 1 comparing to (6.5)) up to a perturbation taking the form of a boundary-term. More precisely, we systematically study the particular class of Lipschitz continuous maps $\Phi = (\Phi_1, \Phi_2) \in \mathrm{Lip}(S^2, \mathbf{R}^2)$ and $\alpha \in \mathrm{Lip}(S^2)$ such that for every smooth $m \in C^\infty(\Omega, S^2)$, the following holds:

$$\begin{aligned} &\nabla \cdot \{\Phi(m)\} + \alpha(m) \nabla \cdot m' \\ &\quad \leq \varepsilon |\nabla m|^2 + \frac{1}{\varepsilon} g(m_3^2) + \nabla \cdot \{a_\varepsilon(m) \nabla m\} \quad \text{a.e. in } \Omega, \end{aligned} \tag{6.9}$$

where $\varepsilon > 0$ is a small parameter and $a_\varepsilon(x)$ is a linear operator mapping the tangent plane $(T_x S^2)^2$ into $\mathbf{R}^2$, for every $x \in S^2$. In the language of differential geometry, $x \mapsto a_\varepsilon(x)$ is a section of the vector bundle

$$\mathcal{B} := \{(x, a) : x \in S^2, a \in \mathcal{L}((T_x S^2)^2, \mathbf{R}^2)\}$$

based on S^2 with fiber $\mathcal{L}(\mathbf{R}^4, \mathbf{R}^2)$. Using the natural differential structure, $\mathcal{B}$ is locally diffeomorphic to $\mathbf{R}^2 \times \mathcal{L}(\mathbf{R}^4, \mathbf{R}^2)$. With the induced topology, *we will always assume that the section* $x \mapsto a_\varepsilon(x)$ *is Lipschitz* (in order for (6.9) to make sense). This notion of generalized entropy is inspired by the work of Jin and Kohn [50] on the Aviles–Giga model. The choice of Lipschitz maps is justified below by the study of Bloch walls where the limit line-energies have a quadratic cost in the angle.

Let us first give the connection between generalized entropies for S^2-valued vector fields and the set of entropies ENT.

Proposition 10. (Ignat–Merlet [42]) *Let* $\Phi \in \mathrm{Lip}(S^2, \mathbf{R}^2)$, $\alpha \in \mathrm{Lip}(S^2)$ *and* a_ε *be a Lipschitz section of* $\mathcal{B}$ *such that* (6.9) *holds for every* $m \in C^\infty(\Omega, S^2)$. *Then* (3.2) *holds in the sense that*

$$\frac{d}{d\theta}\Phi(z) \cdot z = 0, \quad \textit{for almost every } z \in S^1, \tag{6.10}$$

where $\frac{d}{d\theta}\Phi(z)$ *denotes the tangential derivative of the restriction* $\Phi|_{S^1}$ *on the horizontal circle* $S^1 := S^1 \times \{0\} \subset S^2$.

Conversely, let $\Phi \in C^\infty(S^2, \mathbf{R}^2)$ *satisfying* (3.2) *and* $\partial_{m_3}\Phi \equiv 0$ *on* S^1 (m_3-*symmetric entropies* $\Phi(m', m_3) = \Phi(m', -m_3)$ *do satisfy this condition*). *Moreover, we assume a stronger restriction on* g *than* (6.1), *i.e. there exists* $K > 0$ *such that* $g(t) \geq Kt$ *for every* $t \in [0, 1]$. *Then there exist a constant* $C > 0$ *and* $\alpha \in C^\infty(S^2)$ *such that* $C\Phi$ *satisfies* (6.9) *with* $a_\varepsilon \equiv 0$ *for every* $m \in C^\infty(\Omega, S^2)$ *and every* $\varepsilon > 0$.

The above proposition justifies the name of generalized entropies. The differences with respect to Definition 1 consist in defining our entropies on S^2 (which is the target manifold of our vector fields m in this subsection) and in asking for Φ to be *only* Lipschitz continuous. Observe that the inequality (6.9) implies the following necessary pointwise bounds on generalized entropies (that hold for every potential $g \geq 0$ on $\mathbf{R}_+$, so that (6.1) is not necessary here).

Lemma 2. (Ignat–Merlet [42]) *Let* $\varepsilon > 0$, $(\Phi = (\Phi_1, \Phi_2), \alpha) \in \mathrm{Lip}(S^2, \mathbf{R}^2) \times \mathrm{Lip}(S^2)$ *and* a_ε *be a Lipschitz section of* $\mathcal{B}$ *such that* (6.9) *holds for every* $m \in C^\infty(\Omega, S^2)$. *For every* $\tau \in [-\pi, \pi)$, *we set*

$$\begin{aligned} \nu_\tau &= (-\sin\tau, \cos\tau, 0) \in S^2 \quad \textit{and} \\ \Psi_\tau &:= \nu_\tau \cdot \Phi = -\sin\tau\Phi_1 + \cos\tau\Phi_2 \in \mathrm{Lip}(S^2). \end{aligned}$$

Then for almost every point $m \in S^2$, *we have*

$$|D\Psi_\tau(m) + \alpha(m)\Pi_m\nu_\tau| \leq 2\sqrt{g(m_3^2)}, \tag{6.11}$$

where $D\Psi_\tau(m) \in T_mS^2$ *is the gradient of* Ψ_τ *at* m *and* Π_m *denotes the orthogonal projection onto* T_mS^2.

Let us now explain how the generalized entropies are used for proving lower bound for $E_{\varepsilon,\beta}$ (under the condition (6.1)). Assume that $E_{\varepsilon,\beta}(m_\varepsilon) \leq C$. As explained before, Claim 1 holds, so we may assume that $m_\varepsilon \to m_0$ in $L^1(\Omega)$ and

m_0 satisfies (2.1). Moreover, using the *DKMO*-entropies, we know that all entropy productions of m_0 are measures so that by [20] we can define the jump set $J(m_0)$ of m_0. The question is whether $\mathcal{I}_f$ is a lower bound (in the sense of Γ-convergence) of $E_{\varepsilon,\beta}$ where f and g are related by (5.3). To simplify the presentation, we focus on the following periodic setting corresponding to a zoom around a jump point $x \in J(m_0)$ of wall angle θ. More precisely, we consider the periodic strip

$$\Omega = \frac{\mathbf{R} \times \mathbf{R}}{\mathbb{Z}}$$

and we consider $m \in H^1_{\mathrm{loc}}(\Omega, S^2)$ with angle transitions imposed by the limit condition at infinity

$$\lim_{x_1 \to \pm\infty} m(x_1, \cdot) = m^{\pm} = (\cos\theta, \pm\sin\theta, 0) \quad \text{in } L^2\left(\frac{\mathbf{R}}{\mathbb{Z}}\right). \tag{6.12}$$

The aim is to obtain the following lower bound: If $\beta = \beta(\varepsilon) \ll \varepsilon \ll 1$, then

$$f(|m^+ - m^-|) \le \liminf_{\varepsilon \downarrow 0} E_{\varepsilon,\beta}(m_\varepsilon); \tag{6.13}$$

in other words, (6.13) is equivalent by proving that one-dimensional transition layers are asymptotically optimal as $\varepsilon \to 0$. For that purpose, we introduce the following notion of adapted triplet:

Definition 7. For $\theta \in (0, \pi)$, we will say that a triplet $(\Phi = (\Phi_1, \Phi_2), \alpha) \in \mathrm{Lip}(S^2, \mathbf{R}^2) \times \mathrm{Lip}(S^2)$ is adapted to the jump (m^-, m^+) if

$$\Phi_1(m^+) - \Phi_1(m^-) = [\Phi(m^+) - \Phi(m^-)] \cdot \mathbf{e}_1 = f(|m^+ - m^-|) \tag{6.14}$$

and there exists $\varepsilon_0 > 0$ such that for every $0 < \varepsilon \le \varepsilon_0$ one can construct a Lipschitz section a_ε of $\mathcal{B}$ for which (6.9) holds for every map $m \in C^\infty(\Omega, S^2)$.

The existence of a triplet $(\Phi = (\Phi_1, \Phi_2), \alpha)$ satisfying (6.9) and (6.14) would solve (6.13). Indeed, notice first that

$$\begin{aligned} \left| \int_\Omega \alpha(m) \nabla \cdot m' \right| &\le \|\nabla \cdot m'\|_{\dot{H}^{-1}(\Omega)} \|\nabla[\alpha(m)]\|_{L^2(\Omega)} \\ &\le \|\nabla \alpha\|_{L^\infty} \sqrt{\frac{\beta}{\varepsilon}} E_{\varepsilon,\beta}(m). \end{aligned} \tag{6.15}$$

Then integrating (6.9) on Ω and taking into account the boundary conditions (6.14), we would deduce (6.13).

Aviles–Giga model. Let us apply this theory to the case of the quadratic potential $g(t) = t^2$ in the Aviles–Giga model. The following generalized entropy was used by Jin and Kohn [50]. The idea comes from the scalar conservation laws where the entropy production through shocks is asymptotically cubic in the limit of small jumps. Therefore, smooth entropies seem to be adapted for the energy G_ε given in

(5.13) defined for vector fields $m \in H^1_{\mathrm{div}}(\Omega, \mathbf{R}^2)$. For that, let $\Phi : \mathbf{R}^2 \to \mathbf{R}^2$ be the following smooth extension of the entropy given in Example 1:

$$\Phi(z) = \left(2z_2(1 - z_1^2) - \frac{2}{3}z_2^3, 2z_1(1 - z_2^2) - \frac{2}{3}z_1^3\right), \quad \forall\, z \in \mathbf{R}^2. \tag{6.16}$$

(Notice that Φ is not a *DKMO*-entropy.) Then setting $\alpha(z) = 4z_1z_2$ for $z = (z_1, z_2) \in \mathbf{R}^2$, one checks that (6.9) holds for the triplet (Φ, α) (as maps defined on $\mathbf{R}^2$) and the section $a_\varepsilon(z)(U, V) = 2\varepsilon z_2(V_1, -U_1)$ with $U = (U_1, U_2) \in \mathbf{R}^2$, $V = (V_1, V_2) \in \mathbf{R}^2$. This means that for smooth maps $m : \Omega \to \mathbf{R}^2$ with $\nabla \cdot m = 0$ in Ω, one has

$$\begin{aligned}\nabla \cdot \{\Phi(m)\} &= 2(1 - |m|^2)(\partial_1 m_2 + \partial_2 m_1)\\ &\le \varepsilon|\nabla m|^2 + \frac{(1 - |m|^2)^2}{\varepsilon} + 2\varepsilon\nabla \cdot \begin{pmatrix} m_2\partial_2 m_1 \\ -m_2\partial_1 m_1\end{pmatrix}.\end{aligned} \tag{6.17}$$

Moreover, (6.14) is satisfied for $f(t) = \frac{t^3}{3}$. Therefore, one obtains (6.13) for G_ε and also, for $E_{\varepsilon,\beta}$; one can extend it to a general domain Ω so that $\mathcal{I}_f$ is a lower bound of G_ε and $E_{\varepsilon,\beta}$.

Remark 13. Let us explain how the formula (6.16) was obtained; this strategy can be used in general when searching for generalized entropies (6.9). Suppose that we are looking for a triplet (Φ, α) satisfying (6.9), i.e. for every $m \in C^\infty(\Omega, \mathbf{R}^2)$,

$$\begin{aligned}&\nabla \cdot \{\Phi(m)\} + \alpha(m)\nabla \cdot m\\ &\quad \le \varepsilon|\nabla m|^2 + \frac{1}{\varepsilon}(1 - |m|^2)^2 + \nabla \cdot \{a_\varepsilon(m)\nabla m\} \quad \text{a.e. in } \Omega,\end{aligned}$$

where $\varepsilon > 0$ is a small parameter and $x \mapsto a_\varepsilon(x)$ is a Lipschitz map from $\mathbf{R}^2$ into the space of linear operators $\mathcal{L}(\mathbf{R}^4, \mathbf{R}^2)$. Then by Lemma 2, we deduce that

$$|\nabla\Phi_1(m) + \alpha(m)\mathbf{e}_1| \le 2|1 - |m|^2| \quad \text{for every } m \in \mathbf{R}^2. \tag{6.18}$$

Also, assume that (6.14) is satisfied, i.e. $\Phi_1(m^+) - \Phi_1(m^-) = \frac{|m^+ - m^-|^3}{3}$ for every jump $m^\pm = (\cos\theta, \pm\sin\theta)$ in direction $\mathbf{e}_1$ with $\theta \in (0, \frac{\pi}{2})$. Then, let us define $\varphi(t) := \Phi_1(\cos\theta, t\sin\theta)$ for $t \in [-1, 1]$. Inequality (6.18) yields

$$\left|\frac{d\varphi}{dt}(t)\right| = \sin\theta|\mathbf{e}_2 \cdot \nabla\Phi_1(\cos\theta, t\sin\theta)| \le 2\sin^3\theta|1 - t^2|, \quad t \in (-1, 1).$$

On the other hand, (6.14) yields

$$0 = -\frac{8}{3}\sin^3\theta + \varphi(1) - \varphi(-1) = \int_{-1}^{1} \left\{\frac{d\varphi}{dt}(t) - 2\sin^3\theta(1 - t^2)\right\} dt \le 0.$$

So the integrand vanishes and we have $\frac{d\varphi}{dt}(t) = 2\sin^3\theta(1 - t^2)$. Consequently, one recovers the formula of Φ_1 in (6.16).

We recall that the Γ-convergence program is not completely solved for the Aviles–Giga model: The difficulty consists in the upper bound construction for admissible configurations m_0 since the recovery sequences have been constructed *only* for BV configurations m_0 (see Conti and De Lellis [17] and Poliakovsky [66]). For general (non-BV) limiting finite-energy configurations m_0, the problem is still open. Another open question consists in proving that the viscosity solution (5.12) is asymptotically a minimizer of energy G_ε as $\varepsilon \to 0$ under the boundary condition $m = n^\perp$ on $\partial\Omega$. We prove now Theorem 9 that answers this question in a particular case:

Proof of Theorem 9. We use the strategy of Jin–Kohn (see Proposition 5.1 in [50]). Let $m : \Omega \to \mathbf{R}^2$ be a smooth map with $\nabla\cdot m = 0$ in Ω and $m = n^\perp$ on $\partial\Omega$ and Φ be the generalized entropy given at (6.16). Using a suitable rotation $R \in \mathrm{SO}(2)$, we may assume that $\nu_\star = \mathbf{e}_1$. Then by (6.17), we have that

$$\int_\Omega \nabla\cdot\{\Phi(m)\}dx \le G_\varepsilon(m) + 2\varepsilon\int_\Omega \nabla\cdot\begin{pmatrix} m_2\partial_2 m_1 \\ -m_2\partial_1 m_1\end{pmatrix}dx. \tag{6.19}$$

Stokes' theorem leads to

$$\int_\Omega \nabla\cdot\begin{pmatrix} m_2\partial_2 m_1 \\ -m_2\partial_1 m_1\end{pmatrix}dx = \int_{\partial\Omega} -m_2\nabla^\perp m_1\cdot n d\mathcal{H}^1 = \int_{\partial\Omega} n_1\partial_\tau n_2 d\mathcal{H}^1 =: C$$

since $\nabla^\perp m_1\cdot n = \partial_\tau m_1$ with $\tau = -n^\perp = -m$ be the tangent vector field at $\partial\Omega$ and the constant C depends only on the geometry[d] of Ω. Also, Stokes' theorem yields

$$\begin{aligned}\int_\Omega \nabla\cdot\{\Phi(m)\}dx &= \int_{\partial\Omega}\Phi(n^\perp)\cdot n d\mathcal{H}^1 = \int_\Omega \nabla\cdot\{\Phi(m_\star)\}dx \\ &\overset{(3.6)}{=} \int_J [\Phi(m_\star^+) - \Phi(m_\star^-)]\cdot\mathbf{e}_1 d\mathcal{H}^1 \overset{(6.14)}{=} \frac{1}{3}\int_J |m_\star^+ - m_\star^-|^3 d\mathcal{H}^1;\end{aligned}$$

hence, (5.14) holds true. In the general case of a vector field $m \in H^1_{\mathrm{div}}(\Omega, \mathbf{R}^2)$ with $m = n^\perp$ on $\partial\Omega$, one can approximate m in strong H^1-topology by smooth vector fields (satisfying the same divergence and boundary constraints) and then (5.14) immediately follows by passing to the limit. $\square$

The model for the Bloch wall. A second application is given by the linear potential $g(t) = t$ and is arising in micromagnetics in the study of Bloch walls, i.e. for every $m \in H^1(\Omega, S^2)$,

$$E_{\varepsilon,\beta}(m) = \int_\Omega \left(\varepsilon|\nabla m|^2 + \frac{1}{\varepsilon}m_3^2 + \frac{1}{\beta}||\nabla|^{-1}\nabla\cdot m|^2\right)dx,$$

where $\beta = \beta(\varepsilon) \ll \varepsilon \ll 1$. The expected line-energy corresponds to a quadratic cost $f(t) = t^2$. This case is more delicate than the Aviles–Giga model, since smooth

[d]For smooth boundary $\partial\Omega$, we have

$$C = -\frac{1}{2}\int_{\partial\Omega}\tau\cdot\partial_\tau n d\mathcal{H}^1 = -\frac{1}{2}\int_{\partial\Omega}\kappa d\mathcal{H}^1,$$

where κ is the curvature of $\partial\Omega$ and we used that $\partial_\tau n = \kappa\tau$.

entropies are no longer suited to quadratic jumps. This motivates our choice of considering generalized entropies with discontinuous gradients.

First, let us mention that Lipschitz *DKMO*-entropies can detect the quadratic costs over the singular set of limiting configurations. This relies on a control of the entropy production by the energy. In fact, this control is obtained using an improvement of inequality (6.5) via the control of $|\nabla m_3|^2$ by the energy density of $E_{\varepsilon,\beta}$. If $\beta \ll \varepsilon \ll 1$, Φ is a *DKMO*-entropy and $m_\varepsilon \in H^1(\Omega, S^2)$, by (6.4) and (6.15) one gets

$$\limsup_{\varepsilon\to 0}\left|\int_\Omega \nabla\cdot\{\Phi(m_\varepsilon)\}\zeta\right| \le \tilde{C}_\Phi\|\zeta\|_\infty \limsup_{\varepsilon\to 0} E_{\varepsilon,\beta}(m_\varepsilon) \quad \text{for every } \zeta \in C_c^\infty(\Omega),$$

where $\tilde{C}_\Phi = \|\Psi\|_\infty$. The advantage of the above inequality consists in having the R.H.S. only dependent on the L^∞-norm of Ψ (controlled by the Lipschitz norm of the *DKMO*-entropy Φ) whereas in (6.5) the constant C_Φ depends on the $C^{1,1}$-norm of Φ. For this reason, if Φ is a Lipschitz continuous map satisfying (3.2) and m_0 is a strong limit of $\{m_\varepsilon\}$ satisfying $\limsup_{\varepsilon\downarrow 0} E_{\varepsilon,\beta}(m_\varepsilon) < \infty$, then $\nabla\cdot\{\Phi(m_0)\}$ is a measure of finite total mass. In [42], we construct a Lipschitz entropy $\Phi = (\Phi_1, \Phi_2)$ that satisfies (6.14) and leads to (6.13) up to a constant. Moreover, we proved that $\mathcal{I}_f$ is a lower bound of $E_{\varepsilon,\beta}$ (up to a constant):

Theorem 12. (Ignat–Merlet [42]) *Let $\Omega \subset \mathbf{R}^2$ be a bounded domain. Assume that the family $\{m_\varepsilon\}_{\varepsilon\downarrow 0} \subset H^1(\Omega, S^2)$ converges to m_0 in $L^1(\Omega)$ and $\beta = \beta(\varepsilon) \ll \varepsilon \ll 1$. Then*

$$\mathcal{I}_f(m_0) \le C \liminf_{\varepsilon\downarrow 0} E_{\varepsilon,\beta}(m_\varepsilon),$$

with some $C > 1$ (in fact, one can choose $C = \sqrt{4+\pi^2}$).

In order to get the desired inequality (6.13) (with $C = 1$), we analyze the existence of adapted triplets. For the 180° Bloch wall (i.e. the biggest possible jump $\theta = \frac{\pi}{2}$), we have a positive answer.

Proposition 11. (Ignat–Merlet [42]) *There exists a smooth triplet $(\Phi = (\Phi_1, \Phi_2), \alpha)$ adapted to the jump $(-\mathbf{e}_2, \mathbf{e}_2)$. Consequently, (6.13) holds for $\theta = \frac{\pi}{2}$.*

For smaller jumps, we only have a partial result. If $m^\pm$ is the jump of angle $\theta \in (0, \frac{\pi}{2})$ in (6.12), we define the spherical cap

$$S_\theta := \{m \in S^2 : m_1 \ge \cos\theta\}$$

and the set of vector fields taking values into the cap S_θ and adapted to the jump (m^-, m^+):

$$\mathcal{C}_\theta := \{m \in H^1_{\text{loc}}(\Omega, S^2) \colon (6.12) \text{ holds and } m(x) \in S_\theta \text{ for a.e. } x \in \Omega\}.$$

Then one can find a triplet $(\Phi = (\Phi_1, \Phi_2), \alpha)$ that is adapted to a jump (m^-, m^+) if we restrict our study to configurations of $\mathcal{C}_\theta$.

Proposition 12. (Ignat–Merlet [42]) *For every $\theta \in (0, \frac{\pi}{2})$ and every $\varepsilon > 0$, there exists a smooth triplet $(\Phi_\theta, \alpha_\theta) \in C^\infty(S_\theta, \mathbf{R}^3)$ and a smooth section a_ε of $\mathcal{B}$ such that* (6.14) *and* (6.9) *hold for every $m \in C^\infty(\Omega, S_\theta)$. Consequently, if $\{m_\varepsilon\} \subset \mathcal{C}_\theta$, then* (6.13) *holds true.*

We remark that there is no general recipe for constructing adapted triplets. However, Lemma 2 gives a very useful tool in this context.

Despite Propositions 11 and 12, we prove in [42] that for small jumps, the necessary conditions in Lemma 2 are not compatible with condition (6.14). Consequently, there is no triplet $(\Phi = (\Phi_1, \Phi_2), \alpha)$ adapted to a fixed small jump for general configurations (when the vector fields cover the entire sphere S^2):

Theorem 13. (Ignat–Merlet [42]) *There exists $\eta > 0$ such that for $0 < \theta < \eta$, there is no triplet $(\Phi = (\Phi_1, \Phi_2), \alpha)$ adapted to the jump (m^-, m^+).*

However, we strongly believe that (6.13) holds for every angle θ. The conjecture that $\mathcal{I}_f$ is the Γ-limit energy of our 2D model is supported by Theorem 5. In other words, it is not possible to asymptotically decrease the energy by substituting a 1D transition layer by a 2D mesoscopic structure obtained by assembling together 1D transition layers. (This does not rule out the possibility of having 2D microscopic structures at smaller scale than ε inside the transition layers). Moreover, numerical simulations performed in the periodic two-dimensional context indicates that the microscopic transition layers (for $\varepsilon > 0$) are indeed one-dimensional.

6.3. *A zigzag pattern*

We analyze here a modified Aviles–Giga model that arises in micromagnetics where the optimal transitions are no longer one-dimensional, but involve two-dimensional microstructure. Even if the limit energy is not of the form $\mathcal{I}_f$, the method of generalized entropies is also fruitful in this case. The model is the following: We define the functional:

$$F_\varepsilon(m) = \int_\Omega \left(\varepsilon |\nabla m|^2 + \frac{1}{\varepsilon} m_2^2 + \frac{1}{\varepsilon^s} ||\nabla|^{-1} \nabla \cdot m|^2 \right) dx,$$

for $\varepsilon > 0$ small, $m \in H^1(\Omega, S^2)$ defined on a domain $\Omega \subset \mathbf{R}^2$ and $s \in (1, 2)$ (this is a technical assumption). Remark that F_ε penalizes the m_2 component comparing to G_ε (or $E_{\varepsilon,\beta}$) penalizing the m_3 component.

Limiting energy. Suppose that we have a family of maps $m_\varepsilon \in H^1(\Omega, S^2)$ with

$$\limsup_{\varepsilon \downarrow 0} F_\varepsilon(m_\varepsilon) < \infty. \tag{6.20}$$

What can we say about the asymptotic behavior of m_ε and the energy $F_\varepsilon(m_\varepsilon)$ as $\varepsilon \downarrow 0$?

As before, it is natural to study this question in the framework of Γ-convergence. To this end, we first need to fix a topology on the space of admissible magnetizations. The strong $L^1(\Omega, \mathbf{R}^3)$-topology was used for the previous models, but it turns out that F_ε is not coercive enough to deduce compactness from (6.20) in this space. Another possibility is the weak* topology in $L^\infty(\Omega, \mathbf{R}^3)$. Clearly, the limit $m = (m', m_3)$ (as $\varepsilon \downarrow 0$) must have a vanishing second component m_2 and a vanishing distributional divergence $\nabla \cdot m = \nabla \cdot m' = 0$ in Ω. However, we obtain more information about the limit if we first apply a nonlinear transformation to m. In order to do so, we use spherical coordinates (φ, ϑ) so that

$$m = (\cos\varphi \cos\vartheta, \sin\varphi, \cos\varphi \sin\vartheta).$$

The quantity that we need to study is

$$\psi = \sin\vartheta - \vartheta\cos\vartheta,$$

at least if we work in the hemisphere where $|\vartheta| \leq \frac{\pi}{2}$. We will show that as long as ϑ remains sufficiently small, the functional

$$F_0(\psi) = 2\sup\left\{\int_\Omega \frac{\partial v}{\partial x_1}\psi dx : v \in C_0^1(\Omega) \text{ with } \sup_\Omega |v| \leq 1\right\} \tag{6.21}$$

can be identified as the limiting energy. For a sufficiently regular ψ, this is of course

$$F_0(\psi) = 2\int_\Omega \left|\frac{\partial \psi}{\partial x_1}\right| dx.$$

The lack of a penalization of $\frac{\partial\psi}{\partial x_2}$ means that we can have very rough limiting configurations. On the other hand, almost every restriction to a horizontal line $\Omega \cap (\mathbf{R} \times \{x_2\})$ will be a function of bounded variation. There can be jumps, but these jumps contribute to the energy proportionally to the jump height. It is convenient to imagine here that the magnetization depends only on x_1, and then we can think of a jump as a domain wall. It is worth noting that in general, the wall energy given by F_0 is *not* achieved by a one-dimensional transition between the two states on either side of the wall (as in the Aviles–Giga model). Instead, in order to obtain the optimal limiting energy given by F_0, a transition with an additional zigzag structure is required.

Adapted triplet. In order to obtain that F_0 is an optimal lower bound we will use the same strategy based on generalized entropies. More precisely, we study the particular class of Lipschitz continuous maps $\Phi = (\Phi_1, \Phi_2) \in \mathrm{Lip}(S^2, \mathbf{R}^2)$ and $\alpha \in \mathrm{Lip}(S^2)$ such that for every smooth $m \in C^\infty(\Omega, S^2)$, there holds

$$\nabla \cdot \{\Phi(m)\} + \alpha(m)\nabla \cdot m \leq \varepsilon|\nabla m|^2 + \frac{1}{\varepsilon}m_2^2 \quad \text{a.e. in } \Omega, \tag{6.22}$$

where $\varepsilon > 0$ is a small parameter. In (6.22), we skip the last term on the R.H.S. of (6.9) since it is not important in the sequel. The condition (6.22) yields the corresponding necessary pointwise bounds for an admissible triplet $(\Phi = (\Phi_1, \Phi_2), \alpha)$ as in Lemma 2 where $g(m_3^2)$ is to be replaced by m_2^2. As explained above, the expected limit energy for a jump of angle $\theta \in (0, \frac{\pi}{2}]$, i.e.

$$m^{\pm} = (\cos\theta, 0, \pm\sin\theta) \in S^2 \tag{6.23}$$

is given by

$$F(\theta) = 2(\psi(\theta) - \psi(-\theta)) = 4(\sin\theta - \theta\cos\theta).$$

The periodic case. For simplicity, we first focus as before on the periodic situation

$$\Omega = \frac{\mathbf{R} \times \mathbf{R}}{\mathbb{Z}}.$$

For a fixed transition angle $\theta \in (0, \frac{\pi}{2})$, we set the jump directions $m^{\pm}$ given by (6.23) and we consider vector fields (periodic in the tangential direction x_2 to the wall) with the desired transition imposed at the boundary:

$$M(\theta) := \left\{ m \in H^1_{\mathrm{loc}}(\Omega, S^2) : \lim_{x_1 \to \pm\infty} m(x_1, \cdot) = m^{\pm} \text{ in } L^2\left(\frac{\mathbf{R}}{\mathbb{Z}}\right) \right\}.$$

Similar to (6.14), we will say that a triplet $(\Phi = (\Phi_1, \Phi_2), \alpha) \in \mathrm{Lip}(S^2, \mathbf{R}^3)$ is adapted to the jump (m^-, m^+) if

$$\Phi_1(m^+) - \Phi_1(m^-) = F(\theta) \tag{6.24}$$

and there exists $\varepsilon_0 > 0$ such that for any $0 < \varepsilon \leq \varepsilon_0$, inequality (6.22) holds for every map $m \in C^\infty(\Omega, S^2)$.

We shall see that surprisingly this context is opposite to the Bloch wall model where we could find an adapted triplet for the largest angle, but not for small angles. Here, we prove the existence of adapted triplet for walls of small transition angles and non-existence for the biggest angle.

Proposition 13. (Ignat–Moser [44]) *There exist an angle $\theta_0 \in (0, \frac{\pi}{2})$ and a Lipschitz triplet $(\Phi = (\Phi_1, \Phi_2), \alpha)$ that is adapted to the jump $m^{\pm}$ for every $\theta \in (0, \theta_0]$.*

For the biggest jump $\pm\mathbf{e}_3$, we prove a nonexistence result. This result suggests that the zigzag pattern may not be optimal for large angles.

Proposition 14. (Ignat–Moser [44]) *There is no smooth triplet $(\Phi = (\Phi_1, \Phi_2), \alpha)$ adapted to the jump $m^{\pm}$ for $\theta = \frac{\pi}{2}$.*

As we have already seen in Sec. 6.2, the existence of adapted triplets is useful for proving the optimal lower bound for F_ε. Indeed, we prove the desired asymptotic minimal value of F_ε on the set $M(\theta)$ for small transition angles θ:

Theorem 14. (Ignat–Moser [44]) *There exists an angle $\theta_0 \in (0, \frac{\pi}{2})$ such that the following holds: for every $\theta \in (0, \theta_0]$,*

$$\min_{m_\varepsilon \in M(\theta)} F_\varepsilon(m_\varepsilon) = F(\theta) + o(1) \quad \text{as } \varepsilon \to 0.$$

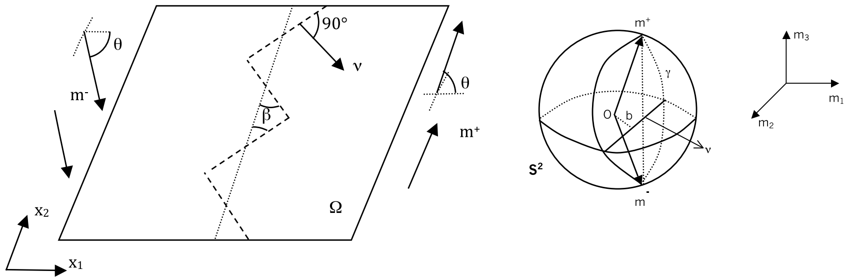

Fig. 10. The zigzag pattern.

The idea of the proof is to match an upper bound coming from the zigzag wall construction with the lower bound based on adapted triplets in Proposition 13. Let us explain the heuristics of deducing the upper bound in Theorem 14 for a wall angle θ. Let $\beta \in [0, \frac{\pi}{2})$ and consider in $\mathbf{R}^3$ the plane containing the two points $m^{\pm} \in S^2$ so that $\nu = (\cos\beta, -\sin\beta, 0)$ is the normal vector to the plane (see Fig. 10). The construction will involve a transition path from m^- to m^+ along the geodesic γ on S^2 within this plane. More precisely, we define

$$b = \cos\theta\cos\beta \quad \text{and} \quad \sigma = \arcsin\frac{\sin\theta}{\sqrt{1-b^2}};$$

the smallest arc γ connecting $m^{\pm}$ on the circle of radius $\sqrt{1-b^2}$ whose plane is perpendicular to ν is given by

$$\gamma(t) = b\nu + \sqrt{1-b^2}(\sin\beta\cos t, \cos\beta\cos t, \sin t) \tag{6.25}$$

for $-\sigma \le t \le \sigma$. For a transition along $\gamma = (\gamma_1, \gamma_2, \gamma_3)$, the expected energy per unit wall length is

$$K(\beta) = 2\int_{-\sigma}^{\sigma} \gamma_2(t)|\dot{\gamma}(t)|dt.$$

In order to keep the magnetostatic energy small, we will have to use this transition across pieces of a zigzag wall that are tilted with respect to $\{0\} \times (0,1)$ by the angle β (see Fig. 10). This increases the length of the wall by the factor $\frac{1}{\cos\beta}$, and in the limit we expect the energy density

$$h(\beta) = \frac{K(\beta)}{\cos\beta}. \tag{6.26}$$

One can check that h is a decreasing function and concludes that

$$\inf_{0\le\beta<\frac{\pi}{2}} h(\beta) = \lim_{\beta\to\frac{\pi}{2}^-} h(\beta) = F(\theta).$$

Observe that the energy cost of a transition of small angle θ is cubic, so that it is asymptotically cheaper than the quadratic energy cost of a Bloch wall transition of the same angle.

Γ-*convergence for small transition angles.* We now concentrate on families of uniformly bounded energy configurations $\{m_\varepsilon \in H^1(\Omega, S^2)\}$ in a smooth bounded simply-connected domain $\Omega \subset \mathbf{R}^2$, i.e. (6.20) holds. The aim is to establish the structure of limiting configurations of such families and to justify that F_0 is their limit energy (according to the Γ-convergence method). The first issue is to find the appropriate topology for the desired Γ-convergence result. Obviously, (6.20) entails $m_{\varepsilon,2} \to 0$ strongly in $L^2(\Omega)$. However, families $\{m_\varepsilon\}$ satisfying (6.20) are in general *not* relatively compact in the strong L^1-topology and the limiting configurations m are not necessarily taking values into S^2 (in general, one only has $|m| \leq 1$ a.e. in Ω). Therefore, one alternative would be to choose the weak* L^∞-topology for $\{(m_{\varepsilon,1}, m_{\varepsilon,3})\}$. Rather than studying the limiting behavior of $(m_{\varepsilon,1}, m_{\varepsilon,3})$, we focus on the quantity

$$\psi_\varepsilon = f(m_\varepsilon), \tag{6.27}$$

where $f : S^2 \to \mathbf{R}$ is the function defined by

$$f(m) = \begin{cases} \dfrac{1}{4} F\left(\arctan\left(\dfrac{m_3}{m_1}\right)\right) & \text{if } m_1 > 0, \\ 2 + \dfrac{1}{4} F\left(\arctan\left(\dfrac{m_3}{m_1}\right)\right) & \text{if } m_1 < 0 \text{ and } m_3 \geq 0, \\ -2 + \dfrac{1}{4} F\left(\arctan\left(\dfrac{m_3}{m_1}\right)\right) & \text{if } m_1 < 0 \text{ and } m_3 < 0, \end{cases}$$

extended continuously where $m_1 = 0$ and $m_2 \neq \pm 1$ (here, $\arctan : \mathbf{R} \to (-\frac{\pi}{2}, \frac{\pi}{2})$). This function has a discontinuity along the semicircle $\{m \in S^2 : m_3 = 0,\ m_1 \leq 0\}$, and from a geometric point of view, it would be more appropriate to regard f as a function from S^2 into $\frac{\mathbf{R}}{4\mathbb{Z}}$. Since we work mostly in a hemisphere below, we keep $\mathbf{R}$ as the target anyway. The discontinuities at the poles $\pm\mathbf{e}_2$, of course, are unavoidable. Since $|\psi_\varepsilon| \leq 2$ a.e. in Ω, we choose the weak* L^∞-topology for $\{\psi_\varepsilon\}$ as appropriate for the Γ-convergence result. Extending (6.21) to the limiting functional $F_0 : L^\infty(\Omega) \to [0, \infty]$, we prove the following Γ-convergence result for small transition angles:

Theorem 15. (Ignat–Moser [44]) *There exists an angle $\theta_0 \in (0, \frac{\pi}{2})$ such that the following holds true*:

(1) (*Compactness and lower bound*) *Let $\{m_\varepsilon\} \subset H^1(\Omega, S^2)$ with* (6.20). *Consider the family $\{\psi_\varepsilon\}$ associated to $\{m_\varepsilon\}$ via* (6.27). *Then for subsequences*,

$$\psi_\varepsilon \overset{*}{\rightharpoonup} \psi \quad \text{in } L^\infty(\Omega) \quad \text{and} \quad m_{\varepsilon,2} \to 0 \quad \text{in } L^2(\Omega). \tag{6.28}$$

If $|\psi_\varepsilon| \leq \frac{1}{4}F(\theta_0)$ a.e. in Ω for every small $\varepsilon > 0$, then

$$F_0(\psi) \leq \liminf_{\varepsilon \downarrow 0} F_\varepsilon(m_\varepsilon).$$

(2) (*Upper bound*) *For every* $\psi \in L^\infty(\Omega)$ *with* $|\psi| \le \frac{1}{4}F(\theta_0)$ *a.e. in* Ω, *there exists a family* $\{m_\varepsilon\} \subset H^1(\Omega, S^2)$ *such that* (6.28) *holds and*

$$F_0(\psi) = \lim_{\varepsilon \downarrow 0} F_\varepsilon(m_\varepsilon).$$

We are aware of only one other situation where the Γ-limit is explicitly known for a problem involving similar microstructures: The problem leading to cross-tie walls in thin ferromagnetic films (see [1, 68, 69]). As shown in Fig. 6, the cross-tie wall consists in a mixture of vortices and Néel walls (one-dimensional transition layers similar to Bloch walls, but taking values only in S^1). Remarkably, the function $\sin\theta - \theta\cos\theta$ plays an important role in that context as well, although this may be a mere coincidence.

7. Micromagnetics

Ferromagnetic materials are widely used in nowadays as technological tools, especially for magnetic data storage. The modeling of very small ferromagnetic particles is based on the micromagnetic theory. The micromagnetic model states that ferromagnetic materials can be described by a 3D vector-field distribution, called *magnetization*, where the stable configurations correspond to (local) minimizers of the micromagnetic energy. The associated variational problem is nonconvex and nonlocal. Moreover, it is a multi-scale system involving both intrinsic parameters (depending on the nature of the ferromagnetic material) and extrinsic parameters (coming from the geometry of the sample). According to the relative smallness of these parameters, different asymptotic regimes appear and lead to formation of various patterns of the magnetization.

The qualitative and quantitative analysis of pattern formation is an extensively explored topic. Generically, a pattern (stable state) consists in large uniformly magnetized 3D regions (*magnetic domains*) separated by narrow transition layers (*domain walls*) where the magnetization varies very rapidly. Depending on the length scales of the system, the experiments predict different type of domain walls: Wall defects (*Néel walls, Bloch walls, asymmetric Néel walls, asymmetric Bloch walls* etc.), interior vortices (*Bloch lines*), boundary vortices or different type of microstructures: *Cross-tie walls*, *zigzag walls* etc. The main goal is to give a mathematical justification of the physical prediction on the formation and characterization of these defects. Classical methods of functional analysis are often insufficient to detect these phenomena of loss of regularity. New approaches need to be developed in order to implement geometric measure theory contributing to the analysis of partial differential equations and calculus of variations.

7.1. *The general three-dimensional model*

The magnetization of a ferromagnetic sample $\Omega \subset \mathbf{R}^3$ is created by the spontaneous alignment of electron spins and can be described in the non-dimensionalized form

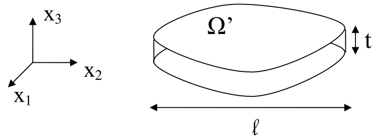

Fig. 11. A ferromagnetic sample.

by a 3D unit-length vector field

$$m : \Omega \to S^2.$$

Let us assume that the sample is a cylinder, i.e.

$$\Omega = \Omega' \times (0, t),$$

where Ω' is the cross-section of the sample of diameter ℓ and t is the thickness of the cylinder (see Fig. 11). According to micromagnetics, stable magnetizations in Ω are described by (local) minimizers of the energy functional defined as:

$$E^{3\mathrm{D}}(m) = d^2 \int_\Omega |\nabla m|^2 dx + Q \int_\Omega \varphi(m) dx + \int_{\mathbf{R}^3} |\nabla U|^2 dx \\ - 2 \int_\Omega H_{\mathrm{ext}} \cdot m dx. \tag{7.1}$$

In the following we explain the four components of the micromagnetic energy $E^{3\mathrm{D}}$.

- The first-term, called exchange energy is due to short range interactions of spins and favors parallel alignment of neighboring spins. The constant d is the exchange length and corresponds to an intrinsic parameter of the material of the order of nanometers.
- The second-term in (7.1) represents the anisotropy energy that penalizes certain magnetization axes. The anisotropy energy density $\varphi \geq 0$ is a non-negative function with symmetry properties inherited from the crystalline lattice. The preferred directions of magnetization are the zeros of φ. Typically, we have uniaxial or multi-axial anisotropy (e.g. $\varphi(m) = 1 - m_1^2$ that favors the direction $(\pm 1, 0, 0)$) and surface anisotropy (e.g. $\varphi(m) = m_3^4$ where the easy plane is the horizontal one). The quality factor Q is a second intrinsic parameter of the material that measures the strength of the anisotropy energy relative to the stray-field. According to the values of Q, we distinguish two classes of materials: Soft materials if $Q < 1$ and hard materials if $Q > 1$.
- The third-term of $E^{3\mathrm{D}}$ is the stray-field energy and is created by long range interactions between electron spins modeled by the static Maxwell equation. More precisely, the stray-field potential $U : \mathbf{R}^3 \to \mathbf{R}$ is determined by

$$\Delta U = \nabla \cdot (m 1_\Omega) \quad \text{in } \mathbf{R}^3, \\ \text{i.e.} \quad \int_{\mathbf{R}^3} \nabla U \cdot \nabla \zeta dx = \int_\Omega m \cdot \nabla \zeta dx, \quad \forall \zeta \in C_c^\infty(\mathbf{R}^3). \tag{7.2}$$

By the electrostatic analogy, two types of charges generate the potential U: Volume charges with density given by the divergence of m in the interior of the sample Ω and surface charges represented by the normal component of the magnetization on the boundary of Ω. Therefore, this nonlocal term favors domain patterns that achieve flux closure.

- The last term in (7.1) denotes the external field energy generated by an applied external field $H_{\text{ext}} : \mathbf{R}^3 \to \mathbf{R}^3$. It favors alignment of the magnetization with H_{ext}.

More details about the mathematical modeling of micromagnetics can be found in the book of Hubert and Schäfer [33] or in the overview of DeSimone, Kohn, Müller and Otto [27].

We will concentrate on the analysis of *global* minimizers of energy (7.1). In fact, physically accessible *local* minima share the same features as the ground state (see DeSimone, Kohn, Müller, Otto and Schäfer [25]). It is a variational problem relying on the nonconvex constraint $|m| = 1$ and the nonlocality of the stray-field energy due to (7.2). On the other hand, four length scales are involved in the system: Two intrinsic parameters (d and Q) and two extrinsic scales (t and ℓ). Our approach is based on asymptotic analysis, taking advantage of the presence of small ratios involving these parameters. The combination of nonlocality and nonconvexity with the multi-scale nature of the variational problem leads to a rich pattern formation of the magnetization.

7.2. *A reduced thin-film model*

In the following, we are interested in thin ferromagnetic films where we expect the nucleation of several singular patterns of the magnetization (like Néel walls, Bloch lines and boundary vortices). The main issue is to identify the scaling law of the minimum energy and the pattern of the magnetization that achieves this minimum.

Heuristics and scaling. We will heuristically explain in the following the separation of energy scales in the regime of thin-films. The balance between the energy terms is responsible for the formation of certain type of walls in function of certain regimes. The ansatz is the following: We assume that the magnetic film $\Omega = \Omega' \times (0, t)$ with $\ell = \operatorname{diam}(\Omega')$ has a small aspect ratio

$$h := \frac{t}{\ell} \ll 1 \tag{7.3}$$

so that the variations of m in the vertical variable x_3 are strongly penalized by the energy. Therefore, we assume that m is *invariant in x_3-direction* and depends only on the in-plane variables $x' = (x_1, x_2)$:

$$m = (m', m_3)(x') : \Omega' \to S^2 \quad \text{and} \quad m \text{ varies on length scales} \gg \frac{t}{\ell}. \tag{7.4}$$

It is also assumed that the external field is in-plane and invariant in x_3, i.e.

$$H_{\text{ext}} = (H'_{\text{ext}}(x'), 0).$$

Here and below, the dash $'$ always indicates a 2D quantity. We always denote $a \ll b$ if $\frac{a}{b} \to 0$; also, $a \lesssim b$ if $a \leq Cb$ for some universal constant $C > 0$.

Rescaling in the length ℓ of Ω', i.e. $\tilde{x}' = \frac{x'}{\ell}$, $\tilde{\Omega}' = \frac{\Omega'}{\ell}$, $\tilde{m}(\tilde{x}') = m(x')$ and $\tilde{H}'_{\text{ext}}(\tilde{x}') = H'_{\text{ext}}(x')$, the exchange energy, anisotropy and external field energy can be written as

$$\begin{aligned}\int_\Omega (d^2|\nabla m|^2 + Q\varphi(m) - 2H_{\text{ext}} \cdot m)dx \\ = td^2 \int_{\tilde{\Omega}'} |\tilde{\nabla}' \tilde{m}|^2 d\tilde{x}' + t\ell^2 \int_{\tilde{\Omega}'} (Q\varphi(\tilde{m}) - 2\tilde{H}'_{\text{ext}} \cdot \tilde{m}')d\tilde{x}'.\end{aligned} \tag{7.5}$$

What is the appropriate scaling law of the stray-field energy? For configurations (7.4), the static Maxwell equation (7.2) turns into:

$$\Delta U = \nabla' \cdot m' 1_\Omega + m \cdot \nu 1_{\partial\Omega} \quad \text{in } \mathbf{R}^3, \tag{7.6}$$

where ν is the unit outer normal vector on $\partial\Omega$. Therefore, the volume charges are given by the in-plane flux $\nabla' \cdot m'$ and the surface charges on the top and the bottom side of the cylinder ($x_3 \in \{0, t\}$) are represented by the out-of-plane component m_3 of the magnetization. Equation (7.6) is a transmission problem that can be solved explicitly using the Fourier transform $\mathcal{F}(\cdot)$ in the horizontal variables (see e.g. [51, 37]) and one computes:

$$\begin{aligned}\int_{\mathbf{R}^3} |\nabla U|^2 dx = t \int_{\mathbf{R}^2} f\left(\frac{t}{2}|\xi'|\right) \left|\frac{\xi'}{|\xi'|} \cdot \mathcal{F}(m' 1_{\Omega'})\right|^2 d\xi' \\ + t \int_{\mathbf{R}^2} g\left(\frac{t}{2}|\xi'|\right) |\mathcal{F}(m_3 1_{\Omega'})|^2 d\xi',\end{aligned}$$

where

$$g(s) = \frac{1 - e^{-2s}}{2s} \quad \text{and} \quad f(s) = 1 - g(s) \text{ for every } s \geq 0.$$

Approximating $g(s) \approx 1$ and $f(s) \approx s$ if $s = o(1)$ and as above, rescaling in the length scale ℓ of Ω', we obtain the following estimate of the stray-field energy:

$$\begin{aligned}\int_{\mathbf{R}^3} |\nabla U|^2 dx \approx \frac{t^2\ell}{2} \|(\tilde{\nabla}' \cdot \tilde{m}')_{ac}\|^2_{\dot{H}^{-\frac{1}{2}}(\mathbf{R}^2)} \\ + \frac{t^2\ell}{2\pi} \left|\log \frac{\ell}{t}\right| \int_{\partial\tilde{\Omega}'} (\tilde{m}' \cdot \tilde{\nu})^2 d\mathcal{H}^1 + t\ell^2 \int_{\tilde{\Omega}'} \tilde{m}_3^2,\end{aligned} \tag{7.7}$$

(see e.g. [23, 51]). This is due to the assumption (7.4), so that indeed the stray-field energy asymptotically decomposes into three terms in the thin-film regime: The first one is penalizing the volume charges

$$(\tilde{\nabla}' \cdot \tilde{m}')_{ac} = \tilde{\nabla}' \cdot \tilde{m}' 1_{\tilde{\Omega}'}$$

as homogeneous $\dot{H}^{-\frac{1}{2}}$-seminorm and induces the leading order of the energy of Néel walls, a second-term penalizing the lateral charges $\tilde{m}' \cdot \tilde{\nu}$ in the L^2-norm and responsible for the nucleation of boundary vortices, as well as the third-term that counts the surface charges $\tilde{m}_3$ on the top and bottom of the cylinder and leading to formation of Bloch lines.

Summing up (7.5) and (7.7), we deduce the following reduced 2D thin-film energy:

$$\begin{aligned}\tilde{E}^{2\mathrm{D}}(\tilde{m}) &= td^2 \int_{\tilde{\Omega}'} |\tilde{\nabla}'\tilde{m}|^2 d\tilde{x}' + \frac{t^2\ell}{2} \int_{\mathbf{R}^2} ||\tilde{\nabla}'|^{-\frac{1}{2}} (\tilde{\nabla}' \cdot \tilde{m}')_{ac}|^2 d\tilde{x}' \\ &\quad + \frac{t^2\ell}{2\pi} \left|\log \frac{\ell}{t}\right| \int_{\partial\Omega'} (\tilde{m}' \cdot \tilde{\nu})^2 d\mathcal{H}^1 \\ &\quad + t\ell^2 \int_{\tilde{\Omega}'} (\tilde{m}_3^2 + Q\varphi(\tilde{m}) - 2\tilde{H}'_{\mathrm{ext}} \cdot \tilde{m}') d\tilde{x}'. \qquad (7.8)\end{aligned}$$

We will often refer in the following to the above thin-film energy approximation and *we will drop* ˜ *in the sequel.*

According to the specific thin-film regime, three types of singular pattern of the magnetization occur: Néel walls, Bloch lines and boundary vortices. In fact, the formation of one of these patterns depends on the scale ordering of the three terms on the R.H.S. of (7.7). Let us now discuss briefly these patterns (and we will present them in more details in the next sections).

Néel walls. The (symmetric) Néel wall is a transition layer describing a one-dimensional in-plane rotation connecting two (opposite) directions of the magnetization. It is generated by the volume charges $(\nabla' \cdot m')_{ac}$ that give the leading order of the energy of a Néel wall. Observe that this term in (7.7) is related at order of $t^2\ell$ with the limiting stray-field energy generated by the in-plane charges as $h \to 0$:

$$\Delta u_{ac} = (\nabla' \cdot m')_{ac} \mathcal{H}^2 \llcorner \{x_3 = 0\} \quad \text{in } \mathbf{R}^3.$$

More precisely, the homogeneous $\dot{H}^{-\frac{1}{2}}$-seminorm of the in-plane divergence of m' is given by the Dirichlet integral of u_{ac}:

$$\int_{\mathbf{R}^3} |\nabla u_{ac}|^2 dx = \frac{1}{2} \int_{\mathbf{R}^2} ||\nabla'|^{-\frac{1}{2}} (\nabla' \cdot m')_{ac}|^2 dx'. \qquad (7.9)$$

Since a Néel wall is a one-dimensional transition layer in the normal direction x_1 to the wall (i.e. $m = m(x_1)$), the R.H.S. in (7.9) becomes the homogeneous $\dot{H}^{\frac{1}{2}}$-seminorm of the normal component m_1 (on the wall). The Néel wall has two length scales: A core of size

$$\delta := \frac{d^2}{t\ell}$$

and two tails of length scale depending on the confining mechanism. In order that a Néel wall is relevant in a certain regime, one should assume that $\delta \lesssim 1$. The reduced stray-field energy (7.7) per unit length of a Néel wall is of the order of

$$E^{\mathrm{2D}}(\text{Néel wall}) = O\left(\frac{t^2\ell}{|\log\delta|}\right).$$

A detailed description of the Néel wall is done in Sec. 8.

Bloch line. A Bloch line is a regularization of a vortex at the microscopic level of the magnetization that becomes out-of-plane at the center. The prototype of a Bloch line is given by a vector field

$$m : B^2 \to S^2$$

defined in a circular cross-section $\Omega' = B^2$ of a thin-film and satisfying the flux-closure condition:

$$\nabla' \cdot m' = 0 \quad \text{in } B^2 \quad \text{and} \quad m'(x') = (x')^\perp \quad \text{on } \partial B^2. \tag{7.10}$$

(The magnetization is assumed to be invariant in the thickness direction of the film and the word "line" of the Bloch line pattern refers to the vertical direction.) Since the magnetization turns in-plane at the boundary of the disc B^2 (so, $\deg(m', \partial\Omega) = 1$), a localized region is created, that is the core of the Bloch line of size

$$\eta := \frac{d}{\ell},$$

where the magnetization becomes perpendicular to the horizontal plane (see Fig. 12). In order for a Bloch line to be relevant in a certain regime, one should assume that $\eta \lesssim 1$. The reduced energy (7.8) of a configuration (7.10) (in the absence of anisotropy and applied external field) is given by the exchange energy and the surface charges in m_3:

$$E^{\mathrm{2D}}(m) = td^2\left(\int_{B^2} |\nabla' m|^2 dx' + \frac{1}{\eta^2}\int_{B^2} m_3^2 dx'\right).$$

The Bloch line represents the minimizer of this energy under the constraint (7.10). Due to the similarity with the Ginzburg–Landau type functional, the Bloch line corresponds to the Ginzburg–Landau vortex and the energetic cost of a Bloch line (per unit-length) is carried out by the exchange energy outside the vortex core:

$$E^{\mathrm{2D}}(\text{Bloch line}) = O(td^2|\log\eta|)$$

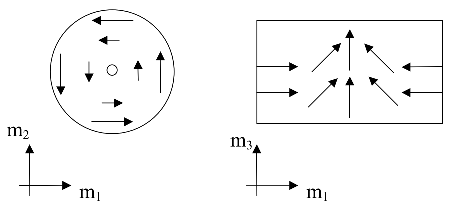

Fig. 12. Bloch line.

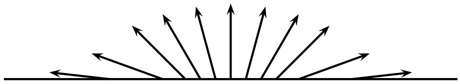

Fig. 13. A micromagnetic boundary vortex.

with the exact prefactor 2π (see e.g. [37]). We will discuss more precisely this singular pattern in Sec. 10.

Boundary vortex. Next we address boundary vortices. A boundary vortex corresponds to an in-plane transition of the magnetization along the boundary from $\nu^\perp$ to $-\nu^\perp$, see Fig. 13. The corresponding minimization problem amounts to the competition between the exchange energy and the lateral surface charges $m' \cdot \nu$:

$$E^{2\mathrm{D}}(m) = td^2\left(\int_{\Omega'} |\nabla' m|^2 dx' + \frac{|\log h|}{2\pi\delta}\int_{\partial\Omega'} (m'\cdot\nu)^2 d\mathcal{H}^1\right)$$

within the set of in-plane magnetizations $m : \Omega' \to S^1$. The minimizer of this energy is a harmonic vector field with values in S^1 driven by a pair of boundary vortices. These have been analyzed in [51, 54, 53, 60, 61]. The transition is regularized on the length scale of the exchange part of the energy, i.e. the core of the boundary vortex has length of size

$$\kappa := \frac{d^2}{t\ell \log\frac{\ell}{t}}.$$

In order that a boundary vortex is relevant in a certain regime, one should assume that $\kappa \lesssim 1$. The cost of such a transition has the energy of leading order of

$$E^{2\mathrm{D}}(\text{Boundary vortex}) = O(td^2|\log\kappa|)$$

with exact prefactor π. Even if they generate the same amount of energy, a boundary vortex is different from a "half" vortex (i.e. regularization of $\frac{x}{|x|}$ in the "half" disc B^2_+): The "half" vortex is tangent at the boundary, i.e. $m'\cdot\nu = 0$ on $B^2_+ \cap \{x_2 = 0\}$ (while the boundary vortex is not), and the boundary vortex is of values into S^1 (while the "half" vortex is not). We will describe in more details boundary vortices in Sec. 11.

Mesoscopic Landau-state in thin-films. At the mesoscopic level in a thin-film, we expect that the magnetization satisfies the flux-closure constraint. It consists in assuming that there are no charges in the sample which would imply that (7.7) vanishes. This type of limit charge-free configurations were predicted in the physics literature (see van den Berg [73]): They are 2D unit-length vector fields of vanishing divergence, i.e.

$$\begin{cases} m_3 = 0, \;\; |m'| = 1 \quad \text{and} \quad \nabla'\cdot m' = 0 \quad \text{in } \Omega', \\ m'\cdot\nu = 0 \quad \text{on } \partial\Omega'. \end{cases} \tag{7.11}$$

This structure reveals the connection with Sec. 2 and explains the formation of jump line-singularities or vortices at the mesoscopic level of the magnetization in thin-films (known in physics as the principle of pole avoidance). We already discussed in Sec. 2 that the method of characteristics yields the nonexistence of continuous solutions of (7.11) in bounded simply connected domains. One of the solutions of (7.11) (in the sense of distributions) is the "viscosity solution" given via the distance function

$$m = \nabla^{\perp}\psi, \quad \text{with } \psi(x') = \mathrm{dist}(x', \partial\Omega')$$

that corresponds to the so-called Landau state for the magnetization m'. The line-singularities for solutions m' are an idealization of domain walls at the mesoscopic level. At the microscopic level, they are replaced by smooth transition layers (as Néel walls, Bloch walls etc.) where the magnetization varies very quickly on a small length scale. Note that the normal component of m' does not jump across these discontinuity lines (because of (7.11)); therefore, the normal vector of the mesoscopic wall is determined by the angle between the mesoscopic levels of the magnetization in the adjacent domains (called wall angle).

Regimes. An important step in our analysis consists in identifying reduced models valid in appropriate regimes where the behavior of the singular patterns described above is easier to understand. The choice of the asymptotic regimes will correspond to the energy ordering of the three patterns (Néel walls, Bloch lines and boundary vortices); the choice of the scaling law of the minimal energy determines the constraints of the model (imposed by the patterns of higher energy order) and the singular patterns that are to be neglected (of lower energy order). With these choices, the mathematical approach is based on asymptotic analysis by proving the matching of upper and lower bounds for the energy (in the spirit of Γ-convergence).

Let us now discuss the possible choices of ordering. First of all, we are interested in thin-film regimes (i.e. $h = \frac{t}{\ell} \ll 1$) where all three singular patterns are relevant, meaning that they are contained by the sample:

$$\delta \ll 1, \quad \eta \ll 1, \quad \kappa \ll 1,$$

leading to $t \ll \ell$ and $d \ll \ell$. (In fact, if the Néel wall is relevant, i.e. $\delta \ll 1$, then also the Bloch line and the boundary vortex are contained, i.e. $\eta \ll 1$ and $\kappa \ll 1$.) Second, one can check that

$$E^{2\mathrm{D}}(\text{Boundary vortex}) \lesssim E^{2\mathrm{D}}(\text{Néel wall})$$
$$\text{or} \quad E^{2\mathrm{D}}(\text{Boundary vortex}) \lesssim E^{2\mathrm{D}}(\text{Bloch line}),$$

meaning that a boundary vortex never induces the leading order of the total energy (see [46]). Therefore, one has the following three choices of ordering:

(i)
$$\max\{E^{2\mathrm{D}}(\text{Boundary vortex}), E^{2\mathrm{D}}(\text{Bloch line})\} \ll E^{2\mathrm{D}}(\text{Néel wall}),$$

equivalent to $|\log h| \ll \frac{1}{\delta|\log\delta|}$. A slightly more general regime was treated in [23], where $|\log h| \ll \frac{1}{\delta}$ and the scaling law of the minimum energy in (7.8) is of the order $t^2\ell$. In this case, the 3D stray-field energy (7.7) reduces to (7.9) (at order $t^2\ell$) and the reduced model is rigorously justified via the Γ-convergence method (see [23]): The limiting configurations are invariant in the vertical direction x_3 (justifying the assumption (7.4)), but they are not in-plane since Bloch lines may appear in the reduced model. The regime in [23] is appropriate for permalloy films of diameter of tens of microns and thickness of the order of tens of nanometers. So, it can be achieved experimentally, though not by numerical simulation which is generally restricted to a thickness of the order of sub-microns.

(ii)

$$E^{2\mathrm{D}}(\text{Boundary vortex}) \ll E^{2\mathrm{D}}(\text{Néel wall}) \ll E^{2\mathrm{D}}(\text{Bloch line}),$$

equivalent to

$$\log|\log h| \ll \frac{1}{\delta|\log\delta|} \ll |\log h|. \tag{7.12}$$

It means that the aspect ratio $h = h(\delta)$ is exponentially small with respect to the Néel wall core δ; in particular, $t \ll d \ll \ell$. This regime is treated in [40] where the choice of the scaling law of the minimal energy is of the order of Néel walls, i.e. $\frac{t^2\ell}{|\log\delta|}$. Therefore, due to (7.12), Bloch lines are avoided (since they are too expensive), so that the limiting configurations as $h \to 0$ are x_3-invariant and they are in-plane, i.e. $m \in S^1$. The boundary vortices do not contribute to the leading order of minimal energy (since they are lower order). In Sec. 9, we discuss this reduced model: The goal is to prove that the optimal pattern of the magnetization on circular cross-section Ω' is a peculiar vortex structure, driven by a 360° Néel wall coupled with a pair of boundary vortices at $\partial\Omega'$.

(iii)

$$E^{2\mathrm{D}}(\text{Néel wall}) \ll E^{2\mathrm{D}}(\text{Boundary vortex}) \ll E^{2\mathrm{D}}(\text{Bloch line}), \tag{7.13}$$

equivalent to

$$\frac{1}{\delta|\log\delta|} \ll \log|\log h|.$$

In Sec. 10, we discuss this reduced model. This is part of [46] where the scaling law of the minimal energy is of the order of Bloch lines $O(td^2|\log\eta|)$. However, in [46], we did not focus on the level of minimal energy, but rather on metastable configurations where boundary vortices are strongly penalized, so that the limiting configurations as $h \to 0$ are assumed to be charges-free on the lateral surface, i.e. $m' \cdot \nu = 0$ on $\partial\Omega'$. Indeed, vanishing lateral surface charges would be physical relevant for a global minimizer *only* if boundary vortices were more expensive than both the Néel walls and Bloch line contribution. As explained above, this assumption is never satisfied in the regime $h \ll 1$ and $\delta \ll 1$. Therefore, the stray-field energy (7.7) (in the absence of the middle term in R.H.S.) is not adapted for studying global minimizers in the regime (7.13), but rather for metastable states with vanishing normal component at the lateral surface.

8. Néel Wall

The Néel wall is a dominant transition layer in thin ferromagnetic films (in the regime presented in Sec. 7.2). It is characterized by a one-dimensional in-plane rotation connecting two (opposite) directions of the magnetization. It has two length scales: A small core with fast varying rotation and two logarithmically decaying tails. In order for the Néel wall to exist, the tails have to be contained. There are three confining mechanisms for the Néel wall tails: The anisotropy of the material, the steric interaction with the sample edges and the steric interaction with the tails of neighboring Néel walls. In the following, we describe these models that correspond to three nonconvex and nonlocal variational problems depending on a small parameter:

Model 1. Confinement of Néel wall tails by anisotropy. The model is derived from (7.8) as follows (we skip $\tilde{}$ in (7.8)): We assume the quality factor Q to be of the order of the aspect ratio h (for simplicity, set $Q = \frac{t}{\ell} \ll 1$), i.e. the material is soft; we also assume that the material anisotropy density is given by $\varphi(m) = m_1^2$ and we impose an applied field $H'_{\text{ext}} = \frac{t}{\ell}(\cos\theta, 0)$. Renormalizing the energy (7.8) at order $t^2\ell$, we may assume in the regime $h = \frac{t}{\ell} \ll 1$ that the section $\Omega' = \frac{\mathbf{R}\times\mathbf{R}}{\mathbb{Z}}$ is a periodic strip and the admissible configurations are in-plane magnetizations depending on one variable (normal to the wall) and satisfy the following boundary conditions (that enforce a transition as in (6.12)):

$$m = m(x_1), \quad m_3 = 0 \quad \text{and} \quad m(\pm\infty) = m^{\pm} := (\cos\theta, \pm\sin\theta, 0), \tag{8.1}$$

where $\theta \in (0, \pi)$ is the wall angle (see Fig. 14). Therefore, by (7.8), we derive the following functional whose behavior is to be studied asymptotically as $\delta \downarrow 0$:

$$m \mapsto \delta\|m\|^2_{\dot{H}^1} + \frac{1}{2}\|m_1\|^2_{\dot{H}^{\frac{1}{2}}} + \|m_1 - \cos\theta\|^2_{L^2}, \tag{8.2}$$

where we recall that $\delta = \frac{d^2}{t\ell}$ plays the role of the core of the transition.

Observe that the energy (8.2) is invariant under translation. Since configurations m of finite energy are continuous, the boundary conditions in (8.1) enforce a

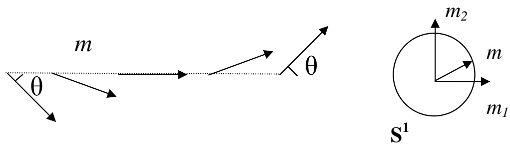

Fig. 14. Néel wall of angle 2θ.

transition (*domain wall*) for the magnetization. One can fix the center of the wall at the origin by setting

$$m(0) = (1, 0).$$

Under these restrictions, a Néel wall corresponds to a minimizer of the energy (8.2).

The variational problem is nonconvex because of the saturation constraint $|m| = 1$ and nonlocal due to the stray-field interaction. It is a nondegenerate problem since the anisotropy term prevents a Néel wall to spread over the complete domain $\mathbf{R}$; therefore, the Néel wall tails are forced to be limited and the energy cannot reach arbitrary small levels. Observe that the energy (8.2) only yields a uniform bound of m_1 in $\dot{H}^{\frac{1}{2}}(\mathbf{R})$ that barely fails to control the $L^\infty(\mathbf{R})$-norm $\|m_1\|_{L^\infty(\mathbf{R})} = 1$. This suggests a logarithmic decay of the energy. Indeed, we prove the following result (see also [21, 40]):

Lemma 3. *Let $I \subset \mathbf{R}$ be a bounded interval and $\delta \ll 1$. For every function $m_1 \in C_c(I)$, the following estimate holds*:

$$\delta\|m_1\|^2_{\dot{H}^1} + \frac{1}{2}\|m_1\|^2_{\dot{H}^{\frac{1}{2}}} \geq \frac{\pi + o(1)}{2|\log \delta|}\|m_1\|^2_{L^\infty} \quad \textit{as } \delta \downarrow 0.$$

The proof of this estimate is based on a duality argument combined with a failing Gagliardo–Nirenberg interpolation embedding

$$BV \cap L^\infty(\mathbf{R}^N) \not\subseteq \dot{H}^{\frac{1}{2}}(\mathbf{R}^N).$$

This failing embedding can be corrected by regularizing the homogeneous $\dot{H}^{\frac{1}{2}}$-seminorm. This perturbation yields a weaker seminorm that is controlled with a logarithmically slow rate having the optimal prefactor $\frac{2}{\pi}$ (see [21]):

For $\delta \ll w$ and for any $\chi : \mathbf{R}^N \to \mathbf{R}$, we have that

$$\int_{\mathbf{R}^N} \min\left\{\frac{1}{\delta}, |\xi|, w|\xi|^2\right\} |\hat{\chi}|^2 d\xi \lessapprox \frac{2}{\pi}\left(\log\frac{w}{\delta}\right)\|\chi\|_{L^\infty}\int_{\mathbf{R}^N}|\nabla\chi|. \tag{8.3}$$

The exact leading order term of the minimal energy in (8.2) was deduced by DeSimone, Kohn, Müller and Otto [22, 24] by matching upper and lower bounds in the case of a 180° Néel wall (i.e. $\theta = \frac{\pi}{2}$):

$$\min_{\substack{(8.1)\\ \theta=\frac{\pi}{2}}}\left(\delta\|m\|^2_{\dot{H}^1} + \frac{1}{2}\|m_1\|^2_{\dot{H}^{\frac{1}{2}}} + \|m_1\|^2_{L^2}\right) = \frac{\pi + o(1)}{2|\log \delta|} \quad \text{as } \delta \downarrow 0. \tag{8.4}$$

The analysis of the structure of a minimizer of (8.4) is rather subtle due to the different scaling behavior of the energy terms in (8.2). Remark that omitting the

$\dot{H}^{\frac{1}{2}}$-seminorm, the formulation of (8.4) in terms of $v := m_2$ corresponds to a variational problem associated to the Cahn–Hilliard model (see Cahn and Hilliard [15]):

$$\min_{\substack{v:\mathbf{R}\to[-1,1] \\ v(0)=0, v(\pm\infty)=\pm 1}} \int_{\mathbf{R}} \left(\frac{\delta}{1-v^2} \left| \frac{dv}{dx_1} \right|^2 + 1 - v^2 \right) dt. \tag{8.5}$$

The minimizer is a transition layer with a single length scale $\sqrt{\delta}$, i.e. $v(x_1) = \tanh(\frac{x_1}{\sqrt{\delta}})$. The first component of the magnetization m_1 would correspond in (8.5) to $\operatorname{sech}(\frac{x_1}{\sqrt{\delta}})$ and the minimal energy is equal to $4\sqrt{\delta}$.

Coming back to our variational problem (8.4), the presence of the nonlocal term as a homogeneous $\dot{H}^{\frac{1}{2}}(\mathbf{R})$-seminorm in competition with the energy (8.5) creates a second length scale of the transition layer. The Néel wall is divided into two regions: A core ($|x_1| \lesssim w_{\text{core}}$) and two tails ($w_{\text{core}} \lesssim |x_1| \lesssim w_{\text{tail}}$). This particular structure enables the magnetization to decrease the energy by a logarithmic factor (8.4). Melcher [56, 57] rigorously established the optimal profile of the Néel wall, i.e. the unique minimizer m of (8.4) with $m_1(0) = 1$ exhibits two uniformly logarithmic tails beyond a core region of the order δ close to the origin (see Fig. 15):

$$m_1(t) \sim \frac{|\log |x_1||}{|\log \delta|} \quad \text{for } \delta < |x_1| < \frac{1}{e}, \quad \text{i.e. } w_{\text{core}} = O(\delta), \;\; w_{\text{tail}} = O(1).$$

We are interested in the asymptotics of the energy (8.2) as $\delta \downarrow 0$. Due to the logarithmic decay (8.4), we consider a new length scale $\varepsilon > 0$ such that

$$\delta = \frac{\varepsilon}{|\log \varepsilon|}$$

and we renormalize the energy (8.2) by a factor $|\log \varepsilon|$ in order that the minimal energy become of the order $O(1)$:

$$E_\varepsilon(m) = \varepsilon \|m\|^2_{\dot{H}^1} + |\log \varepsilon| \left(\frac{1}{2} \|m_1\|^2_{\dot{H}^{\frac{1}{2}}} + \|m_1 - \cos\theta\|^2_{L^2} \right). \tag{8.6}$$

Our goal is to study the Γ-convergence of energies $\{E_\varepsilon\}$ as $\varepsilon \downarrow 0$ and to characterize the limiting configurations of the magnetization. We will prove that the limiting

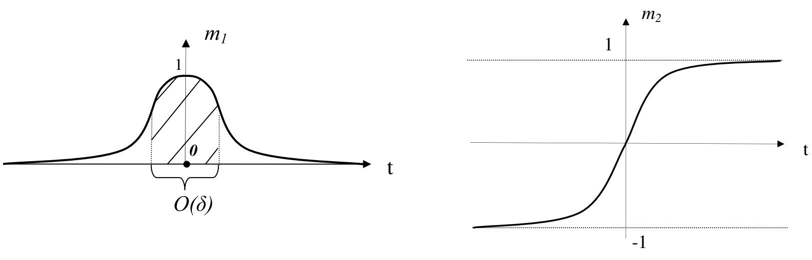

Fig. 15. First and second component of a 180° Néel wall.

configurations are piecewise constant functions of bounded total variation that can take two values $\{m^{\pm} = (\cos\theta, \pm\sin\theta, 0)\}$, i.e. they belong to

$$\mathcal{A} = \left\{ m_0 : \mathbf{R} \to \{m^{\pm}\} : \int_{\mathbf{R}} \left| \frac{dm_0}{dx_1} \right| < \infty \right\}.$$

The Γ-limit energy is proportional to the number of jumps of these configurations and the energetic cost of each jump is $\frac{\pi(1-|\cos\theta|)^2}{2}$; therefore, we define the following energy for any configuration $m_0 \in \mathcal{A}$:

$$E_0(m_0) = \frac{\pi}{2}(1 - |\cos\theta|)^2 \cdot (\text{number of jumps of } m_0). \tag{8.7}$$

Theorem 16. (Ignat [36]) *Let $\theta \in (0, \pi)$. Then*

$$E_\varepsilon \xrightarrow{\Gamma} E_0 \textit{ under the } L^1_{\mathrm{loc}}(\mathbf{R}, S^1)\textit{-topology as } \varepsilon \downarrow 0, \textit{ i.e.}$$

(i) (*Compactness and lower bound*) *If $\{m_\varepsilon : \mathbf{R} \to S^1\}_\varepsilon$ satisfies*

$$\limsup_{\varepsilon\downarrow 0} E_\varepsilon(m_\varepsilon) < +\infty,$$

then for subsequences ε, there exists $m_0 \in \mathcal{A}$ such that $m_\varepsilon \to m_0$ in $L^1_{\mathrm{loc}}(\mathbf{R}, S^1)$ as $\varepsilon \downarrow 0$ and

$$\liminf_{\varepsilon\downarrow 0} E_\varepsilon(m_\varepsilon) \geq E_0(m_0);$$

(ii) (*Upper bound*) *For every $m_0 \in \mathcal{A}$, there exists a family of smooth functions $\{m_\varepsilon : \mathbf{R} \to S^1\}_{\varepsilon\downarrow 0}$ such that $m_\varepsilon - m_0$ has compact support in $\mathbf{R}$ for all ε, $m_\varepsilon - m_0 \xrightarrow{\varepsilon\downarrow 0} 0$ in $L^1(\mathbf{R}, \mathbf{R}^2)$ and*

$$\lim_{\varepsilon\downarrow 0} E_\varepsilon(m_\varepsilon) = E_0(m_0).$$

Remark 14. Observe that the energy of a Néel wall of angle 2θ is quartic in θ for small angles θ:

$$\min_{(8.1)} E_\varepsilon \overset{\varepsilon\downarrow 0}{=} \frac{\pi}{2}(1 - \cos\theta)^2 \approx \frac{\pi}{8}\theta^4 \quad \text{as } \theta \downarrow 0.$$

We mention that the compactness result fails in general under the strict convergence in BV_{loc} even if the limiting configurations are of bounded variation in $\mathbf{R}$. In fact, it is constructed in [45] a sequence of magnetizations $\{m_\varepsilon\}$ satisfying (8.1) and of uniformly bounded energies $E_\varepsilon(m_\varepsilon) \leq C$ such that the sequence of total variations $\{\int |\frac{dm_{1,\varepsilon}}{dx_1}|\}$ blows-up.

Remark 15. One could compare Model 1 with the Aviles–Giga model presented in Sec. 6.2. The nonlocal term $|\log\varepsilon|\|m_1\|^2_{\dot{H}^{\frac{1}{2}}}$ for the energy $E_\varepsilon(m)$ (penalizing nonvanishing divergence configurations m which are here 1D) will amount to a delicate multi-scale structure of the transition layer in Model 1 comparing to the one-scale transition layers in the Aviles–Giga model. Since the behavior of E_ε is quartic in the wall angle, the entropy method (used for the Aviles–Giga) does not

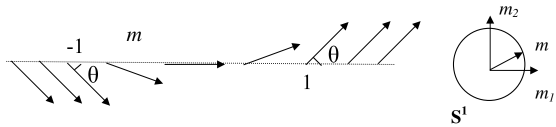

Fig. 16. Néel wall of angle 2θ confined in $[-1,1]$.

apply here. However, we succeed to show that limiting configurations in Model 1 are BV and to deduce the complete Γ-convergence result for our nonlocal functionals.

Model 2. Confinement of Néel wall tails by the finite size of the sample. The constraints are given by:

$$m : \mathbf{R} \to S^1 \quad \text{and} \quad m(\pm x_1) = m^{\pm} \quad \text{for } \pm x_1 \geq 1, \tag{8.8}$$

with $\theta \in (0, \pi)$ (see Fig. 16), whereas the energy functional is:

$$m \mapsto \delta \|m\|^2_{\dot{H}^1} + \frac{1}{2}\|m_1\|^2_{\dot{H}^{\frac{1}{2}}} \tag{8.9}$$

with $\delta > 0$ a small parameter. It models a one-dimensional magnetization in a thin ferromagnetic film of finite width where the effect of crystalline anisotropy and external field is neglected (i.e. $Q = 0$ and $H_{\text{ext}} = 0$ in (7.8) and the energy rescales as for Model 1). The corresponding variational problem was analyzed in [23, 21, 45]. The main difference with respect to Model 1 consists in the confinement of the Néel wall tails by the interaction with the sample edges placed in -1 and 1 in our framework. However, the properties of the transition layer in Model 1 naturally transfer to the structure of the minimizer of (8.9) that satisfies $m(0) = (1, 0)$. It is a two length scale object with a small core of the order δ and two logarithmically decaying tails contained in $[-1, 1]$ and it attains the same level of minimal energy $\frac{\pi+o(1)}{2|\log\delta|}$ as $\delta \downarrow 0$. The stability of 180° Néel walls under arbitrary 2D modulation was proved by DeSimone, Knüpfer and Otto [21]. Moreover, we proved in [45] the optimality of the one-dimensional minimizer, i.e. asymptotically, the Néel wall is the unique minimizer of the associated two-dimensional variational problem in the strip Ω'. As before, by rescaling (8.9), the corresponding energy writes:

$$F_\varepsilon(m) = \varepsilon \|m\|^2_{\dot{H}^1} + \frac{|\log \varepsilon|}{2}\|m_1\|^2_{\dot{H}^{\frac{1}{2}}} \tag{8.10}$$

for a small parameter $\varepsilon > 0$. We proved in [36] the similar asymptotic of F_ε by the Γ-convergence method as $\varepsilon \downarrow 0$ as in Model 1. The difference will consist in having all the walls confined in the interval $[-1, 1]$.

Model 3. Confinement of Néel wall tails by the neighboring Néel walls. The magnetizations are periodic functions such that:

$$\begin{gathered} m = e^{i\varphi}, \\ \varphi : \mathbf{R} \to \mathbf{R} \quad \text{with } \varphi(x_1 + 2) = \varphi(x_1) \quad \text{and} \quad \varphi(x_1 + 1) = \varphi(x_1) + \pi \end{gathered} \tag{8.11}$$

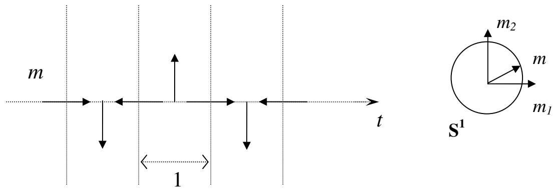

Fig. 17. Periodic array of winding walls.

(see Fig. 17). The energy is given by:

$$m \mapsto \delta \|m\|^2_{\dot{H}^1_{\rm per}} + \frac{1}{2}\|m_1\|^2_{\dot{H}^{\frac{1}{2}}_{\rm per}}, \tag{8.12}$$

for a small parameter $\delta > 0$.

This model was investigated by DeSimone, Kohn, Müller and Otto [24] in order to quantify the repulsive interaction of Néel walls. It consists in considering a periodic array of winding walls at a renormalized distance $w = 2$ in the absence of anisotropy and external field. A transition of 180° is enforced in the middle of each period by the constraint (8.11). Therefore, the tails of a Néel wall are limited by the tails of the neighboring walls at a distance $O(1)$ and we expect that this model generates only 180° Néel walls. As before, the following rescaled energy associated to (8.12):

$$G_\varepsilon(m) = \varepsilon\|m\|^2_{\dot{H}^1_{\rm per}} + \frac{|\log\varepsilon|}{2}\|m_1\|^2_{\dot{H}^{\frac{1}{2}}_{\rm per}}$$

has the same limiting behavior when $\varepsilon \downarrow 0$ as in Model 1.

9. 360° Néel Walls and Vortex Energy

360° *Néel walls.* The aim of the section concerns the special case of 360° Néel walls. For these walls, the magnetization performs a complete rotation across the mesoscopic wall so that it carries a nonzero topological degree. They are characterized by the angle $\alpha \in [0, 2\pi)$ between the mesoscopic direction of the magnetization and the normal direction to the wall (see Fig. 18). We call these transition layers "360° Néel walls of initial angle α". Note that for any mesoscopic Néel wall (with a wall angle smaller than 360°), the condition to be charge free uniquely determines the initial angle α. For 360° Néel walls, the situation is different: In this case, the condition of being charge-free can be achieved for any initial angle α. Our analysis shows that the initial angle α contributes to the leading order energy of the 360° Néel wall. Another peculiarity of 360° Néel walls (of initial angle $\alpha > 0$) with

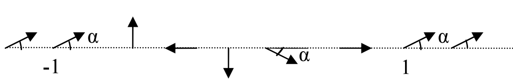

Fig. 18. 360° Néel wall of initial angle α.

respect to general Néel walls comes from their internal structure. It consists of two parts with zero magnetic net charge: A first Néel wall of angle $2\pi - 2\alpha$ and a second Néel wall of angle 2α (see Fig. 18). This means that these two parts only interact by weak dipole–dipole interaction. For this reason the thickness of the 360° Néel wall is much larger than the thickness of the 180° Néel wall. A detailed numerical analysis of the 360° Néel wall, also including the effect of anisotropy and external field, can be found in [63].

The 360° Néel walls we consider in the following are confined by the boundary of the sample (as in Model 2 in Sec. 8). We will assume that the magnetization

$$m = (m_1, m_2) : \mathbf{R} \to S^1$$

only depends on a single variable $x_1 \in \mathbf{R}$. In this case, the specific one-dimensional energy associated to m in our model reduces to the following expression (see (8.10)):

$$F_\varepsilon(m) = \varepsilon \int_{\mathbf{R}} \frac{1}{1-m_1^2} \left| \frac{d}{dx_1} m_1 \right|^2 dx_1 + \frac{|\log \varepsilon|}{2} \int_{\mathbf{R}} \left| \left| \frac{d}{dx_1} \right|^{\frac{1}{2}} m_1 \right|^2 dx_1. \tag{9.1}$$

For our analysis of 360° Néel walls, we assume that the initial direction of the magnetization is given by the angle $\alpha \in [0, 2\pi)$ and a complete rotation is imposed by the following condition:

$$m(x_1) = e^{i\alpha} \quad \text{for } |x_1| \geq 1 \quad \text{and} \quad \deg(m) = 1.$$

In other words, using the lifting $m = e^{i\phi}$, the above condition is equivalent to

$$\phi(x_1) = \begin{cases} \alpha & \text{for } x_1 \leq -1, \\ 2\pi + \alpha & \text{for } x_1 \geq 1. \end{cases} \tag{9.2}$$

We finally mention that 360° Néel walls are a commonly observed structure in thin magnetic films, see [33, p. 457]. They typically arise from (global) topological constraints which can be related to the geometry of the magnetic sample. As we will show in the second part of this section, the 360° Néel wall is a global minimizing structure for magnetic samples with circular cross-section in a certain regime. Note, however, that commonly 360° Néel walls occur as metastable states [33].

Our first result concerns the exact leading order energy of a 360° Néel wall with initial angle α.

Theorem 17. (Ignat–Knüpfer [40]) *Let $m_\varepsilon : \mathbf{R} \to S^1$ be a minimizer of* (9.1) *satisfying* (9.2). *Then m_ε is a smooth map inside* $(-1, 1)$ *and its energetic cost is given by*

$$F_\varepsilon(m_\varepsilon) = \pi(1 + \cos^2 \alpha) + o(1) \quad \text{as } \varepsilon \to 0. \tag{9.3}$$

The result shows that even within the class of 360° Néel walls there is a dependence of the energy with respect to the initial angle α. This result agrees well with a numerical simulation in [63, Fig. 2] where the energetic difference between the two extreme cases $\alpha = 0$ and $\alpha = \frac{\pi}{2}$ by a factor 2 is predicted. Note that we have smoothness in the interior for any critical point of the energy functional (9.1). The main idea for the proof of Theorem 17 is the following: Consider any admissible configuration $m_\varepsilon = (m_{1,\varepsilon}, m_{2,\varepsilon})$ satisfying (9.2) for some given initial angle α. We first prove an optimal lower bound separately for the regions where $m_{1,\varepsilon}$ is larger than $\cos\alpha$ and less than $\cos\alpha$, respectively. These regions correspond to a Néel wall transition of angle $2\pi - 2\alpha$ and 2α, respectively. Then we use the fact that the "interaction" of the nonlocal magnetostatic component of the energy is positive between these two regions.

Vortex induced by $360°$ *Néel wall.* Our second goal is to analyze the behavior of a vortex configuration in ultra thin-films of circular cross-section. As we shall explain in the following, a vortex in our model is a very peculiar structure driven by a $360°$ Néel wall along a radius of a disc, so that the topological degree around the center of the disc is zero. Therefore, it is a configuration completely different from the Bloch line (a structure characteristic of moderately thick ferromagnetic films) or of the so-called Ginzburg–Landau vortices (characteristic to superconductors) that carry a non-zero topological degree.

Let us fix the setting: We use the thin-film reduction (7.8) where we will skip $\tilde{}$. We shall for simplicity ignore the anisotropy and the applied external field (i.e. $Q = 0$ and $H_{\text{ext}} = 0$). It is trivial, however, to include a small anisotropy and an appropriately-scaled applied field energy, since Γ-convergence is insensitive to compact perturbations of the functional. We are interested here in ferromagnetic samples of a thin circular film, i.e. $\Omega' = B_\ell$ is the disc of radius ℓ. We use the two dimensionless parameters $\delta = \frac{d^2}{t\ell}$ as the size of the core of a Néel wall and $h = \frac{t}{\ell}$ as the aspect ratio of the micromagnetic sample. We focus on the regime of ultra thin-films where $h = h(\delta)$ satisfies (7.12) and the energy scaling is chosen at the level of Néel walls. Rescaling the energy (7.8) by $t^2\ell$, we get the following functional energy over the set of configurations $m : B^2 \to S^1$:

$$\begin{aligned}\hat{E}_\delta(m) = \delta \int_{B^2} |\nabla m|^2 dx + \frac{1}{2}\|(\nabla \cdot m)_{ac}\|^2_{\dot{H}^{-\frac{1}{2}}(\mathbf{R}^2)} \\ + \frac{1}{2\pi}|\log h| \int_{\partial B^2} (m \cdot \nu)^2 d\mathcal{H}^1. \end{aligned} \tag{9.4}$$

In this section, we denote the in-plane differential operator by $\nabla = (\partial_{x_1}, \partial_{x_2})$ and since $m \in S^1$, we have $m' \equiv m$ (with $m_3 = 0$). We conjecture that the vortex is asymptotically the minimizer of the above variational problem.

Open Problem 4. *Let* $\delta \ll 1$ *and let* $h = h(\delta)$ *satisfying* (7.12). *If* m_δ *is a minimizer of* (9.4) *for* $\delta > 0$, *then*

$$m_\delta \to m_0(x) := \frac{x^\perp}{|x|} \quad \text{in } L^2(B^2) \quad \text{and} \quad \lim_{\delta\downarrow 0} |\log\delta| \hat{E}_\delta(m_\delta) = E_0\left(\frac{x^\perp}{|x|}\right),$$

where $E_0(\frac{x^\perp}{|x|}) = 2\pi$ *is the energetic cost* (9.3) *of a* $360°$ *Néel wall with vanishing initial angle* $\alpha = 0$.

For the moment, let us simplify the problem by omitting the last term that penalizes the surface charges in (9.4). (We will discuss later the general context of Open Problem 4.) The analysis is based on the following renormalization of two-dimensional micromagnetic energy (already mentioned at Remark 7 in Sec. 2):

$$E_\varepsilon(m) = \varepsilon \int_{B^2} |\nabla m|^2 dx + \frac{|\log \varepsilon|}{2} \int_{\mathbf{R}^2} ||\nabla|^{-\frac{1}{2}} (\nabla \cdot m)_{ac}|^2 dx, \tag{9.5}$$

where ε is a rescaled small parameter corresponding to the Néel core given by

$$\delta = \frac{\varepsilon}{|\log \varepsilon|} > 0.$$

Our viewpoint is based on the method of Γ-convergence: We enforce the formation of a vortex in the limit $\varepsilon \to 0$ by considering families $\{m_\varepsilon\}_{\varepsilon>0}$ of magnetizations that satisfy

$$m_\varepsilon \to \frac{x^\perp}{|x|} \quad \text{in } L^2(B^2) \quad \text{as } \varepsilon \to 0 \tag{9.6}$$

and we define the energy of the vortex by the following relaxed problem:

$$E_0\left(\frac{x^\perp}{|x|}\right) = \inf\left\{\liminf_{\varepsilon\to 0} E_\varepsilon(m_\varepsilon) : \{m_\varepsilon\} \text{ satisfies } (9.6)\right\}. \tag{9.7}$$

Indeed, the infimum in (9.7) is achieved (and nontrivial). We call a minimizing family, every family $\{m_\varepsilon\}$ that satisfies (9.6) and achieves the minimum (9.7), i.e. $\lim_{\varepsilon\to 0} E_\varepsilon(m_\varepsilon) = E_0(\frac{x^\perp}{|x|})$. The L^2-compactness of uniformly bounded energy configurations has been proved in [45].

Note that the minimal level of energy E_ε is trivial and all minima are constant since (9.5) does not penalize surface charges $m \cdot \nu \neq 0$ on ∂B^2 (which is the case of (9.4)). In fact, every finite energy configuration $E_\varepsilon(m) < \infty$ does have surface charges on ∂B^2 and zero winding number on each closed curve in B^2. For this reason, the two constraints of having a degree 1 and the absence of surface charges can only be imposed in the limit $\varepsilon \to 0$ (as in (9.6)). Our analysis shows that asymptotically the vortex state represents the minimum energy E_ε under the constraint (9.6). We conjecture that the vortex is still a minimizer if the constraint (9.6) is relaxed and convergence is only assumed on the boundary ∂B^2 (i.e. $m_\varepsilon \to x^\perp$ in $L^2(\partial B^2)$ as $\varepsilon \to 0$); this is of course a weaker conjecture than Open Problem 4.

Our main result in this direction characterizes asymptotically the energy of the vortex:

Theorem 18. (Ignat–Knüpfer [40]) *Let* $\{m_\varepsilon\}$ *be a minimizing family in* (9.7). *Then we have*

$$E_\varepsilon(m_\varepsilon) = 2\pi + o(1) \quad \textit{as } \varepsilon \to 0,$$

so that $E_0(\frac{x^\perp}{|x|}) = 2\pi$.

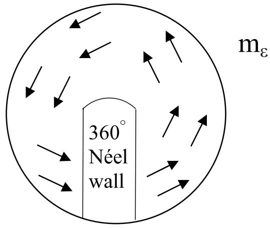

Fig. 19. Microscopic vortex structure at level ε.

Note that this result includes the precise leading constant of the minimal energy. Our construction for the upper bound of the energy is based on the inclusion of a 360° Néel wall of initial angle 0 along a radius of the disc (see Fig. 19). On the other hand, we prove the lower bound of the energy of a vortex in a slightly more general context. More precisely, as in [45], we consider localized stray-fields $H : B^3 \to \mathbf{R}^3$ determined by the static Maxwell's equation in the weak sense: For all $\zeta \in C_c^\infty(B^3)$,

$$\int_{B^3} H \cdot \left(\nabla, \frac{\partial}{\partial z}\right) \zeta dx dz = \int_{B^2} \nabla \cdot m \zeta dx, \tag{9.8}$$

where $B^3 \subset \mathbf{R}^3$ is the unit ball in $\mathbf{R}^3$ and we define the localized micromagnetic energy

$$E_\varepsilon^{\mathrm{loc}}(m, H) = \varepsilon \int_{B^2} |\nabla m|^2 dx + |\log \varepsilon| \int_{B^3} |H|^2 dx dz.$$

Obviously, by (7.9), $E_\varepsilon^{\mathrm{loc}}(m, \nabla u_{ac}) \le E_\varepsilon(m)$ (since $E_\varepsilon^{\mathrm{loc}}$ counts the stray-field energy only inside the ball B^3). We prove the following estimate for the localized energy:

Theorem 19. (Ignat–Knüpfer [40]) *Let* $\{m_\varepsilon\}$ *be a family satisfying* (9.6) *and let* $H_\varepsilon : B^3 \to \mathbf{R}^3$ *be localized stray-fields associated to* m_ε *by* (9.8). *Then we have*

$$E_\varepsilon^{\mathrm{loc}}(m_\varepsilon, H_\varepsilon) \ge 2\pi + o(1) \quad \textit{as } \varepsilon \to 0.$$

Crucial for the estimate of the lower bound is the control of the localized stray-field energy. The main idea relies on a dynamical system argument combined with localized interpolation inequalities similar to (8.3). Since the stray-field energy is created by $\nabla \cdot m_\varepsilon$, by Stokes theorem this implies a control for the net flow of m_ε across the boundary of any subdomain of B^2. The first step of the proof consists in finding such a domain with maximal net flow; as in [21, 45], we consider the flow generated by the vector field $m_\varepsilon^\perp$. Using Stokes theorem, this yields the optimal lower bound for the energy in some particular cases. To get to the general result, a careful analysis is carried out on a partition in small annuli of the domain B^2 by balancing two effects: Rotation versus the length of orbits of the flow.

Discussion on Open Problem 4. While we cannot rigorously prove Open Problem 4, we would like to compare the vortex with the typical counter-candidate

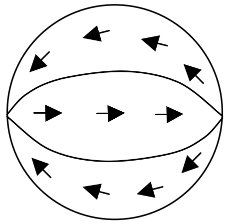

Fig. 20. S-state.

observed in thin ferromagnetic discs, the so-called S-state (see [33]). We show that the vortex has asymptotically lower energy than the S-state (see Fig. 20), thus indicating that the vortex might indeed be global minimizer of the energy. Recall that the vortex corresponds to the viscosity solution of the domain B^2, i.e.

$$m_0(x) = \nabla^\perp \operatorname{dist}(x, \partial B^2).$$

In our regime, the asymptotic cost of a vortex follows by Theorem 18:

$$E_0(m_0) = 2\pi.$$

The limit configuration of the S-state is represented at the mesoscopic level by

$$S(x) = \begin{cases} \nabla^\perp \operatorname{dist}(x, \partial B^2_+) & \text{if } x \in B^2_+, \\ -\nabla^\perp \operatorname{dist}(x, \partial B^2_-) & \text{if } x \in B^2_-, \end{cases}$$

where $B^2_\pm = \{x \in B^2 : \pm x_2 \geq 0\}$ are the upper (respectively, lower) half-discs (see Fig. 20). Let γ be the jump set of the S-state, i.e.

$$\gamma = \gamma^+ \cup \gamma^- \quad \text{and} \quad \gamma^\pm(x_1) = \left(x_1, \pm\frac{1 - x_1^2}{2}\right) \text{ with } x_1 \in (-1, 1).$$

In fact, if we denote by $S^\pm$ the traces of S on γ, one has $S^-(x) = (1, 0)$ and $S^+(x) = \pm\frac{x^\perp}{|x|}$ for $x \in \gamma^\pm$. So, the angle of the jump θ (given by $S^+ = e^{i\theta}S^-$) increases on $\gamma^\pm$ from 90° to 270°. Furthermore, we denote the corresponding asymptotic energy density of a Néel wall connecting the directions S^+ and S^- by $e(S^+, S^-) = \frac{\pi}{2}(1 - \cos\frac{\theta}{2})^2$. Then

$$E_0(S) = \int_\gamma e(S^+, S^-) d\mathcal{H}^1.$$

Therefore, one computes:

$$\int_\gamma e(S^+, S^-) d\mathcal{H}^1 = 2\int_{\gamma^+} e(S^+, S^-) d\mathcal{H}^1 = 2\sqrt{2}\pi > E_0(m_0).$$

The above computation shows that the S-state is asymptotically less favorable than the vortex state in the regime (7.12). It is an open question to rigorously prove that the vortex state indeed is the global minimizer over all planar configurations of (9.4).

10. Landau State

In this section, we investigate a common pattern of the magnetization in thin ferromagnetic films (the Landau state), that corresponds to the global minimizer of the micromagnetic energy in the regime (7.13). For that, we focus on a toy problem rather than on the full physical model: We use the thin-film reduction (7.8) and for simplicity, we ignore the anisotropy and the applied external field (i.e. $Q = 0$ and $H_{\text{ext}} = 0$). So, let $\Omega \subset \mathbf{R}^2$ be a bounded simply-connected domain with a $C^{1,1}$ boundary corresponding to the horizontal section of a ferromagnetic cylinder of small thickness. We consider magnetizations that are invariant in the out-of-plane variable, i.e.

$$m = (m_1, m_2, m_3) : \Omega \to S^2$$

and they are tangent to the boundary $\partial\Omega$, i.e.

$$m' \cdot \nu = 0 \quad \text{on } \partial\Omega, \tag{10.1}$$

where $m' = (m_1, m_2)$ is the in-plane component of the magnetization and ν is the normal outer unit vector to $\partial\Omega$. The assumption (10.1) is not compatible with our regime (7.13) when analyzing the minimal energy since metastable states of the magnetization under the restriction (10.1) are not minimizers of (7.8). Scaling the energy at order of td^2, the reduced energy (7.8) can be written as the following functional:

$$E_{\eta,\delta}(m) = \int_\Omega |\nabla m|^2 dx + \frac{1}{\eta^2} \int_\Omega m_3^2 dx + \frac{1}{2\delta} \int_{\mathbf{R}^2} ||\nabla|^{-\frac{1}{2}} (\nabla \cdot m')|^2 dx,$$

where $\eta = \frac{d}{\ell}$ and $\delta = \frac{d^2}{t\ell}$ are two small positive parameters (standing for the size of the Bloch line core and the Néel wall core, respectively). Here, $x = (x_1, x_2)$ are the in-plane variables with the differential operator $\nabla = (\partial_{x_1}, \partial_{x_2})$. In this section, we will always think of

$$m' \equiv m' \mathbf{1}_\Omega$$

as being extended by 0 outside Ω. Observe that the boundary condition (10.1) is necessary so that the homogeneous $\dot{H}^{-\frac{1}{2}}$-seminorm of $\nabla \cdot m'$ is finite since

$$\nabla \cdot m' = (\nabla \cdot m') \mathbf{1}_\Omega + (m' \cdot \nu) \mathbf{1}_{\partial\Omega} \quad \text{in } \mathbf{R}^2.$$

We are interested in the asymptotic behavior of minimizers of the energy $E_{\eta,\delta}$ in the regime

$$\eta \ll 1 \quad \text{and} \quad \delta \ll 1.$$

The characteristic singular patterns expected in this context are the Néel walls together with topological defects (due to (10.1)) standing for interior vortices (the Bloch lines) or "half" Bloch lines at the boundary. Recall that the energy $E_{\eta,\delta}$ per unit-length of a Néel wall of angle 2θ (with $\theta \in (0, \frac{\pi}{2}]$) is given by:

$$\frac{\pi(1 - \cos\theta)^2 + o(1)}{2\delta|\log\delta|} \quad \text{as } \delta \to 0, \tag{10.2}$$

(see (8.7)). The formation of interior or boundary vortices is explained by the competition between the exchange energy and the penalization of the m_3-component for configurations tangent at the boundary. Indeed, there is no S^1-configuration that is of finite exchange energy and satisfies (10.1). There are only two possible situations:

- If m' does not vanish on $\partial\Omega$, then (10.1) implies that m' carries a nonzero topological degree, $\deg(m', \partial\Omega) = \pm 1$. In this case, we expect the nucleation of an interior vortex of core-scale η (i.e. Bloch line in the micromagnetic jargon). The scaling of the vortex energy is related to the minimal Ginzburg–Landau (GL) energy (see Bethuel, Brezis and Helein [7]):
$$\min_{\substack{m' \in H^1(\Omega, \mathbf{R}^2)\\ m' = \nu^\perp \text{ on } \partial\Omega}} \int_\Omega g_\eta(m') dx = (2\pi + o(1)) |\log \eta| \quad \text{as } \eta \to 0, \tag{10.3}$$
where the GL density energy is given in the following:
$$g_\eta(m') = |\nabla m'|^2 + \frac{1}{\eta^2}(1 - |m'|^2)^2. \tag{10.4}$$
- The second situation consists in having zeros of m' on the boundary. Therefore, we expect that GL boundary vortices do appear. Roughly speaking, they correspond to "half" of an interior vortex where the vector field m' is tangent at the boundary and vanishes at the core; therefore they are different from the micromagnetic boundary vortices that take values into S^1, so they never vanish. Remark the importance of the regularity of $\partial\Omega$ in estimate (10.3). In fact, if $\partial\Omega$ has a corner and the boundary condition $m' = \nu^\perp$ on $\partial\Omega$ in (10.3) is relaxed to (10.1), then estimate (10.3) does not hold anymore, it depends on the angle of the corner. Therefore, at the microscopic level, topological point defects do appear in the Landau state pattern and are induced by (10.1).

The aim of the section is to show compactness of magnetizations energetically $E_{\eta,\delta}$ close to the Landau state in order to rigorously justify the limit behavior (7.11): The delicate issue consists in having the constraint $|m| = 1$ conserved in the limit. For that, we have to evaluate the energetic cost of the Landau state. We expect that the leading order energy of a Landau state is given by the topological point defects and Néel walls. The Landau state configuration consists in several Néel walls and either one interior Bloch line or two "half" Bloch lines placed at the boundary of the sample Ω. Therefore, by (10.2) and (10.3), we expect that the energy of the Landau state has the following order:
$$2\pi |\log \eta| + \frac{A}{\delta |\log \delta|}, \tag{10.5}$$
for some positive $A > 0$ depending on the length and angle of Néel walls.

Main results. First of all, we want to rigorously prove the upper bound (10.5) for the Landau state. Our result gives the exact leading order energy of the Landau state in the case of a stadium domain Ω (see Fig. 7). Note that the Landau state of a stadium consists in a single Néel wall of 180° around the jump set of the viscosity solution (in our example, the length of the wall is equal to $2L$, so that by (10.2), $A = \pi L$ in (10.5)).

Theorem 20. (Ignat–Otto [46]) *Let Ω be a stadium domain (as in Fig. 7). In the regime $\eta \ll \delta \ll 1$, there exists a C^1 vector field $m_{\eta,\delta} : \Omega \to S^2$ that satisfies* (10.1) *and*

$$E_{\eta,\delta}(m_{\eta,\delta}) \leq 2\pi|\log\eta| + \frac{\pi L + o(1)}{\delta|\log\delta|} \quad \text{as } \delta \downarrow 0. \tag{10.6}$$

Observe that the vortex energy in the above estimate is relevant only if its energy costs at least as much as a Néel wall, i.e. $\frac{1}{\delta|\log\delta|} \lesssim |\log\eta|$ (otherwise, the vortex energy would be absorbed by the term $o(\frac{1}{\delta|\log\delta|})$). This regime leads to a size η of the vortex core exponentially smaller than the size δ of the Néel wall core (see Remark 16).

Now we state our main result on the compactness of the S^2-valued magnetizations that have energies near the Landau state. The issue consists in rigorously justifying that the constraint $|m| = 1$ is conserved by the limit configurations as $\eta, \delta \to 0$. The regime where we prove our result corresponds to the case where a topological defect is energetically more expensive than the Néel wall:

Theorem 21. (Ignat–Otto [46]) *Let $\alpha \in (0, \frac{1}{2})$ be an arbitrary constant. We consider the following regime between the small parameters $\eta, \delta \ll 1$:*

$$\eta^{\frac{1}{2}} \lesssim \delta, \tag{10.7}$$

$$\log|\log\eta| \lesssim \frac{1}{\delta|\log\delta|}. \tag{10.8}$$

For each η and δ, we consider C^1 vector fields $m_{\eta,\delta} : \Omega \to S^2$ that satisfy (10.1) *and*

$$E_{\eta,\delta}(m_{\eta,\delta}) - 2\pi|\log\eta| \begin{cases} \leq 2\pi\alpha|\log\eta|, & (10.9) \\ \lesssim \dfrac{1}{\delta|\log\delta|}. & (10.10) \end{cases}$$

Then the family $\{m_{\eta,\delta}\}_{\eta,\delta\downarrow 0}$ is relatively compact in $L^2(\Omega, S^2)$ and any accumulation point $m : \Omega \to S^2$ satisfies

$$\begin{aligned} &m_3 = 0, \quad |m'| = 1 \text{ a.e. } \quad \text{in } \Omega \quad \text{and} \\ &\nabla \cdot m' = 0 \quad \text{distributionally in } \mathbf{R}^2. \end{aligned} \tag{10.11}$$

The proof of compactness is based on an argument of approximating S^2-valued vector fields by S^1-valued vector fields away from a small defect region. This small region consists in either one interior vortex or two boundary vortices. The detection of this region is done in Theorem 22 below and uses some topological methods due to Jerrard [49] and Sandier [70] for the concentration of the Ginzburg–Landau energy around vortices (see also Lin [55], Sandier and Serfaty [71]). Away from this small region, the energy level *only* allows for line-singularities. Therefore, the compactness result for S^1-valued vector fields in [45] applies.

Let us discuss the assumptions (10.7)–(10.10). Inequality (10.10) assures that cutting out the topological defect (one vortex or two boundary vortices), the remaining energy rescaled at the energetic level of Néel walls is uniformly bounded. Inequality (10.9) together with the choice of $\alpha < \frac{1}{2}$ mean that the energy cannot support three "half" vortices and is precisely explained in Theorem 22 below. Inequality (10.8) is imposed due to our method to detect a boundary vortex: It leads to a loss of energy of the order $O(\log|\log\eta|)$ with respect to the expected half energy $\pi|\log\eta|$ of an interior vortex (see Theorem 22 and Proposition 15). This amount of energy could leave room for configurations of Néel walls that may destroy the compactness of $|m'| = 1$. Therefore, to avoid this scenario, (10.8) is imposed. The regime (10.7) is rather technical: It is needed in the approximation argument of S^2-valued vector fields by S^1-valued vector fields away from the vortex balls. In fact, starting from the values of m' on a square grid of size η^β, the S^1-approximation argument requires zero degree of m' on each cell, leading to the condition $\beta < 1-\alpha$; furthermore, the condition $\eta^\beta \lesssim \delta$ is needed in order that the approximating S^1-valued vector fields induce a stray-field energy of the same order of m'. Therefore, (10.7) can be improved to a larger regime

$$\eta^\beta \lesssim \delta \quad \text{for any } \beta < 1-\alpha$$

(Theorem 21 is stated for the value $\beta = \frac{1}{2}$ which is the universal choice for every $\alpha < \frac{1}{2}$.) However, this slightly improved condition is weaker than the complete regime implied by (10.9) as explained in the following remark.

Remark 16. Any limit configuration m' satisfies (10.11). If Ω is a bounded simply-connected domain which is not a disc, then m' has at least one ridge (line-singularity) that corresponds to a Néel wall. Therefore, the minimal energy verifies

$$\min_{(10.1)} E_{\eta,\delta} - 2\pi|\log\eta| \gtrsim \frac{1}{\delta|\log\delta|}.$$

Combining with (10.9), it follows that

$$\frac{1}{\delta|\log\delta|} \lesssim |\log\eta|,$$

in particular, $\eta \lesssim e^{-\frac{1}{\delta|\log\delta|}}$, i.e. the core of the vortex is exponentially smaller than the core of the Néel wall. However, in the proof of Theorem 21, this constraint much stronger than (10.7) is not needed.

We prove the following result of the concentration of Ginzburg–Landau energy around one interior vortex or two boundary vortices for vector fields tangent at the boundary:

Theorem 22. (Ignat–Otto [46]) *Let $\alpha \in (0, \frac{1}{2})$ and $\Omega \subset \mathbf{R}^2$ be a bounded simply-connected domain with a $C^{1,1}$ boundary. Then there exists $\eta_0 = \eta_0(\alpha, \partial\Omega) > 0$ such that for every $0 < \eta < \eta_0$, if $m' : \Omega \to \overline{B^2}$ is a C^1 vector field that satisfies* (10.1) *and*

$$\int_\Omega g_\eta(m')dx \leq 2\pi(1+\alpha)|\log \eta|, \tag{10.12}$$

then there exist either a ball $B(x_1^*, r^*) \subset \Omega$ (called vortex ball) with $r^* = \frac{1}{|\log \eta|^3}$ and

$$\int_{B(x_1^*, r^*)} g_\eta(m')dx \geq 2\pi \left|\log \frac{r^*}{\eta}\right| - C, \tag{10.13}$$

or two balls $B(x_2^*, r^*)$ and $B(x_3^*, r^*)$ (called boundary vortex balls) with $x_2^*, x_3^* \in \partial\Omega$ and

$$\int_{(B(x_2^*, r^*) \cup B(x_3^*, r^*)) \cap \Omega} g_\eta(m')dx \geq 2\pi \left|\log \frac{r^*}{\eta}\right| - C, \tag{10.14}$$

where $C = C(\alpha, \partial\Omega) > 0$ is a constant depending only on α and on the geometry of $\partial\Omega$.

The condition $\alpha < \frac{1}{2}$ is essential in our proof. In fact, if no topological defect exists in the interior (in which case, condition (10.1) induces boundary vortices), we perform a mirror-reflection extension of m' outside the domain. Roughly speaking, the GL energy in the extended domain doubles, i.e. it is of the order $2\pi(2+2\alpha)|\log \eta|$ and the topological degree at the new boundary is equal to two; in order to avoid the formation of three interior vortices in the extended region, we should impose $2 + 2\alpha < 3$, i.e. $\alpha < \frac{1}{2}$.

Observe that the Ginzburg–Landau energy concentration for a boundary vortex in (10.14) has a cost of the order $\pi|\log \eta| - C \log|\log \eta|$ provided that the boundary has regularity $C^{1,1}$. We conjecture that the same energetic cost for a boundary vortex holds true if the boundary has regularity $C^{1,\beta}$, $\beta \in (0,1)$. However, if the boundary regularity is only C^1, then the energetic cost of a boundary vortex may decrease to $(\pi - \frac{C}{\log|\log \eta|})|\log \eta|$ where $C > 0$ is a universal constant. This indicates that the loss of energy of the order $\log|\log \eta|$ in (10.14) could occur for boundary vortices in $C^{1,\beta}$-domains and the order of this energy loss increases to $\frac{|\log \eta|}{\log|\log \eta|}$ for C^1 boundaries as $\beta \to 0$. This claim is supported by the following example for a C^1 boundary domain:

Proposition 15. (Ignat–Otto [46]) *We consider in polar coordinates the following C^1 domain $\Omega = \{(r, \theta) : r \in (0, \frac{1}{20}), |\theta| < \gamma(r) = \frac{\pi}{2} - \frac{1}{\log \log \frac{1}{r}}\}$. For every $0 < \eta < 1$, there exists a C^1-function $m'_\eta : \Omega \cap B_{\frac{1}{200}} \to \mathbf{R}^2$ that satisfies* (10.1) *on $\partial\Omega \cap B_{\frac{1}{200}}$*

and

$$\int_{\Omega \cap B_{\frac{1}{200}}} g_\eta(m'_\eta)dx \leq \left(\pi - \frac{C}{\log|\log \eta|}\right)|\log \eta|,$$

where $C > 0$ is some universal positive constant (independent of η).

11. Boundary Vortices

In this section, we analyze a special thin-film regime where boundary vortices appear. We will assume small aspect ration, i.e. $h = \frac{t}{\ell} \ll 1$ and that the Néel walls have a large core $\delta = \frac{d^2}{t\ell}$, i.e.

$$\delta \gg 1 \quad \text{or} \quad \delta = O(1),$$

which is the opposite context with respect to the ordering presented in Sec. 7.2.

(a) The regime of very small films, characterized by

$$\delta \gg |\log h|$$

was considered by Kohn–Slastikov [51] with the scaling law of minimal energy chosen at the order of $t^2\ell|\log h|$. (In this regime, Néel walls and boundary vortices are not contained by the sample). Then the exchange term in the energy dominates completely (since rescaling by $t^2\ell|\log h|$, its coefficient in (7.8) is equal to $\frac{\delta}{|\log h|} \gg 1$) and the magnetization becomes an in-plane constant vector field. The corresponding reduced energy (in the sense of Γ-convergence) was derived in [51] and is related to earlier work of Carbou [16]. Their result shows that the nonlocal stray-field energy (7.7) reduces to a local contribution of the boundary $\int_{\partial\Omega'}(m' \cdot \nu)^2 d\mathcal{H}^1$.

(b) Slightly larger films, where

$$\delta = \alpha|\log h|$$

with $0 < \alpha < \infty$ and the minimal energy scales as $t^2\ell|\log h|$ were also studied by Kohn–Slastikov [51]. In this context, Néel walls are not contained by the sample, while boundary vortices have a core size of the order $O(1)$. Since in this regime Bloch lines have higher cost than boundary vortices, the limiting magnetizations are still required to be in-plane

$$m' : \Omega' \subset \mathbf{R}^2 \to S^1,$$

but no longer need to be constant. Instead, the exchange energy and the boundary contribution compete, and the rescaled energy $E^{3\mathrm{D}}$ (at the order of $t^2\ell|\log h|$) Γ-converges to

$$E^{2\mathrm{D}}(m') = \alpha \int_{\Omega'} |\nabla m'|^2 dx + \frac{1}{2\pi}\int_{\partial\Omega'}(m' \cdot \nu)^2 d\mathcal{H}^1.$$

A second limit, describing the behavior of $\frac{1}{\alpha}E^{2\mathrm{D}}$ when $\alpha \to 0$, was examined by Kurzke [54, 53]. As there is no $m' \in H^1(\Omega', S^1)$ that satisfies $m' \cdot \nu = 0$

on $\partial\Omega'$ for simply-connected bounded domains Ω', the limit is characterized by *boundary vortices*, whose interaction is governed by a (local) renormalized energy.

(c) The case where $\delta = O(1)$ was studied by Moser [60, 61] when the minimal energy scaling is at order of $\log|\log h|$. Here, all three patterns (Néel walls, boundary vortices, Bloch lines) are contained by the sample and the ordering is given by

$$E^{2\mathrm{D}}(\text{Néel wall}) \ll E^{2\mathrm{D}}(\text{Boundary vortex}) \ll E^{2\mathrm{D}}(\text{Bloch line}),$$

as in regime (iii) in Sec. 7.2. Due to the scaling law of the energy of $O(\log|\log h|)$, both the stray-field (represented by the lateral surface charges) and exchange terms survive in the limit. The balance between these terms produces boundary vortices. The corresponding vortex interaction is nonlocal here, in contrast to the local renormalized energy in [53].

Model. The aim of this section is to show the existence of a boundary vortex regime with purely exchange-driven and local vortex interaction. To do so, we show that the double limit in [51] and [53] can be replaced by a direct approach. The context is the following: Our regime is given by

$$1 \ll \delta \ll |\log h|.$$

Here, the Néel wall is not contained by the sample, but boundary vortices and Bloch lines may nucleate knowing that a boundary vortex energetically costs less than a Bloch line. The scaling law of the minimal energy is chosen at the level of a boundary vortex, i.e. $O(d^2 t|\log\kappa|)$ where we recall that $\kappa = \frac{d^2}{t\ell\log(\frac{\ell}{t})}$. Therefore, our regime is equivalent to the assumption $h \ll 1$ and $\frac{1}{|\log h|} \ll \kappa = \kappa(h) \ll 1$. The full energy $E^{3\mathrm{D}}$ (in the absence of anisotropy and external field) will be rescaled as

$$E_h(m_h) = \frac{1}{h|\log\kappa|}\int_{\Omega_h}|\nabla m_h|^2dx + \frac{1}{\eta^2 h|\log\kappa|}\int_{\mathbf{R}^3}|\nabla U_h|^2dx, \tag{11.1}$$

where

$$\Omega_h = \Omega' \times (0,h)$$

is the rescaled sample and $\Omega' \subset \mathbf{R}^2$ is a $C^{1,\alpha}$ domain with $\operatorname{diam}\Omega' = 1$. (Here, the core of the Block line η can be written in function of the aspect ratio h and the boundary vortex core κ as $\eta^2 = \kappa h|\log h|$.) We highlight the fact that here we consider the full model, i.e. we do not assume invariance of magnetization in the vertical direction x_3. The rescaled configurations $m_h(x) = m(\ell x)$ and the stray-field potential $U_h(x) = \frac{1}{\ell}U(\ell x)$ satisfy

$$m_h : \Omega_h \to S^2, \quad \Delta U_h = \nabla\cdot(m_h \mathbf{1}_{\Omega_h}) \quad \text{in } \mathbf{R}^3. \tag{11.2}$$

Our goal is to derive the reduced model as $h \to 0$ (in the sense of Γ-convergence). Let us first discuss the compactness issue for uniformly bounded energy configurations m_h that yields the correct topology of Γ-convergence. It consists in regarding for averaged magnetization (in x_3-component):

$$\bar{m}_h(x') = \frac{1}{h}\int_0^h m_h(x', x_3)dx_3, \quad x' = (x_1, x_2) \in \Omega'.$$

Then $\bar{m}_h \in H^1(\Omega', \bar{B}^3)$ and the trace of $\bar{m}_h$ on $\partial\Omega'$ belongs to $H^{\frac{1}{2}}(\Omega', \bar{B}^3)$. We will prove relative compactness of $\{\bar{m}_h\}_h$ at the boundary $\partial\Omega'$ in $L^2(\partial\Omega')$ where the limiting configurations m_0 belong to $BV(\partial\Omega', S^1)$. Moreover, the boundary Jacobians associated to the in-plane vector field $\bar{m}'_h$ on the boundary $\partial\Omega'$ are uniformly bounded measures.

Boundary Jacobian. This notion is defined as follows: For every $\bar{m}'_h \in H^1(\Omega', \mathbf{R}^2)$, we denote the (usual) Jacobian of $\bar{m}'_h$ by

$$\mathrm{Jac}(\bar{m}'_h) = \frac{1}{2}\nabla \times (\bar{m}'_h \wedge \nabla \bar{m}'_h) = \partial_{x_1}\bar{m}'_h \wedge \partial_{x_2}\bar{m}'_h \in L^1(\Omega').$$

We call *boundary Jacobian*, the operator $D : H^1(\Omega', \mathbf{R}^2) \to (C^{0,1})^*(\bar{\Omega}')$ defined as

$$\int_{\Omega'} D(\bar{m}'_h)\zeta dx' := \int_{\Omega'} (2\mathrm{Jac}(\bar{m}'_h)\zeta + \bar{m}'_h \wedge \nabla \bar{m}'_h \cdot \nabla^{\perp}\zeta)dx', \quad \text{for every } \zeta \in C^{0,1}(\bar{\Omega}').$$

It is a continuous operator and

$$\int_{\Omega'} D(\bar{m}'_h)\zeta dx' = \int_{\partial\Omega'} \bar{m}'_h \wedge \partial_\tau \bar{m}'_h \zeta d\mathcal{H}^1 \quad \text{if } \bar{m}'_h \in C^1(\bar{\Omega}', \mathbf{R}^2). \tag{11.3}$$

Note that $D(\bar{m}'_h)$ acts only on the boundary $\partial\Omega'$ (which has a natural meaning whenever $\bar{m}'_h \in C^1(\bar{\Omega}')$). Indeed, by density of $C^1(\bar{\Omega}')$ in $H^1(\Omega', \mathbf{R}^2)$ and the continuity of the operator D over $H^1(\Omega', \mathbf{R}^2)$, it means that D can be seen as an operator on the boundary acting on $H^{\frac{1}{2}}(\partial\Omega', \mathbf{R}^2)$ which gives a meaning of the R.H.S. of (11.3) if $\bar{m}'_h \in H^{\frac{1}{2}}(\partial\Omega', \mathbf{R}^2)$.

Vorticity and renormalized energy. We expect that the limiting measure of $\{D(\bar{m}'_h)\}_{h\downarrow 0}$ is the vorticity measure

$$J_0 = \pi \sum_{j=1}^{N} d_j \delta_{a_j}, \tag{11.4}$$

carried by the boundary vortices $a_j \in \partial\Omega'$ of "degree" $d_j \in \mathbb{Z}$ satisfying $\sum_{j=1}^N d_j = 2$. A boundary vortex a_j of "degree" $d_j \in \mathbb{Z}$ corresponds to a jump of size $d_j\pi$ in the lifting of the limit magnetization m_0. More precisely, we introduce a lifting $\psi : \partial\Omega' \to \mathbf{R}$ of the tangent vector $\tau = e^{i\psi}$ on $\partial\Omega'$ such that ψ is continuous on $\partial\Omega'$ except on a jump point with the size of the jump equal to 2π (after a complete turn on $\partial\Omega'$). This explains the above constraint $\sum_j d_j = 2$. The limit magnetization $m_0 = e^{i\varphi_0}$ belongs to $BV(\partial\Omega', S^1)$ and has the property that $\psi - \varphi_0$ is a piecewise constant function with values into $\pi\mathbb{Z}$, so that the total variation of $\psi - \varphi_0$ coincides with the mass of the vorticity measure:

$$J_0 = \partial_\tau(\psi - \varphi_0) \quad \text{on } \partial\Omega' \quad \text{and} \quad \|J_0\|_{\mathcal{M}(\partial\Omega')} = \int_{\partial\Omega'} |\partial_\tau(\psi - \varphi_0)| = \pi \sum_{j=1}^{N} |d_j|.$$

This result is very similar to the Ginzburg–Landau type functionals, the difference here residing in the concentration of the Jacobian on the boundary rather than at the interior of the domain. Similar to [7], we define the solution V of the inhomogeneous Neumann problem:

$$\begin{cases} \Delta V = 0 & \text{in } \Omega', \\ \dfrac{\partial V}{\partial \nu} = \partial_\tau \psi - J_0 & \text{on } \partial\Omega', \end{cases}$$

and let $R \in C(\bar{\Omega}')$ be the continuous harmonic function in Ω' given by

$$R(x') := V(x') - \sum_{j=1}^{N} d_j \log|x' - a_j|, \quad x' \in \Omega'.$$

The renormalized energy corresponding to $\{(a_j, d_j)\}$ is defined as follows:

$$W(\{(a_j, d_j\}) = -\pi \sum_{1 \le i < j \le N} d_i d_j \log|a_i - a_j| + \frac{1}{2} \int_{\partial\Omega'} V \partial_\tau \psi - \frac{\pi}{2} \sum_{j=1}^{N} d_j R(a_j).$$

Main result. We prove the following Γ-convergence result:

Theorem 23. (Ignat–Kurzke [41]) *Assume that $h \ll 1$ and let $\kappa = \kappa(h)$ be such that $\frac{1}{|\log h|} \ll \kappa \ll 1$.*

(1) (*Compactness and lower bound*) *If $m_h : \Omega_h \to S^2$ is a sequence of magnetizations such that*

$$\limsup_{h \to 0} E_h(m_h) < \infty,$$

then for a subsequence, the x_3-averaged magnetizations $\bar{m}_h \to m_0 = e^{i\varphi_0}$ in $L^2(\partial\Omega')$ where $\psi - \varphi_0 \in BV(\partial\Omega', \pi\mathbb{Z})$ and averaged boundary Jacobians $\{D(\bar{m}'_h)\}_{h \downarrow 0}$ converge to a vorticity measure $J_0 = \partial_\tau(\psi - \varphi_0)$ of the form (11.4). *The energy satisfies the following lower bound*:

$$\liminf_{h \to 0} E_h(m_h) \ge \|J_0\|_{\mathcal{M}(\partial\Omega')}.$$

Furthermore, if the "degrees" d_j belong to $\{\pm 1\}$ for every $1 \le j \le N$, then we have the following optimal lower bound at the second order of the energy:

$$\liminf_{h \to 0} |\log \kappa| (E_h(m_h) - \|J_0\|_{\mathcal{M}(\partial\Omega')}) \ge W(\{a_j, d_j\}) + \gamma_0 \|J_0\|_{\mathcal{M}(\partial\Omega')},$$

where $\gamma_0 = 1 - \log 2$ and W is the renormalized energy defined above.

(2) (*Upper bound*) *Given a configuration of disjoint boundary points $a_j \in \partial\Omega'$ and $d_j \in \mathbb{Z}$ with $\sum_{j=1}^N d_j = 2$, there exists a family of magnetizations $m_h : \Omega_h \to S^2$ such that the averaged magnetizations $\bar{m}_h \to m_0 = e^{i\varphi_0}$ in $L^2(\partial\Omega')$ where $\partial_\tau\varphi_0 = \partial_\tau\psi - J_0$ and the boundary Jacobians $\{D(\bar{m}_h')\}_{h\downarrow 0}$ converge to the vorticity measure J_0 and*

$$\lim_{h\to 0} E_h(m_h) = \pi \sum_{j=1}^N |d_j|.$$

Furthermore, if $|d_j| = 1$ for all $j = 1, \ldots, N$, then m_h can be chosen such that

$$\lim_{h\to 0} |\log\kappa|(E_h(m_h) - \pi N) = W(\{a_i, d_i\}) + \pi N\gamma_0.$$

Our strategy in proving this theorem is as follows. First, we reduce the energy $E_h(m_h)$ to a simplified functional defined for averaged magnetizations $\bar{m}_h$:

$$\bar{E}_h(\bar{m}_h) = \frac{1}{|\log\kappa|}\left(\int_{\Omega'} |\nabla'\bar{m}_h|^2 dx' + \frac{1}{\eta^2}\int_{\Omega'} (1 - |\bar{m}_h'|^2) dx' + \frac{1}{2\pi\kappa}\int_{\partial\Omega'} (\bar{m}_h \cdot \nu)^2 d\mathcal{H}^1\right).$$

In fact, the energy $\bar{E}_h(\bar{m}_h)$ is close to $E_h(m_h)$ up to $o(\frac{1}{|\log\kappa|})$ (note that $o(1)$ would suffice for the first leading order of the Γ-limit development). This is done by a careful series of estimates that improve in a more quantitative way results of Carbou [16] and Kohn–Slastikov [51]. Then we show that the averaged magnetizations $\bar{m}_h'$ can be approximated by S^1-vector fields with small energy error, using an argument related to the one explained in Sec. 10. This allows us to show compactness of the boundary Jacobians based on a new argument that avoids rearrangement inequalities used initially in [54]. Finally, we show the Γ-convergence result. Essentially, the idea here is to reduce to the pure boundary vortex regime using η-compactness type estimates.

12. Cross-Over from Symmetric to Asymmetric Walls

We have already presented the (symmetric) Néel wall in Sec. 8 as an x_3-invariant transition layer that is predominant in thin-films. For thicker-films, we expect that asymmetric walls (i.e. varying in the x_3-direction) become favorable as stray-field free transition layers. In this section, we are interested in the critical regime of the cross-over from symmetric to asymmetric walls in soft ferromagnetic films.

Model. We consider a magnetic material $\Omega \subset \mathbf{R}^3$ with the easy axis $e_2 = \begin{pmatrix} 0 \\ 1 \\ 0 \end{pmatrix}$ driven by an anisotropy density $Q\varphi(m)$ with $\varphi(m) = m_1^2 + m_3^2$. The domain wall is set to be parallel to the x_2x_3-plane as in Fig. 21. In order to deal with arbitrary

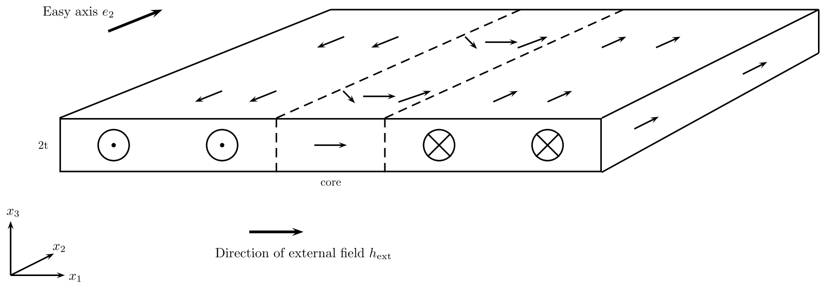

Fig. 21. A 180° domain wall perpendicular to x_1-direction.

wall angles $\theta \in [0, \frac{\pi}{2}]$ between the directions

$$m^{\pm} = (\cos\theta, \pm\sin\theta, 0),$$

we apply an external field $H_{\text{ext}} = Q(\cos(\theta), 0, 0)$ in the normal direction to the wall plane. The aim consists in studying the specific energy of a domain wall per unit length in x_2-direction and to understand the behavior of the transition layer that achieves the minimal energy. Hence, the admissible magnetizations are considered to be x_2-invariant and connect the two mesoscopic directions $m^{\pm}$ inside the x_1x_3-plane:

$$m = m(x_1, x_3) \in S^2, \quad (x_1, x_3) \in \omega := \mathbf{R} \times (-t, t), \;\; m(\pm\infty, \cdot) = m^{\pm}. \tag{12.1}$$

Rescaling in the thickness variable t, i.e. $\tilde{x} = \frac{x}{t}$, $\tilde{\omega} = \frac{\omega}{t}$, $\tilde{m}(\tilde{x}) = m(x)$, $\tilde{U}(\tilde{x}) = \frac{U(x)}{t}$, the specific energy (per unit-length in x_2) is given by

$$\begin{aligned} \tilde{E}_{2\text{D}}(\tilde{m}) = d^2 \int_{\tilde{\omega}} |\tilde{\nabla}\tilde{m}|^2 d\tilde{x} + t^2 \int_{\mathbf{R}^2} |\tilde{\nabla}\tilde{U}|^2 d\tilde{x} \\ + Qt^2 \int_{\tilde{\omega}} ((\tilde{m}_1 - \cos(\theta))^2 + \tilde{m}_3^2) d\tilde{x}, \end{aligned} \tag{12.2}$$

where the differential operator $\tilde{\nabla}$ refers to the variables $\tilde{x} = (\tilde{x}_1, \tilde{x}_3)$ and $\tilde{U} : \mathbf{R}^2 \to \mathbf{R}$ is the 2D stray-field potential given by

$$\tilde{\Delta}\tilde{U} = \tilde{\nabla} \cdot (\tilde{m} 1_{\tilde{\omega}}) \quad \text{in } \mathbf{R}^2.$$

Observe that the scaling of the stray-field energy is the same as for the Bloch wall, i.e.

$$\int_{\mathbf{R}^2} |\tilde{\nabla}\tilde{U}|^2 d\tilde{x} = \|\tilde{\nabla} \cdot (\tilde{m} 1_{\tilde{\omega}})\|^2_{\dot{H}^{-1}(\mathbf{R}^2)}.$$

Throughout the section, *we skip* ˜.

Symmetric walls. As we explained in Sec. 8, in the regime of thin-films (corresponding to small thickness t), the (symmetric) Néel wall m is the favorable transition layer: $\frac{\partial m}{\partial x_3} = 0$ in ω (i.e. $m = m(x_1)$ is invariant in x_3) and $m_3 = 0$ in ω (i.e. $m \in S^1$). It is a two length scale objects with a core of size $w_{\text{core}} = O\frac{d^2}{t}$ and two logarithmically decaying tails $w_{\text{core}} \lesssim |x_1| \lesssim w_{\text{tail}} = O\frac{t}{Q}$. Even if it does not satisfy the flux-closure constraint, it is invariant with respect to the group of symmetries generated by the charges $\nabla \cdot m$ in ω and $m_3 = 0$ on $\partial\omega$:

(1) $x_1 \to -x_1$, $x_3 \to -x_3$, $m_2 \to -m_2$;
(2) $x_1 \to -x_1$, $m_3 \to -m_3$, $m_2 \to -m_2$;
(3) $x_3 \to -x_3$, $m_3 \to -m_3$;
(4) Id.

The specific energy of a Néel wall is given by

$$E_{2\text{D}}(\text{symmetric Néel wall}) = O\left(t^2 \frac{1}{\log \frac{w_{\text{tail}}}{w_{\text{core}}}}\right) = O\left(t^2 \frac{1}{\log \frac{t^2}{d^2 Q}}\right)$$

(see e.g. [65, 27]).

Asymmetric walls. The main feature of an asymmetric wall relies on the flux-closure, i.e. it is a smooth transition layer m that satisfies (12.1) and

$$m : \omega \to S^2, \quad \nabla \cdot m = 0 \quad \text{in } \omega \quad \text{and} \quad m_3 = 0 \quad \text{on } \partial\omega. \tag{12.3}$$

Observe that $m' = (m_1, m_2) : \partial\omega \to S^1$ since m_3 vanishes on $\partial\omega$, so that one can define a topological degree for m' on $\partial\omega$ (where $\partial\omega$ is the closed "infinite" curve $(\mathbf{R} \times \{\pm 1\}) \cup (\{\pm\infty\} \times [-1, 1])$). The physical experiments predict two types of asymmetric walls related to the breaking of symmetries and the degree of m' on $\partial\omega$:

(1) For small angles θ, the system prefers the so-called asymmetric Néel wall. The main features amount to the conservation of symmetry (1) and (4) and in having a vanishing degree of m' on $\partial\omega$ (see Fig. 22). Due to symmetry (1), the asymmetric Néel wall has the m_2 component vanishing on a curve symmetric with respect to the center of the wall (by $x \to -x$). Moreover, m_2 is not monotone at the surface $|x_3| = 1$.
(2) For large angles θ, the system prefers the so-called asymmetric Bloch wall. In fact, as the angle θ grows, there is a breaking of symmetry with respect

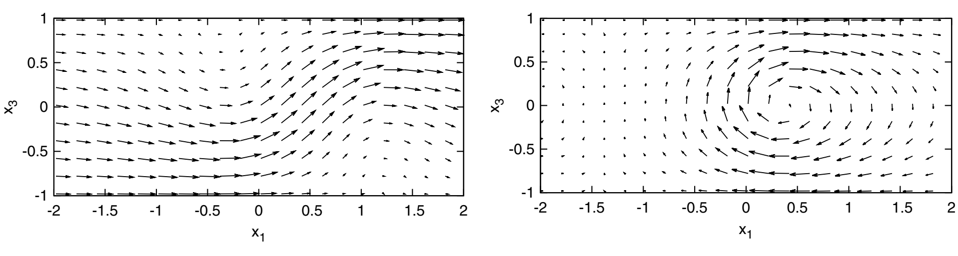

Fig. 22. Asymmetric Néel wall (on the left) and asymmetric Bloch wall (on the right). Numerics (made by L. Döring).

to the asymmetric Néel wall, so that the asymmetric Bloch wall conserves only the trivial symmetry (4). Another difference consists in the nonvanishing topological degree on $\partial\omega$ carried by asymmetric Bloch wall (i.e. $\deg(m', \partial\omega) = 1$). Then a vortex defect of (m_1, m_3) is nucleated at the center of the wall, and the curve of zeros of m_2 is no longer symmetric with respect the center of the wall (see Fig. 22). Moreover, the m_2-component is expected to be monotone at the surface $|x_3| = 1$.

The asymmetric wall has a single length scale $w_{\text{core}} \sim t$ and the specific energy is carried out by the exchange energy of the order (see e.g. [65, 27])

$$E_{2\mathrm{D}}(\text{asymmetric wall}) = O(d^2).$$

Regime. We focus on the challenging regime of soft materials and thickness t close to the exchange length d where we expect the cross-over in the scaling energy of symmetric walls (Néel wall) and asymmetric walls:

$$Q \ll 1 \quad \text{and} \quad |\log Q| \sim \left(\frac{t}{d}\right)^2.$$

Rescaling the energy (12.2) by d^2 and setting

$$\rho := Q\frac{t^2}{d^2} \ll 1 \quad \text{and} \quad \lambda := \frac{t^2}{d^2|\log\rho|} > 0,$$

then $\lambda = O(1)$ is a tuning parameter in the system and the rescaled energy, which is to be minimized, can be written as:

$$E_\rho(m) = \int_\omega |\nabla m|^2 dx + \lambda|\log\rho| \int_{\mathbf{R}^2} |\nabla U|^2 dx + \rho\int_\omega ((m_1 - \cos(\theta))^2 + m_3^2) dx$$

under the constraint

$$m : \omega = \mathbf{R} \times [-1, 1] \to S^2, \quad m(\pm\infty, \cdot) = m^\pm,$$
$$U : \mathbf{R}^2 \to \mathbf{R}, \quad \Delta U = \nabla \cdot (m1_\omega) \quad \text{in } \mathbf{R}^2.$$

To fix the center of the transition we set

$$\bar{m}_2(0) := \fint_{-1}^{1} m_2(0, x_3) dx_3 = 0.$$

Main result. We are interested in understanding the dependence in the wall angle θ of the asymptotic behavior of the minimal energy E_ρ and to describe the qualitative properties of minimizing transition layers as $\rho \to 0$.

We expect the following scenario (for $\rho \ll 1$): For small angles $0 \le \theta \le \theta^* = \theta^*(\lambda)$, the transition layer is symmetric, i.e. driven by the (symmetric) Néel wall, so that the minimal energy amounts to the logarithmic decaying tails of the Néel wall. In fact, if λ is very small, then the system will always prefer the symmetric transition layer. However, for larger λ, there exists a critical angle θ^* where a bifurcation occurs: An asymmetric wall becomes favorable to nucleate into the core of the transition. In fact, for large wall angles $\theta > \theta^*$, the optimal transition layer has a core driven by the exchange energy where the transition layer is charge-free, while outside the core, it preserves the tails of the symmetric wall (driven by the stray-field energy). The splitting into the core and the tails is determined by an angle θ_{in} of the asymmetric part of the wall. In fact, the angle θ_{in} optimizes the balance between the energy of asymmetric part of the transition in the core (turning from $-\theta_{\text{in}}$ to θ_{in}) and the energy of the symmetric part of the wall inside the tails (where the transition completes the rotation by an angle $\theta_{\text{out}} = \theta - \theta_{\text{in}}$).

This separation of the minimal energy is justified by the following Γ-convergence result at the level of minimizers:

Theorem 24. (Döring–Ignat–Otto [29]) *Let* $\theta \in (0, \frac{\pi}{2}]$. *As* $\rho \to 0$ *we have the following splitting of the minimal energy*:

$$\min_{(12.1)} E_\rho \to \min\left\{E_{\text{asym}}(\theta_{\text{in}}) + \lambda E_{\text{sym}}(\theta - \theta_{\text{in}}) : \theta_{\text{in}} \in \left[0, \frac{\pi}{2}\right]\right\}, \tag{12.4}$$

where the asymmetric wall energy is given by

$$E_{\text{asym}}(\theta_{\text{in}}) := \min_{(12.3)} \left\{ \int_\omega |\nabla m|^2 dx \,\middle|\, \bar{m}_2(0) = 0, \right.$$
$$\left. m(\pm\infty, \cdot) = (\cos(\theta_{\text{in}}), \pm\sin(\theta_{\text{in}}), 0) \right\} \tag{12.5}$$

while the symmetric wall energy can be written for $\theta_{\text{out}} = \theta - \theta_{\text{in}}$ *as*:

$$E_{\text{sym}}(\theta_{\text{out}}) := 2\pi(\cos(\theta_{\text{in}}) - \cos(\theta))^2.$$

Observe now that the symmetric part of the energy is quartic for small angles θ (as the Néel wall), i.e. $E_{\text{sym}} \lesssim \theta^4$. Therefore, in order to understand the bifurcation at the critical angle θ^* (when both symmetric and asymmetric walls are favorable), by (12.4) we need to compute the asymptotic expansion of the asymmetric energy at order θ^4 as $\theta \to 0$. For that, we will prove

$$E_{\text{asym}}(\theta) = E_0\theta^2 + E_1\theta^4 + o(\theta^4),$$

with some positive constants $E_0 > 0$ and $E_1 > 0$ that we compute explicitly. This allows us to heuristically determine a critical angle θ^*, at which the symmetric Néel wall loses stability and an asymmetric core is generated. Moreover, a new path of stable critical points with increasing inner wall angle θ_{in} branches off of $\theta_{\text{in}} = 0$ (see Fig. 23).

Leading order of E_{asym}: We will determine the first leading order term $E_0\theta^2$ of the asymmetric wall energy when the transition angle $\theta \to 0$. Moreover, we prove the asymptotic behavior of an asymmetric transition layer m_θ:

$$m_\theta = (\cos\theta, (\sin\theta)m_2^*, 0) + O(\theta^2), \quad \text{as } \theta \to 0,$$

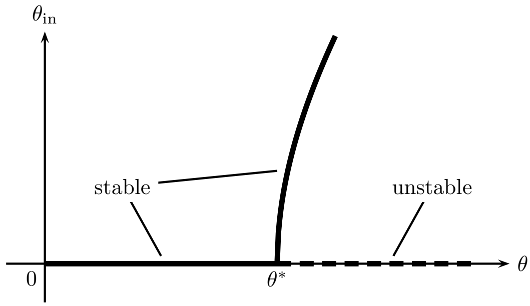

Fig. 23. Bifurcation diagram for the angle θ_{in} of the asymmetric core part, depending on the global wall angle θ.

where m_2^* is a minimizing transition layer of the following problem

$$E_0 = \min \left\{ \int_\omega |\nabla f|^2 dx \,\middle|\, f : \omega \to \mathbf{R}, f(\pm\infty, \cdot) = \pm 1, \right.$$

$$\left. \fint_{-1}^{1} f^2(\cdot, x_3) dx_3 = 1, \bar{f}(0) = 0 \right\}. \tag{12.6}$$

The asymptotic analysis is done by matching upper and lower bounds in the spirit of the Γ-convergence at the level of minimizers:

Theorem 25. (Döring–Ignat–Otto [28]) *The leading order coefficient of* E_{asym} *is given by*:

$$E_0 = \lim_{\theta \to 0} \frac{E_{\text{asym}}(\theta)}{\theta^2},$$

where E_0 *is the minimal energy value* (12.6). *There are only two minimizers of* E_0 *corresponding to* $\sigma \in \{\pm 1\}$ *that we explicitly determine*:

$$m_2^*(x) = \tanh\left(\frac{\pi}{2} x_1\right) + \sigma\sqrt{2} \sin\left(\frac{\pi}{2} x_3\right) \sqrt{1 - \tanh^2\left(\frac{\pi}{2} x_1\right)}, \quad x = (x_1, x_3) \in \omega.$$

Moreover, one computes $E_0 = 4\pi$.

The above theorem already justifies the physical prediction on the asymmetric Néel wall: First of all, observe that m_2^* is a non-monotone function on the surface $\{|x_3| = 1\}$, so that the same behavior is conserved by the second component of the asymmetric Néel wall. Second, observe that the curve where m_2^* vanishes is symmetric with respect to the origin, so that the zeros of the second component of an asymmetric Néel wall conserves the same symmetry (as predicted by numerical simulations in Fig. 22).

Second leading order of E_{asym}: We will now determine the second leading order term $E_1\theta^4$ of the asymmetric wall energy in the asymptotic of the transition angle

$\theta \to 0$. Moreover, the behavior of the asymmetric transition layer m_θ is expected to have the following second order expansion in θ:

$$m_\theta = (\cos\theta, (\sin\theta) m_2^*, 0) + (\sin^2\theta)\hat{m} + O(\theta^3), \quad \text{as } \theta \to 0, \tag{12.7}$$

where m_2^* is a minimizing transition layer of E_0 (given by Theorem 25) and $\hat{m}$ has the following components:

$$\hat{m}_1 = \frac{1-(m_2^*)^2}{2}, \quad \hat{m}_2 = 0 \quad \text{and} \quad \partial_{x_3}\hat{m}_3 = \partial_{x_1}\frac{(m_2^*)^2}{2} \ \text{ in } \omega,$$

where $\hat{m}_3$ is uniquely determined by the boundary condition $\hat{m}_3 = 0$ on $\partial\omega$. Using this heuristic expansion (12.7), one computes that

$$\int_\omega |\nabla m_\theta|^2 dx = \theta^2 E_0 + \theta^4 E_1 + o(\theta^4)$$

with some exact constant

$$E_1 = \frac{304}{105}\pi.$$

The following result rigorously proves the above second order term of E_{asym} by matching upper and lower bound:

Theorem 26. (Döring–Ignat–Otto [28]) *We have the following second-leading order coefficient*

$$E_1 = \lim_{\theta\to 0} \frac{(E_{\text{asym}}(\theta) - \theta^2 E_0)}{\theta^4}.$$

Now we can rigorously justify the supercritical bifurcation in the wall angle from symmetric to asymmetric optimal profile (as shown in Fig. 23). By Theorem 26, we have that

$$E_{\text{asym}}(\theta) = 4\pi\theta^2 + \frac{304}{105}\pi\theta^4 + o(\theta^4). \tag{12.8}$$

If θ is the transition wall angle, it means by Theorem 24 that:

$$\begin{aligned} \min_{(12.1)} E_\rho = &\min_{\theta_{\text{in}}\in[0,\frac{\pi}{2}]} (E_{\text{asym}}(\theta_{\text{in}}) + 2\pi\lambda(\cos(\theta_{\text{in}}) - \cos(\theta))^2) \\ &+ o(1) \quad \text{as } \rho \to 0, \end{aligned} \tag{12.9}$$

where θ_{in} is the angle of the inner asymmetric core part. For small θ, combining with (12.8), the R.H.S. of (12.9) as function of $\theta_{\text{in}} \in [0, \theta]$ has the unique critical point $\theta_{\text{in}} = 0$ if $\theta \le \theta^*$ where the bifurcation angle θ^* is given by

$$\theta^* = \arccos\left(1 - \frac{E_0}{2\pi\lambda}\right) + o(1), \quad \text{as } \theta \to 0.$$

(Observe that θ^* is well-defined provided that $\lambda \ge \frac{E_0}{4\pi}$; therefore, the bifurcation appears only if λ is large enough.) For $\theta > \theta^*$, the optimal splitting angle θ_{in} becomes positive and the symmetric wall becomes unstable under symmetry-breaking perturbations; hence, the asymmetric wall becomes favored by the system. Moreover, the second variation of the R.H.S. of (12.9) at θ^* is positive so that the bifurcation from symmetric to asymmetric wall is supercritical.

References

1. F. Alouges, T. Rivière and S. Serfaty, Néel and cross-tie wall energies for planar micromagnetic configurations, *ESAIM Control Optim. Calc. Var.* **8** (2002) 31–68.
2. L. Ambrosio, C. De Lellis and C. Mantegazza, Line energies for gradient vector fields in the plane, *Calc. Var. Partial Differential Equations* **9** (1999) 327–255.
3. L. Ambrosio, B. Kirchheim, M. Lecumberry and T. Rivière, On the rectifiability of defect measures arising in a micromagnetics model, in *Nonlinear Problems in Mathematical Physics and Related Topics*, II, Int. Math. Ser., Vol. 2 (Kluwer/Plenum, 2002), pp. 29–60.
4. P. Aviles and Y. Giga, A mathematical problem related to the physical theory of liquid crystal configurations, in *Miniconference on Geometry and Partial Differential Equations*, 2 (Canberra, 1986), Proc. Centre Math. Anal. Austral. Nat. Univ., Vol. 12 (Austral. Nat. Univ., 1987), pp. 1–16.
5. P. Aviles and Y. Giga, The distance function and defect energy, *Proc. Roy. Soc. Edinburgh Sect. A* **126** (1996) 923–938.
6. P. Aviles and Y. Giga, On lower semicontinuity of a defect energy obtained by a singular limit of the Ginzburg–Landau type energy for gradient fields, *Proc. Roy. Soc. Edinburgh Sect. A* **129** (1999) 1–17.
7. F. Béthuel, H. Brezis and F. Hélein, *Ginzburg–Landau Vortices*, Progress in Nonlinear Differential Equations and their Applications, Vol. 13 (Birkhäuser, 1994).
8. F. Bethuel and X. M. Zheng, Density of smooth functions between two manifolds in Sobolev spaces, *J. Funct. Anal.* **80** (1988) 60–75.
9. S. Bianchini, C. De Lellis and R. Robyr, SBV regularity for Hamilton–Jacobi equations in $\mathbb{R}^n$, *Arch. Rational Mech. Anal.* **200** (2011) 1003–1021.
10. J. Bourgain, H. Brezis and P. Mironescu, Lifting in Sobolev spaces, *J. Anal. Math.* **80** (2000) 37–86.
11. J. Bourgain, H. Brezis and P. Mironescu, $H^{\frac{1}{2}}$ maps with values into the circle: Minimal connections, lifting, and the Ginzburg–Landau equation, *Publ. Math. Inst. Hautes Études Sci.* **99** (2004) 1–115.
12. H. Brezis, P. Mironescu and A. C. Ponce, $W^{1,1}$-maps with values into S^1, in *Geometric Analysis of PDE and Several Complex Variables*, Contemp. Math., Vol. 368 (Amer. Math. Soc., 2005), pp. 69–100.
13. W. F. Brown, *Micromagnetics* (Wiley Interscience, 1963).
14. L. A. Caffarelli and M. G. Crandall, Distance functions and almost global solutions of eikonal equations, *Comm. Partial Differential Equations* **35** (2010) 391–414.
15. J. W. Cahn and J. E. Hilliard, Free energy of a nonuniform system I. Interfacial energy, *J. Chem. Phys.* **28** (1958) 258–267.
16. G. Carbou, Thin layers in micromagnetism, *Math. Models Methods Appl. Sci.* **11** (2001) 1529–1546.
17. S. Conti and C. De Lellis, Sharp upper bounds for a variational problem with singular perturbation, *Math. Ann.* **338** (2007) 119–146.
18. J. Dávila and R. Ignat, Lifting of BV functions with values in S^1, *C. R. Math. Acad. Sci. Paris* **337** (2003) 159–164.
19. C. De Lellis, An example in the gradient theory of phase transitions, *ESAIM Control Optim. Calc. Var.* **7** (2002) 285–289.
20. C. De Lellis and F. Otto, Structure of entropy solutions to the eikonal equation, *J. Eur. Math. Soc.* **5** (2003) 107–145.
21. A. DeSimone, H. Knüpfer and F. Otto, 2d stability of the Néel wall, *Calc. Var. Partial Differential Equations* **27** (2006) 233–253.

22. A. DeSimone, R. V. Kohn, S. Müller and F. Otto, Magnetic microstructures — a paradigm of multiscale problems, in *ICIAM 99* (Edinburgh), (Oxford Univ. Press, 2000), pp. 175–190.
23. A. Desimone, R. V. Kohn, S. Müller and F. Otto, A reduced theory for thin-film micromagnetics, *Comm. Pure Appl. Math.* **55** (2002) 1408–1460.
24. A. Desimone, R. V. Kohn, S. Müller and F. Otto, Repulsive interaction of Néel walls, and the internal length scale of the cross-tie wall, *Multiscale Model. Simul.* **1** (2003) 57–104.
25. A. DeSimone, R. V. Kohn, S. Müller, F. Otto and R. Schäfer, Two-dimensional modelling of soft ferromagnetic films, *R. Soc. Lond. Proc. Ser. A Math. Phys. Eng. Sci.*, **457** (2001) 2983–2991.
26. A. DeSimone, S. Müller, R. V. Kohn and F. Otto, A compactness result in the gradient theory of phase transitions, *Proc. Roy. Soc. Edinburgh Sect. A* **131** (2001) 833–844.
27. A. DeSimone, S. Müller, R. V. Kohn and F. Otto, Recent analytical developments in micromagnetics, in *The Science of Hysteresis*, Vol. 2 (Elsevier, 2005), pp. 269–381.
28. L. Döring, R. Ignat and F. Otto, Asymmetric domain walls of small angle in micromagnetics, preprint.
29. L. Döring, R. Ignat and F. Otto, Cross-over from symmetric to asymmetric transition layers in micromagnetics, preprint.
30. M. Giaquinta, G. Modica and J. Souček, *Cartesian Currents in the Calculus of Variations*, II, Ergebnisse der Mathematik und ihrer Grenzgebiete. 3. Folge. A Series of Modern Surveys in Mathematics [Results in Mathematics and Related Areas. 3rd Series. A Series of Modern Surveys in Mathematics], Vol. 38 (Springer-Verlag, 1998).
31. Y. Giga, M. Kubo and Y. Tonegawa, Magnetic clusters and fold energies, *Proc. Roy. Soc. Edinburgh Sect. A* **137** (2007) 23–40.
32. F. Golse, P.-L. Lions, B. Perthame and R. Sentis, Regularity of the moments of the solution of a transport equation, *J. Funct. Anal.* **76** (1988) 110–125.
33. A. Hubert and R. Schäfer, *Magnetic Domains: The Analysis of Magnetic Microstructures* (Springer-Verlag, 1998).
34. R. Ignat, On an open problem about how to recognize constant functions, *Houston J. Math.* **31** (2005) 285–304.
35. R. Ignat, The space $\mathrm{BV}(S^2, S^1)$: Minimal connection and optimal lifting, *Ann. Inst. H. Poincaré Anal. Non Linéaire* **22** (2005) 283–302.
36. R. Ignat, A Γ-convergence result for Néel walls in micromagnetics, *Calc. Var. Partial Differential Equations* **36** (2009) 285–316.
37. R. Ignat, A survey of some new results in ferromagnetic thin films, in *Séminaire: Équations aux Dérivées Partielles. 2007–2008*, Sémin. Équ. Dériv. Partielles, pages Exp. No. VI, 21 (École Polytech., 2009).
38. R. Ignat, Gradient vector fields with values into S^1, *C. R. Math. Acad. Sci. Paris* **349** (2011) 883–887.
39. R. Ignat, Two-dimensional unit-length vector fields of vanishing divergence, *J. Funct. Anal.* **262** (2012) 3465–3494.
40. R. Ignat and H. Knüpfer, Vortex energy and 360° Néel walls in thin-film micromagnetics, *Comm. Pure Appl. Math.* **63** (2010) 1677–1724.
41. R. Ignat and M. Kurzke, An effective model for boundary vortices in thin-film micromagnetics, in preparation.
42. R. Ignat and B. Merlet, Lower bound for the energy of Bloch walls in micromagnetics, *Arch. Rational Mech. Anal.* **199** (2011) 369–406.
43. R. Ignat and B. Merlet, Entropy method for line-energies, *Calc. Var. Partial Differential Equations* **44** (2012) 375–418.

44. R. Ignat and R. Moser, A zigzag pattern in micromagnetics, *J. Math. Pures Appl.* **98** (2012) 139–159.
45. R. Ignat and F. Otto, A compactness result in thin-film micromagnetics and the optimality of the Néel wall, *J. Eur. Math. Soc.* **10** (2008) 909–956.
46. R. Ignat and F. Otto, A compactness result of Landau state in thin-film micromagnetics, *Ann. Inst. H. Poincaré Anal. Non Linéaire* **28** (2011) 247–282.
47. P.-E. Jabin, F. Otto and B. Perthame, Line-energy Ginzburg–Landau models: Zero-energy states, *Ann. Sc. Norm. Super. Pisa Cl. Sci.* **1** (2002) 187–202.
48. P.-E. Jabin and B. Perthame, Compactness in Ginzburg–Landau energy by kinetic averaging, *Comm. Pure Appl. Math.* **54** (2001) 1096–1109.
49. R. L. Jerrard, Lower bounds for generalized Ginzburg–Landau functionals, *SIAM J. Math. Anal.* **30** (1999) 721–746.
50. W. Jin and R. V. Kohn, Singular perturbation and the energy of folds, *J. Nonlinear Sci.* **10** (2000) 355–390.
51. R. V. Kohn and V. V. Slastikov, Another thin-film limit of micromagnetics, *Arch. Rational Mech. Anal.* **178** (2005) 227–245.
52. S. N. Kružkov, First order quasilinear equations with several independent variables, *Mat. Sb.* (*N.S.*) **81** (1970) 228–255.
53. M. Kurzke, Boundary vortices in thin magnetic films, *Calc. Var. Partial Differential Equations* **26** (2006) 1–28.
54. M. Kurzke, A nonlocal singular perturbation problem with periodic well potential, *ESAIM Control Optim. Calc. Var.* **12** (2006) 52–63.
55. F. H. Lin, Vortex dynamics for the nonlinear wave equation, *Comm. Pure Appl. Math.* **52** (1999) 737–761.
56. C. Melcher, The logarithmic tail of Néel walls, *Arch. Rational Mech. Anal.* **168** (2003) 83–113.
57. C. Melcher, Logarithmic lower bounds for Néel walls, *Calc. Var. Partial Differential Equations* **21** (2004) 209–219.
58. P. Mironescu, Lifting of S^1-valued maps in sums of Sobolev spaces, preprint.
59. P. Mironescu, S^1-valued Sobolev mappings, *Sovrem. Mat. Fundam. Napravl.* **35** (2010) 86–100.
60. R. Moser, Ginzburg–Landau vortices for thin ferromagnetic films, *AMRX Appl. Math. Res. Express* **1** (2003) 1–32.
61. R. Moser, Boundary vortices for thin ferromagnetic films, *Arch. Rational Mech. Anal.* **174** (2004) 267–300.
62. F. Murat, Compacité par compensation: Condition nécessaire et suffisante de continuité faible sous une hypothèse de rang constant, *Ann. Scuola Norm. Sup. Pisa Cl. Sci.* (*4*) **8** (1981) 69–102.
63. C. B. Muratov and V. V. Osipov, Theory of 360° domain walls in thin ferromagnetic films, *J. Appl. Phys.* **104** (2008) 053908.
64. M. Ortiz and G. Gioia, The morphology and folding patterns of buckling-driven thin-film blisters, *J. Mech. Phys. Solids* **42** (1994) 531–559.
65. F. Otto, Cross-over in scaling laws: A simple example from micromagnetics, in *Proc. of the Int. Congress of Mathematicians*, Vol. III (Beijing, 2002) (Higher Ed. Press, 2002), pp. 829–838.
66. A. Poliakovsky, Upper bounds for singular perturbation problems involving gradient fields, *J. Eur. Math. Soc.* **9** (2007) 1–43.
67. T. Rivière, Dense subsets of $H^{\frac{1}{2}}(S^2, S^1)$, *Ann. Global Anal. Geom.* **18** (2000) 517–528.
68. T. Rivière and S. Serfaty, Limiting domain wall energy for a problem related to micromagnetics, *Comm. Pure Appl. Math.* **54** (2001) 294–338.

69. T. Rivière and S. Serfaty, Compactness, kinetic formulation, and entropies for a problem related to micromagnetics, *Comm. Partial Differential Equations* **28** (2003) 249–269.
70. E. Sandier, Lower bounds for the energy of unit vector fields and applications, *J. Funct. Anal.* **152** (1998) 379–403.
71. E. Sandier and S. Serfaty, *Vortices in the Magnetic Ginzburg–Landau Model*, Progress in Nonlinear Differential Equations and their Applications, Vol. 70 (Birkhäuser, 2007).
72. L. Tartar. Compensated compactness and applications to partial differential equations, in *Nonlinear Analysis and Mechanics*: *Heriot-Watt Symposium*, Vol. IV, Res. Notes in Math., Vol. 39 (Pitman, 1979), pp. 136–212.
73. H. A. M. van den Berg, Self-consistent domain theory in soft-ferromagnetic media. II, Basic domain structures in thin film objects, *J. Appl. Phys.* **60** (1986) 1104–1113.